DEVELOPMENT OF GRAIN-ORIENTED 3.5 PERCENT Si-Fe ALLOYS

A Thesis Submitted
In Partial Fulfilment of the Requirements
for the Degree of
MASTER OF TECHNOLOGY

A. A. BAND

POST GRADUATE OFFICE
This thesis has been approved
for the award of the Degree of
Master of Technology (M. Tech.)
in accordance with the
regulations of the Indian
Institute of Technology Kanpur
Dated. 16-2-72

to the

DEPARTMENT OF METALLURGICAL ENGINEERING
INDIAN INSTITUTE OF TECHNOLOGY KANPUR
JANUARY 1972

POST GRADUATE OFFICE
Submitted on 1.2.72

CERTIFICATE

This is to certify that this work on ' Development of Grain-oriented 3.5% Si-Fe alloys ' has been carried under my supervision and it has not been submitted elsewhere for a degree.

(K.P. Gupta)
Professor and Head
Department of Metallurgical Engineering
Indian Institute of Technology , Kanpur

ACKNOWLEDGEMENTS

The author wishes to express his sincere gratitude to Dr. K.P. Gupta, Professor and Head of the Department of Metallurgical Engineering, who acted as thesis supervisor, for his able guidance, lively interest, inspiration and useful suggestions in every step involved in this project and presentation of this thesis.

The author is highly indebted to Dr. G.S. Murty, Assistant Professor of Metallurgical Engineering Department for his sincere suggestions and many fruitful discussions.

The author wishes to express his thanks to Dr. A.R. Das and Dr. D. Chakravarty for their suggestions in setting up equipment for magnetic testing.

The author wishes to express his hearty thanks to h co-workers Mr. M.L. Narula, and Mr. J.V. Kumar for their co-operation, help, inspiration and discussions in setting u equipment for melting, heat treatment and magnetic testing, and for the help they extended in carrying out this investigation.

Thanks are also due to Mr. K.P. Mukherjee and Mr.N. Yadav of Metallurgical Engg. Department for their kind help in taking micrographs and texture study respectively and availing of facilities.

The author wishes to express his thanks to Mr.B. Sharma and Mr. R.K. Prasad of Ceramics Lab. for their kind help in making and sintering of crucibles.

Contd.

I.I.T. KANPUR
CENTRAL LIBRARY
Acc. No. A 19896

17 JUN 1972

Thesis
669.141
B221

V
JUNE '76

ME-1972-M-BAN-DEV

Thanks are due to the staff of all the Metallurgy Workshops for fabrication of various equipments required for this project.

Thanks are also due to Mr. Arora and Mr.Srivastava of Graphic Arts for their kind help in designing and drawing of Goniometer and tracings of the Pole figures respectively.

The author wishes to thank the staff of the predision Workshop, Central Workshop, Glass-blowing shop for fabrication of various equipments needed in the project.

The author wishes to express sincere thanks to Mr. S.K. Si, Mr. S.K. Gupta and Mr. Raghuram, students of Metallurgical Engineering Department for helping in setting up various equipments.

The author also is indebted to M/s. Mahindra & Mahindra for sending Grain-oriented Si-steel free of cost.

The author acknowledges the financial support of Hindustan Steel Ltd. (India) which made this work possible for investigation.

Finally thanks are due to Mr. S.N. Gupta for his careful and excellent typing.

A.A. Band

SYNOPSIS

The present investigation involves the study of deformation and recrystallization characteristics of high purity and commercial purity 3.5% Si-F_e alloys. This investigation involved the study of a few process variables, such as the amount of reduction, intermediate annealings, atmosphere, recrystallization time and temperatures for the production of right textures. The work on high purity alloy has shown that only sharp cold rolled texture can be produced in this case, either by straight heavy reduction or by low reduction followed by primary recrystallization for long periods and a high temperature anneal. No secondary recrystallization textures could be observed in this case. However, commercial purity alloy showed a strong but possibly slightly imperfect cube-on-edge texture.

CONTENTS

I INTRODUCTION

INTRODUCTION

Silicon-Iron alloys with up to 5% Si have enjoyed a constant improvement through research and control of production methods so as to produce better properties for electrical use. The most significant improvement in this direction was based on the observations by Kaya and Honda [1] and Williams [2] that single crystals of pure Fe and Fe-Si alloys can be magnetised more easily in the [100] direction than in the [110] and [111] directions; the third direction being the hardest direction for magnetisation (Fig.1 & 2). Steel sheets used in transformer cores undergo repeated cycles of magnetisation and demagnetisation and are required to have high permeability in the direction of applied field, and low core losses. This requires that the sheets should have preferred grain orientation so that as many grains as possible have their easy directions of magnetisation parallel to the direction of magnetisation in the transformer cores. Since preffered grain orientation in sheets is achieved by rolling (and also by subsequent heat treatment) this easy direction of magnetisation of grains should become parallel to the rolling direction. The importance of texture is evident from Fig.3. Another significant discovery was by Hadfield [45] who observed that the addition of silicon to substantially pure iron greatly improves the magnetic

properties of Fe-Si alloys. Silicon in Fe causes a small drop in magnetic induction at saturation, increases resistivity and beyond about 3% Si in Fe the permeability increases rapidly and reaches a maximum at about 6% Si (Fig. 4). Besides, it provides uniformly large grain size throughout the matrix which is helpful in secondary recrystallization. However, addition of Si beyond 5% makes the material brittle (Fig.5). Hence all commercial alloys normally contain less than 4.5% Si.

From the single crystal magnetic data on Fe-Si alloys it is apparent (Fig.6) that the ideal orientation of grains for producing better magnetic properties will be:

1. A cube face of grains parallel to the rolling plane and a cube edge parallel to the rolling direction i.e. (100) [001] texture or cube texture, so that there will be two easiest directions of magnetisation lying on the rolling plane. (Fig.7(a)).

2. A diagonal (110) plane parallel to the rolling plane and a cube edge parallel to the rolling direction, i.e. (110) [001] texture or cube on edge texture, so that there will be an easy and a medium easy direction of magnetisation lying on the rolling plane (Fig.7(b)).

Fig. 1. Magnetization curve for pure Fe single Crystals.

Fig. 2. Magnetization curve for Fe — Si alloy Single Crystals.

Fig. 3. Magnetic properties of grain oriented 3% Si-Fe alloy (A) & Hot-rolled 4% Si-Fe alloy (B).

Fig. 4. Variation in saturation induction B_S, maximum permeability μ_m, curie temperature θ and resistivity ρ as a function of % Si in Fe.

Fig. 5. Tensile strength of Fe-Si alloys for different concentrations of Si.

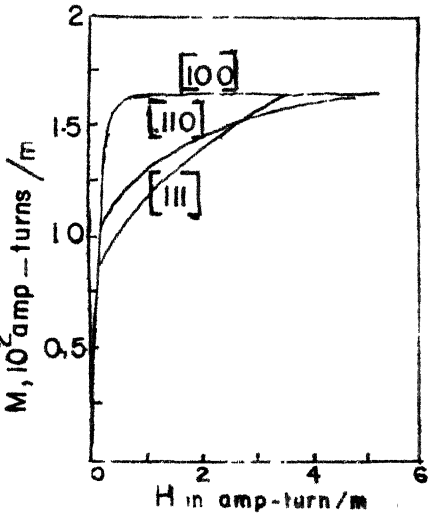

FIG-1

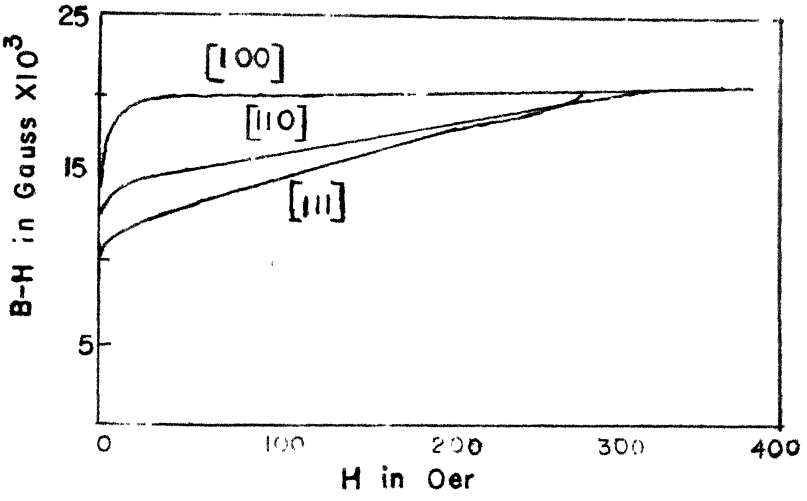

FIG-2.

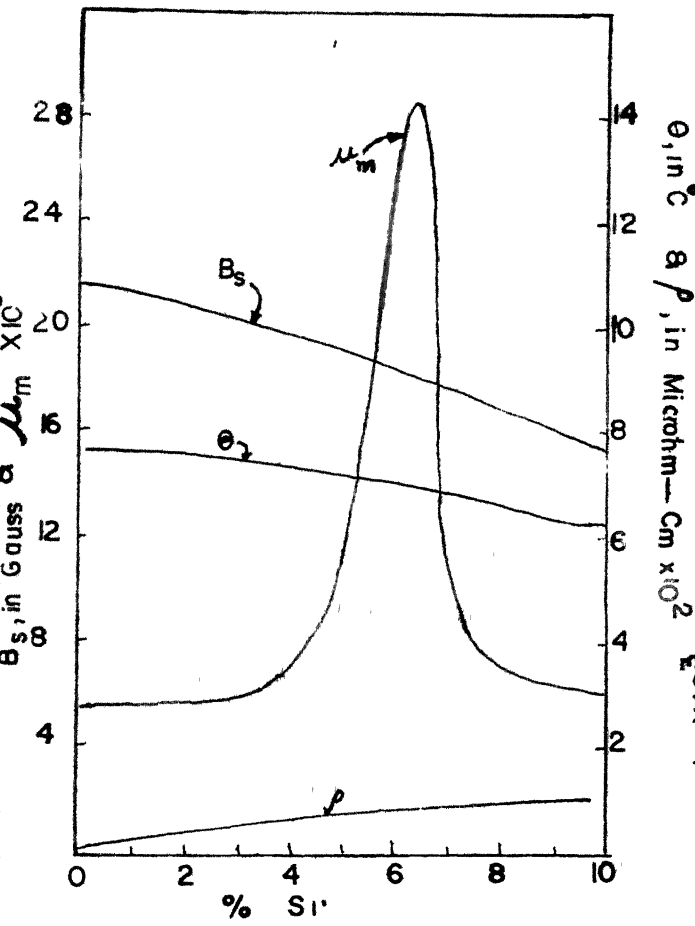

FIG-4

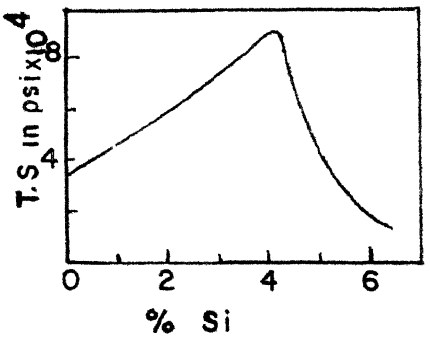

FIG-5.

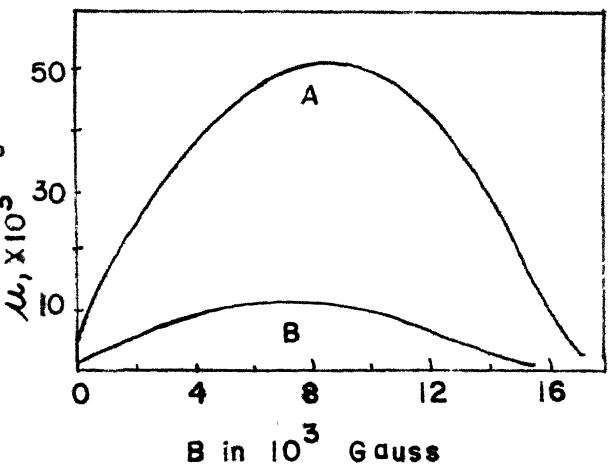

FIG-3

3. A (100) plane parallel to the rolling plane and [011] direction parallel to the rolling direction so that there will be two easy directions of magnetisation on the rolling plane at 45° to the rolling direction. When properly oriented this will be equivalent to cube texture (Fig.7(c)).

The method of producing any of the grain oriented textures can be divided into two basic catagories, 1) The texture produced by cold deformation, with or without any heat treatment so as to retain the cold rolled texture 2) The texture produced by cold-rolling followed by suitable annealing so as to produce a completely new texture known as annealing texture . While the (100) [011] texture can be produced by cold rolling only (followed by annealing or no annealing, the other two textures, (100) [001] and (110) [001] , can be produced only by suitable high temperature annealing following a suitable percent reduction.

When b.c.c. metals and alloys, such as Fe and Fe-Si alloys, are cold rolled they invariably produce a cold rolled texture (100) [011] [3,24,9,38] with [011] direction parallel (with a few degrees deviation) to the rolling direction and (100) plane parallel (with a few degrees to as large as about 45° deviation from the ideal orientation around the rolling direction) to

Fig. 6. Planes and directions of cubic crystals that are important for better magnetic properties in b.c.c. metals.

Fig. 7. Crystal orientation with respect to rolling plane (the plane of the sheets) and the rolling directions (R.D.) to give (a) cube texture, (b) cube on edge texture (c) cold rolled texture.

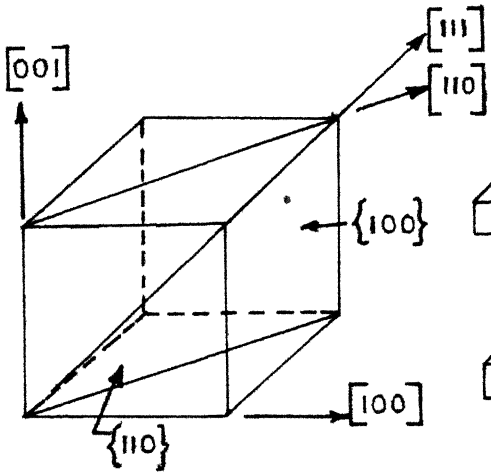

Fig. 6

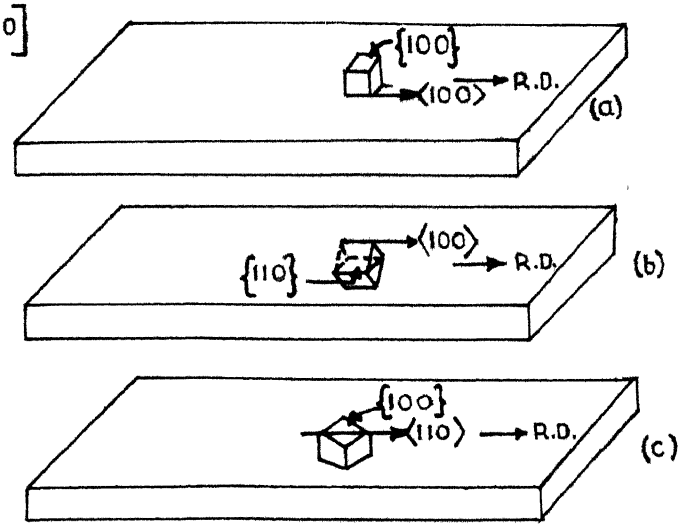

Fig. 7

the rolling plane. The sharpness in this texture has been achieved either by rolling in two perpendicular directions[4,5,6] or by partial recrystallization at temperatures below 675°C[7]. Cross rolling or partial recrystallization sharpens the cold-rolled textures by reducing the minor textures (111) [1$\bar{1}$0] and (111) [11$\bar{2}$] which are usually associated with the (100) [0$\bar{1}$1] texture. Further, it has been observed[8] that reductions more than 70% are essential for producing sharp cold-rolled texture in b.c.c. metals and alloys. Brown[9] indicated that the cold rolled texture is invariably dependent on the procedure adopted in the cold reduction stage. For example, in one stage cold-reduction produces sharp (100) [0$\bar{1}$1] texture whereas a two or three stage process, i.e. cold reductions followed by intermediate annealings, produce complex duplex texture.

Annealing of cold-rolled material above the recrystallization temperature produces primary recrystallization followed by primary grain growth. If, however, there are conditions favourable to produce stable grain structure (primary grain growth inhibition) which may be due to a) a strong single orientation[23] (texture inhibition) b) dispersed second phase[10] (dispersed phase inhibition) c) thermal grooving[11], high temperature annealing brings about a new process known as secondary recrystallization. In this process certain favourably oriented grains grow to very large

size consuming many of the unfavourably oriented grains. For Fe-Si alloys these grains usually have the cube-on-edge orientation with respect to the rolling plane and rolling direction. However, in certain cases cube orientation with respect to rolling plane and rolling direction has also been observed.

The annealing of the cold rolled material to produce secondary recrystallization in sheets of thickness 0.025" to 0.014" may be done in two ways- (a) isothermal annealing at a suitable temp. or (b) a suitable constant rate of heating with or without a short isothermal treatment at final temperature. When constant heating rates are used normally no separate primary recrystallization treatment is given to the material. Heating rates varying from 30°C/hr[12,14] to 100°C/hr.[13] have been used. However, it has been suggested[14] that a good heating rate is 30°C - 60°C/hr. At high heating rates the number of growth centres increase, time for complete recrystallization becomes short and the perfection in texture becomes poor.[14] In isothermal treatment temperatures above and below 800°C are used for secondary and primary recrystallization respectively. For secondary recrystallization, which produces magnetic orientation, the stabilization of grain size is achieved in the primary recrystallization stage.

The primary recrystallization texture is usually strongly developed (100) [011] texture[12] provided the cold reduction is high and annealing temperature is low. However, in most of the reported cases weak secondary textures (111) [112][12,13] (110) [001][12] are also observed; the secondary texture becomes prominent i.e., the primary texture becomes more random, if the specimen is processed through more number of intermediate annealings[9].

Much to the understanding of production of secondary recrystallization textures (110) [001] and (100) [001] has been done by Dunn and his coworkers[15-20], May and Turnbull[12], Wiener[21] and Detert[22]. The general method of producing secondary recrystallization texture appear to be similar, i.e., it requires after the primary recrystallization of the heavily cold-rolled material, a secondary recrystallization treatment. The methods of producing these two textures are so similar that the differences in conditions under which (110) [001] and (100) [001] textures can be produced do not become apparent. The secondary recrystallization takes place due to selective growth of preferentially oriented grains. Wiener[21] and Detert[22] suggested that the growth of (100) or (110) grains depend on the relative surface energies(σ), the one having lower surface would grow at the expense of the other. Measurements of thermal etch pits have shown that when

grins with (100) face parallel to rolling plane grow then $\sigma(100) < \sigma(110)$, but the difference is only very small, being approximately 70 ergs/cm^2[23]. From this observation as well as from other similar observations[24], it appears that surface energy has an important role to play in determining the final texture produced by annealing. Surface energy is dependent on the atmosphere used and is expected to be dependent on the variations in impurities present in the atmosphere. Wiener[21] and Foster[25] studied the amount of cube texture and cube texture growth rate as a function of oxygen content (Figs.8(a)&(b)). The available data, however, gives contradictory results making it difficult to understand the effect of atmosphere. As for example, while Wiener[21] using argon atmosphere containing less than 35 ppm oxygen produced (110) [001] texture and in 10^{-4} mm Hg vacuum a cube texture, Dunn and his coworkers[26-29] obtained cube-on-edge texture in high vacuum (5×10^{-5} mm of Hg) and cube texture in commercial purity argon gas containing O_2 as impurity. Similarly, the presence (in trace quantity) or absence of H_2S gas in hydrogen gas (which is commenly used as a suitable atmosphere) has been found to produce cube or cube on edge texture, respectively[30]. Annealing atmosphere also appears to have a considerable effect on the perfection of textures produced. While increase in nitrogen content

Fig. 8. Effect of oxygen in the formation of cube texture in 3% Si Fe alloy.

(A) Amount of cube texture as a function of oxygen content.

(a) 0.001% O_2, (b) 0.0033% O_2,
(c) 0.0042% O_2, (d) 0.0059% O_2.

(B) Cube texture growth rate as a function of oxygen content.
Single strips annealed in hydrogen at 1200°C

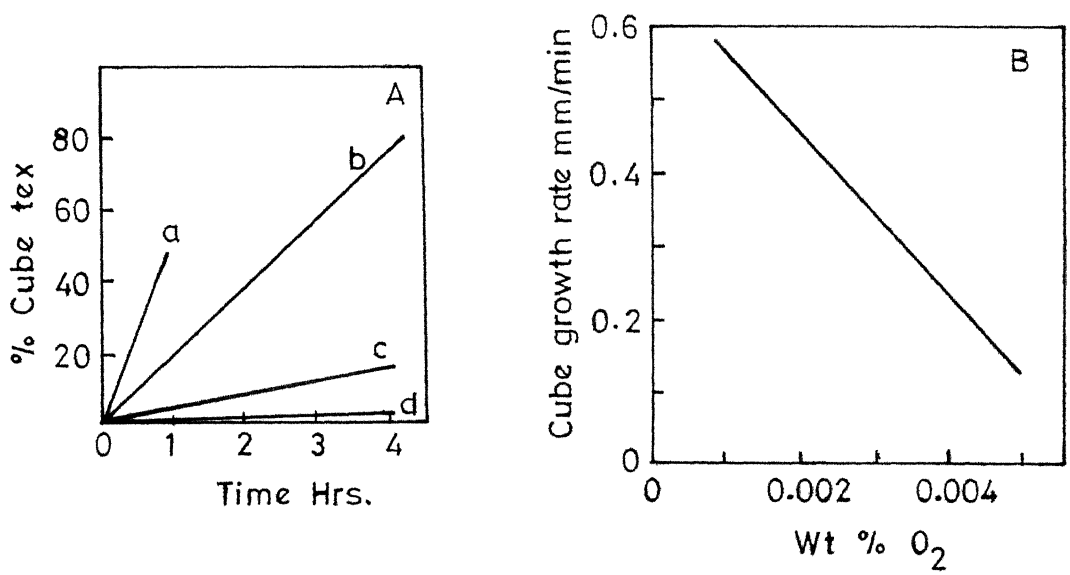
A
% Cube tex
80
60
40
20
a
b
c
d
0
1
2
3
4
Time Hrs.
B
Cube growth rate mm/min
0.6
0.4
0.2
0
0
0.002
0.004
Wt % O_2

FIG. 8

from 0.005% to 0.001% tends to produce larger size of grains and more perfect grain orientation, the growth completely stops if the nitrogen content exceeds 0.015%[31].

Dunn and coworkers[15,17,19] starting with oriented (001) [110] and (111) [112] single crystals of 3.25% Si-Fe alloy, on giving 70% reduction and subsequent annealing, showed that the production of cube on edge texture in b c c metals and alloys require the presence of either a (110) [001] or a weak (111) [112] textures in the material which developes during the primary recrystallization process.

The work on the development of cube texture in Fe-Si alloys is very limited. After Sixtus[32] first produced the texture several investigators confirmed it[33-35]. While most of the work is on commercial purity alloys, Dunn and Walters[36] produced this texture in high purity Fe-Si alloys. In either case the common feature is that the surfaces were cleaned before heat treatment. Atmosphere used varied from high vacuum to purified argon as described earlier. The experimental procedure involved heavy cold reduction followed by primary and secondary recrystallization.

The cube-on-edge texture was first produced by Goss[37] and later by many investigators[9,12,24,38]. The method usually involves hot rolling of ingots above 800°C followed by cold rolling (at room temperature[12,24] or elvated temperatures[37]), with or without intermediate annealing in the temperature range of 900-950°C for 1 to 5 mins, further cold reduction to the final size followed by primary and secondary recrystallization at constant temperatures[12] or by heating at a constant rate of heating[14].

The essential difference in the work of different investigators lies in the employment of different stages of reduction, amount of reduction, the number of intermediate annealings given before reduction to final size and choice of the recrystallization temperatures. For practical purposes, usually Fe-Si alloys are rolled into 0.014" thick sheets. In laboratory practice, many investigators have used forged ingots for hot rolling. The final reduction after intermediate annealing in many cases were more than 50%. The total reductions varied between 75%[38] and 95%[39].

The deformation and recrystallization study with a 3.5% Si-Fe alloy does not appear to have been done in the past, but a lot of work has been done with silicon content varying between 3% to 3.5%. Corcoran and Wiener[38] studied two alloys, made by melting in argon atmosphere

high purity silicon, electrolyte Mn and Fes of compositions 1) 3.4% Si, and 0.14% Mn, 0.001% S and 0.001% O_2 and 2) 3.39% Si, 0.14% Mn, 0.015% S and 0.001% O_2. They hot forged the ingots to bars of $1\frac{1}{2}$" x $1\frac{1}{2}$" size which were hot rolled to 0.1" thickness sheets at 970°C and cold rolled to a thickness of 0.025". Heat treatments for 2 mins or more were done in dry hydrogen atmosphere and for times less than 2 mins in a salt pot furnace. The cold rolled texture was found to be a strong (100) [011] texture with (111) [112] as a minor texture. Secondary recrystallization produced a strong (110) [001] texture.

May and Turnbull[42] starting with 2.84% - 3.34% Si, 0.003% - 0.006% C, 0.0% to 0.110% Mn and 0 % to 0.46% S alloys, hot forged between 1000°C - 800°C followed by hot rolling to 0.2" thickness and finally cold rolled to 0.014" thickness through two intermediate annealings at 950°C for 5 mins at 0.1" and 0.28" thickness. The primary and secondary recrystallization treatments were performed in H_2 atmosphere. The final recrystallization texture was found to be (110) [001] . Harker and Decker[24] starting with hot rolled 0.125" thick strips of composition 3.25% Si and small amounts of C, Mn S and phosphorous, cold rolled to 0.014" in two stages, intermediate anneal was given at 950°C

for 5 mins in H_2 atmosphere. They found strong (100) [011] cold-rolled texture and (110) [$\bar{0}$01] final recrystallization texture.

The available large volume of data does not give a single procedure to be followed and often gives contradictory processing methods. In view of the tremendous importance of this material and nonavailability of the exact know-how of production method which appears to be developed for each composition and other process variables, the study of grain oriented Fe-Si was undertaken. The present investigation involves the study of deformation and recrystallization characteristics of high purity 3.5% Si-Fe and commercial purity 3.5% Si-Fe alloys with a view to develope the production techni que of the right kind of textures in these alloys for possible commercial exploitation.

II FABRICATION OF EQUIPMENT

To carry out investigation on grain oriented Fe-Si alloys the facilities for controlled atmosphere melting of large amount of material and their heat treatment, quantitative texture work using X-ray diffraction methods and testing the magnetic properties are essential. Since there were only a few ready made equipment available for this work, all the required equipment had to be designed and fabricated.

A) Equipment for preparation of alloys, their forming and heat treatment:

The equipment required for this purpose were:-

1. Controlled atmosphere melting unit.
2. Alumina Crucibles.
3. Protective gas (argon) purification train.
4. Controlled atmosphere heat treatment furnace.
5. Hot forging and hot and cold rolling facilities.

Of these only a 20 KW spark gap high frequency generator, hot forging and cold rolling facilities were available. Hence all other equipment were designed and fabricated.

1. Controlled atmosphere induction melting unit:-

An induction coil, 6" O.D. x 7.5" high, suitable for use with the 20 K.W. generator was used with a one end closed vycor tube fitted with water cooled flange, ports

for evacuation, gas inlet and a sight hole. The furnace has been described in detail elsewhere(40). The complete assembly is shown in Fig. 9 .

2. Crucibles:

Since big size high purity alumina crucibles were not available, alumina crucibles of two sizes, 2" dia x 2½" long and 2.3" dia. x 5" long, were fabricated. Plaster of paris mould was used for slip casting the crucibles from a slip (p_H = 3.5) containing 99% pure Al_2O_3 powder mixed with 2.5% Na_2Co_3. The crucibles were presintered at 900°C for 3½ hours and then sintered at 1365°C and finally sintered in the induction furnace using a graphite crucible as a susceptor. Induction heating was done slowly at first to raise the temperature to 1550°C in 2½ hours and then sintered at 1650°C for 1 hour. Gas firing at 1750°C and oil firing at 1650°C was also used with only limited success.

3. Gas purification train & Heat treatment Furnaces:

Since grain orientation treatment is very much dependant on furnace atmosphere and the gas content of the material control of furnace atmosphere during melting and heat treatment, especially with regard to oxygen and nitrogen, is very essential. In order to avoid oxygen and nitrogen pick up . inert atmosphere was required for both

Fig. 9 Controlled Atmosphere High Frequency Induction Melting Furnace.

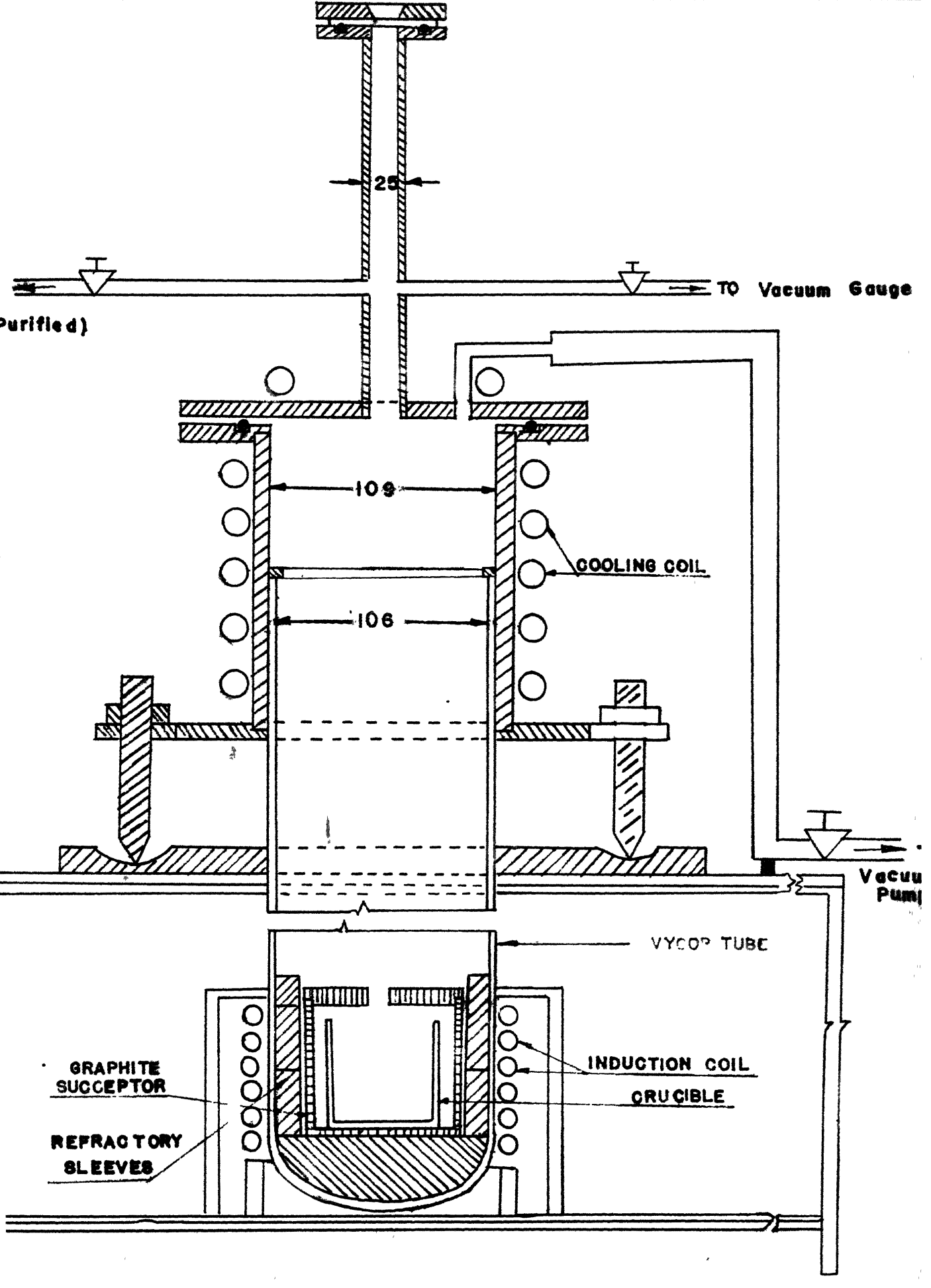

Dimensions in m.m

the purposes. Argon gas was chosen as the best available atmosphere. The available bottled argon gas normally contain small amounts of O_2, N_2 and moisture. To remove these effectively a gas purification train was made using copper-chip and Ti - Chip furnaces to remove N_2, O_2 etc. and silca gel, anhydrous fused $CaCl_2$ and P_2O_5 for removing water vapour. The schematic gas purification train layout is shown in Fig.10 .

Heat treatment furnaces:- Grain orientation treatment of pure and commercial purity Fe-Si alloys require heat treatment temperature ranging from 400°C to 1350°C. For all low temperature annealings up to 1100°C, Kanthal-A heating element of total resistance 100 ohms was used for constructing the furnace. This furnace had a provision for flushing with argon gas. The details of the furnaces for gas purification and heat treatment are described elsewhere[40]. The inter connection of the furnace and the gas train is shown in Fig.10 . On the exit side of the furnace an oil bubbler seal was used to maintain a positive pressure in the furnace tube as well as to maintain and indicate a desired flow rate of gas. The gas purification train and the annealing furnace were mounted on a four-wheeled trolley so that the whole set could be easily transported from the melting site to the forming site.

Vacuum annealing furnaces:- The argon gas annealing furnace described above was found satisfactory for heat

treatment of thick specimens. In spite of purification of argon gas some surface oxidation was found to occur possibly due to (1) siliminite furnace tube (Indian made) not being perfectly impervious to gases (2) the impurity content of the argon gas (O_2, N_2 and H_2O vapour) which varied considerably from cylinder to cylinder. Since the purification system had a limited capacity it could not function, due to large variations in impurities in the gas, properly. Since annealing of thin specimens were involved in the subsequent work, two vacuum annealing furnaces were constructed. One resistance heating furnace (resistance 60 ohms) with a 1" dia. vycor heat treatment tube was set up for primary recrystallization of specimen. This furnace could go up to a temperature of 1000°C. The other furnace, a Globar tube furnace provided with an imported, impervious, one end closed sillimanite tube (of 2.3" internal dia), which could go up to 1350°C, was used for secondary recrystallization. The open end of the heat treatment tubes were fitted with water cooled brass flanges and with provisions for introducing specimen without breaking vacuum and argon gas flushing. An ultimate vacuum of 40-50 μ of Hg could be achieved through the use of a single stage mechanical pump. With the specimen charging device a stainless steel boat containing Ti chips was attached so that it entered the hot zone first and took care of the traces of O_2 and N_2 in the heat treatment tube. The schematic drawing is shown in Fig. 11 . Specimens as thin as 0.003" could be

annealed in the furnace without any oxidation.

4. Rolling facility:

Hot rolls:- Two alloy steel rolls were forged and heat treated (normalised) at the Ordenance Factory, Kanpur and machined to size (Fig.12). The hardness of the roll surface was Rockwell C 30.

Adjustable Guide:- Since a texture is developed during cold rolling and changes its characteristics if rolling direction vary, an adjustable guide (Fig.13) was fabricated to eliminate accidental rotation of the small specimens during feeding into the rolls.

B) Equipment for texture study:

Texture Goniometer:- If X-ray diffraction pattern of a textured sheet specimen, initially mounted perpendicular to the incident beam with rolling direction vertical, is taken by a transmission pin hole camera, the resulting photograph will contain discontinuous Debye rings and the pattern will be symmetrical about the vertical line (rolling direction) through the centre of the film. However, if the sheet is now rotated around the rolling direction and another photograph is taken, the diffraction pattern will show change in the position and intensity of the streaks on the Debye rings. This is due to the fact that the difference in the number of favourably oriented grains cause change in the intensity

Fig. 10 Gas Purification Train and
Heat Treatment Furnace Interconnection.

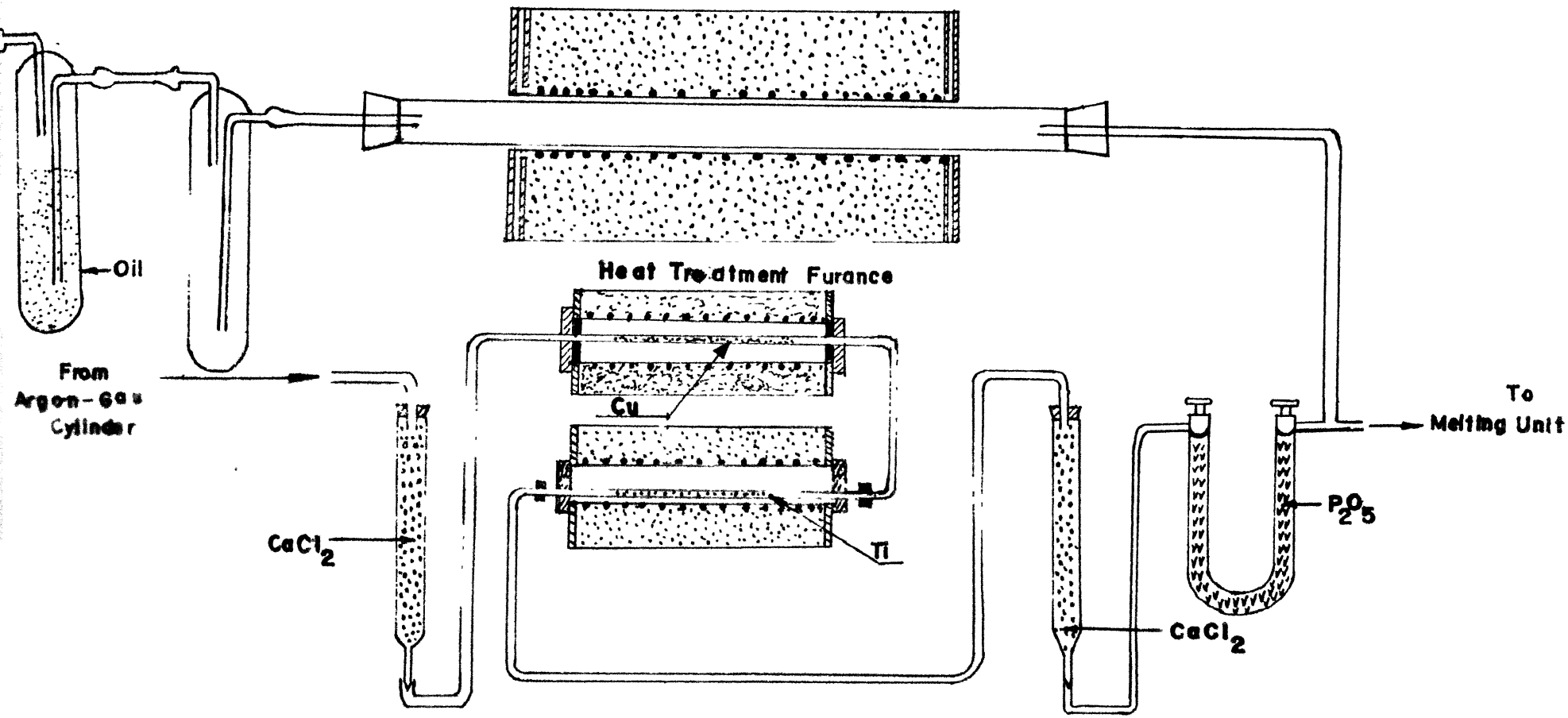
Oil
From
Argon-Gas
Cylinder
Heat Treatment Furance
Cu
Ti
$CaCl_2$
$CaCl_2$
P_2O_5
To
Melting Unit

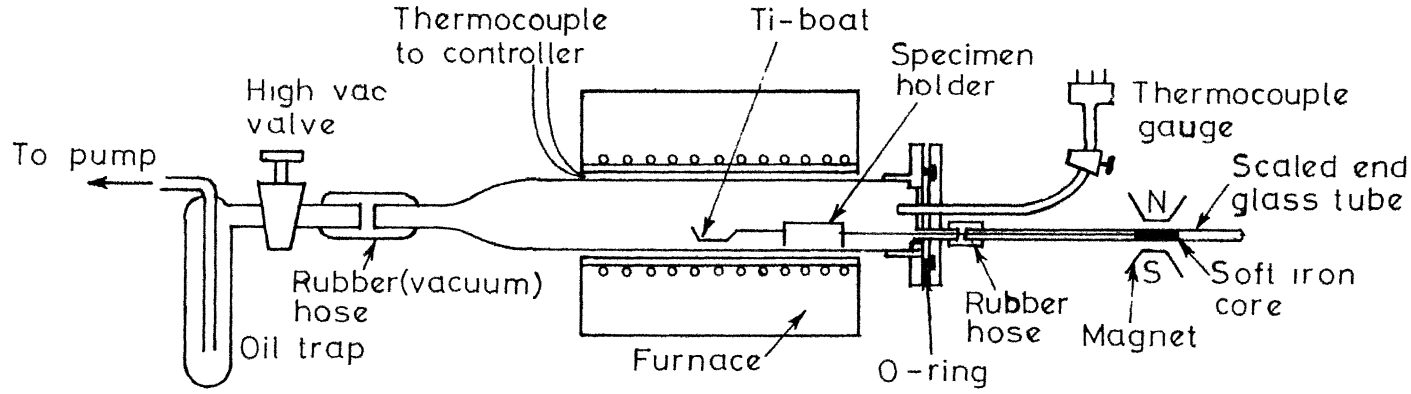

Fig.11 Vacuum annealing furnace

Fig. 12 Forged hot roll dimension

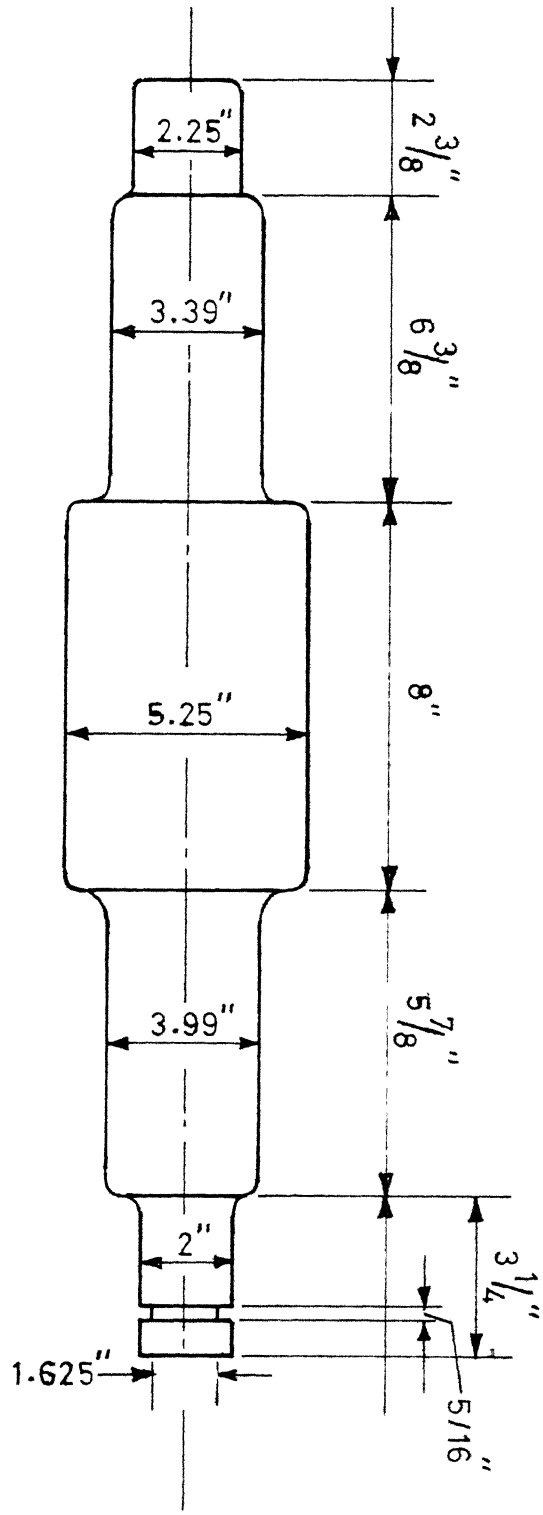
2.25"
2 3/8"
3.39"
6 3/8"
5.25"
8"
3.99"
5 7/8"
2"
3 1/4"
1.625"
5/16"

Fig. 13 Guide for cold rolling operation

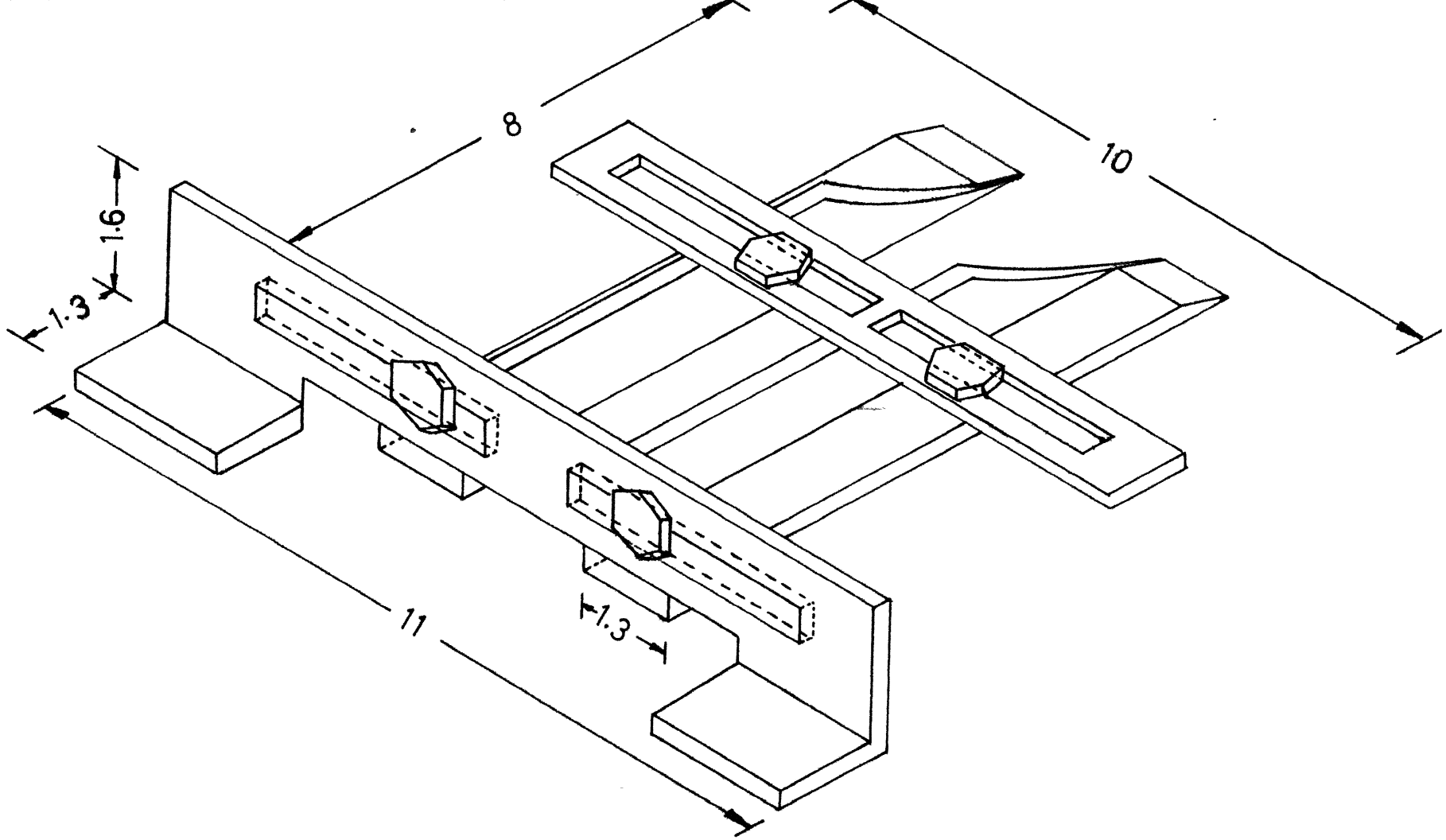

FIG.13. ISOMETRIC VIEW OF THE GUIDE

Dimensions In Inches

and the positional change is due to the difference in the degree of randomness. To determine the complete texture of sheet, it is therefore necessary to measure the distribution of orientation about the rolling direction by taking several diffraction patterns with the sheet normal at various angles to the incident beam. Since the photographic method gives only qualitative information, in recent years methods have been developed for the determination of texture with diffractometer which are capable of quite high precision. Since in a diffractometer only a small portion of the Debye ring is interepted by the fixed counter, the measurement of intensity variation along a whole Debye ring requires specimen rotations around several axes. This is achieved by a specially designed goniometer. There are two types of goniometers - 1) reflection type goniometer and 2) transmission type goniometer. The geometry of both of these techniques are shown in Figs.14 &15, respectively. Either one of them is not suitable for complete texture determination, because of the absorption characteristics of the specimen, the design of the goniometers and the characteristics of the diffractometer geometry. If the pole figure is drawn with normal direction as the pole of the projection, then the transmission method is able to produce texture data between 90° (at the periphery) to 50° in the pole figure diagram, whereas the reflection type produces pole figures between 0° (centre of pole figure) to 70°.

Fig. 14 Ideal specimen geometry in a Sculz type texture Goniometer.

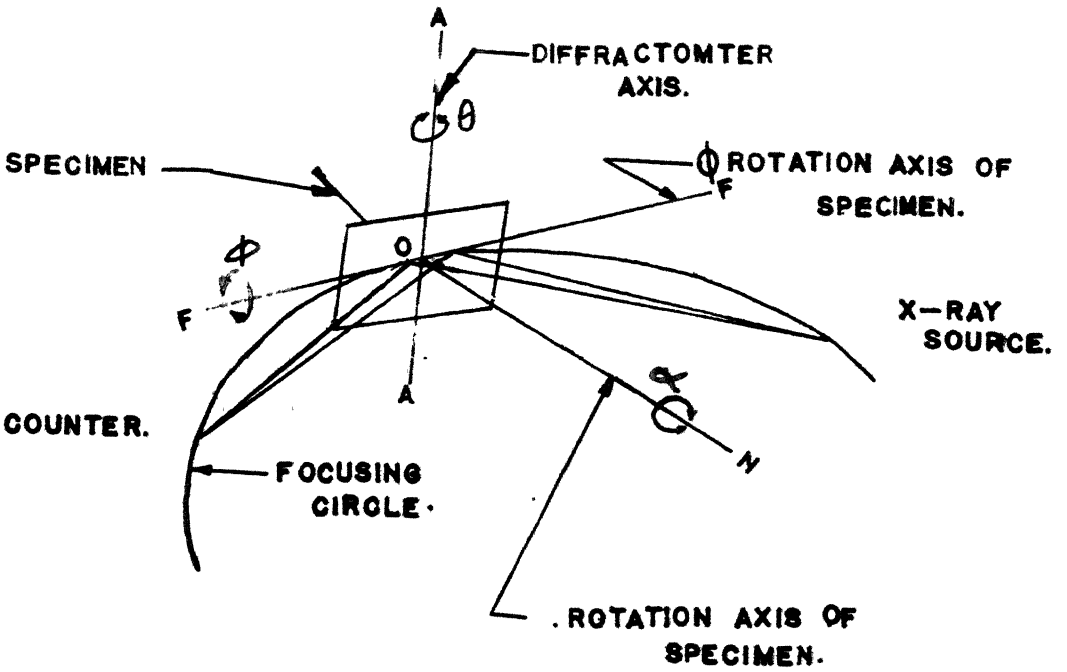

FIG.14. IDEAL SPECIMEN WITH RESPECT TO DIFFRACTOMETER. SPECIMEN SHOWN WITH $\phi = 0$, I.E. PLANE OF SPECIMEN IS PERPENDICULER TO THE PLANE OF FOCUSING CIRCLE.

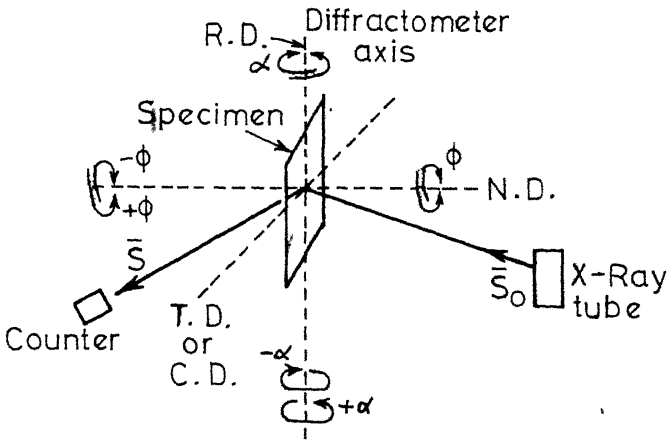

Fig. 15. Diffractometer geometry for transmission technique. The positions of rolling direction (R D) Transverse or cross direction (T.D. or C D) and normal direction (N D) correspond to $\alpha = 0$ and $\phi = 0$

The reflection technique does not require any intensity correction due to the specimen absorption, as is required in case of transmission technique. Moreover, specimen preparation for transmission technique is very laborious.

Considering all these facts, it was thought that texture study will be done by using Sculz reflection type goniometer. Since this goniometer was not available in the laboratory, a reflection type goniometer was designed and fabricated. The goniometer could use 1" x 1" flat specimens and an intensity integration provision was made for oscillation of specimen in its own plane.

Preliminary trials were made with powdered NaCl and 300 mesh Fe powder seived from coarse iron powder. Idealy the variation of the measured intensity (Im) with α (Fig.14) rotation should show no variation in intensity up to $\alpha = 40^{\circ}$. However, the test results indicated a rather sharp drop in intensity within few degrees. The reason for this was traced to fabrication defect ; difficulty in keeping the specimen stage in alignment with the X-ray beam & because specimen translation was not smooth.

Since there was no simple way of rectifying the defect and realising that the alignment will be easier for transmission technique, the goniometer was changed into a transmission type of goniometer. The specimen stage

was redesigned for operation on the same track where reflection stage was supposed to operate. The transmission stage has a 7/8" x 3/4" opening for fixing a thin specimen and to serve as a window for x-rays . The mechanical drive designed for specimen oscillation was a rack and pinion arrangement driven by a specially designed gear which was rotated by a 1 rpm reversing synchronous motor. The gear required special teeth profile. Since such profile cutters were not available gear teeth shaping was done by hand filing which obviously did not produce the right kind of profile. As a result of this the mechanical drive did not work satisfactorily. The mechanical oscillation mechanism was replaced by a simple rack and pinion arrangement driven by an electrically reversing synchronous motor. The circuit diagram for drive motor reversal is shown in Fig.16 . With this arrangement and with a 1 rpm synchronous motor the specimen stage could be oscillated without any difficulty. However, this method restricted the use of higher rpm motors.

(C) Testing of transmission texture goniometer. Decker, Harker and Asp[41] have shown the nature of the variation of measured intensity (Im) with α using a random sample, Ag Br in X-ray film. In order to check the performance of the fabricated goniometer, a similar test was performed using Kodak no screen X-ray film, the data of which, together with the data of Decker, Harker and Asp, is shown in Fig.17. That the intensity does not

change with change in ϕ was also varified. A similar data for variation of intensity with α and ϕ (Fig.18) was obtained for a 3.5% Si-Fe alloy random sample prepared with 300 mesh filed and vacuum annealed powder. To prepare the random specimen of 3.5% Si-Fe alloy, a perspex specimen holder 1" x 7/8" x 0.005" was prepared. The annealed powder mixed with Crylon spray was tapped in the shallow groove (0.005") in the specimen holder and properly levelled off using a clean glass slide. The spray dried quickly leaving a 0.005" thick powder layer firmly attached in the specimen holder. The whole assemply was used as the specimen. The thin perspex sheet beneath the specimen did not cause any difficulty in the calibration.

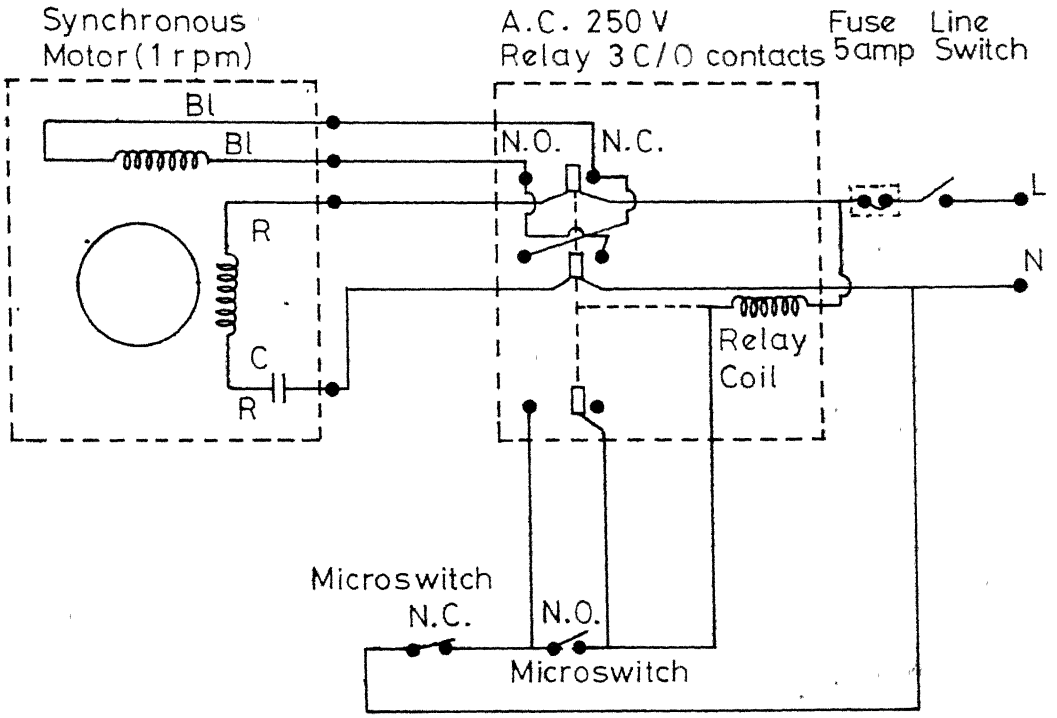

Note Motor shaft operates N.C. & N.C. microswitches for reversing operation

Fig.16 Electrical circuit for reversing synchronous motor for specimen oscillation

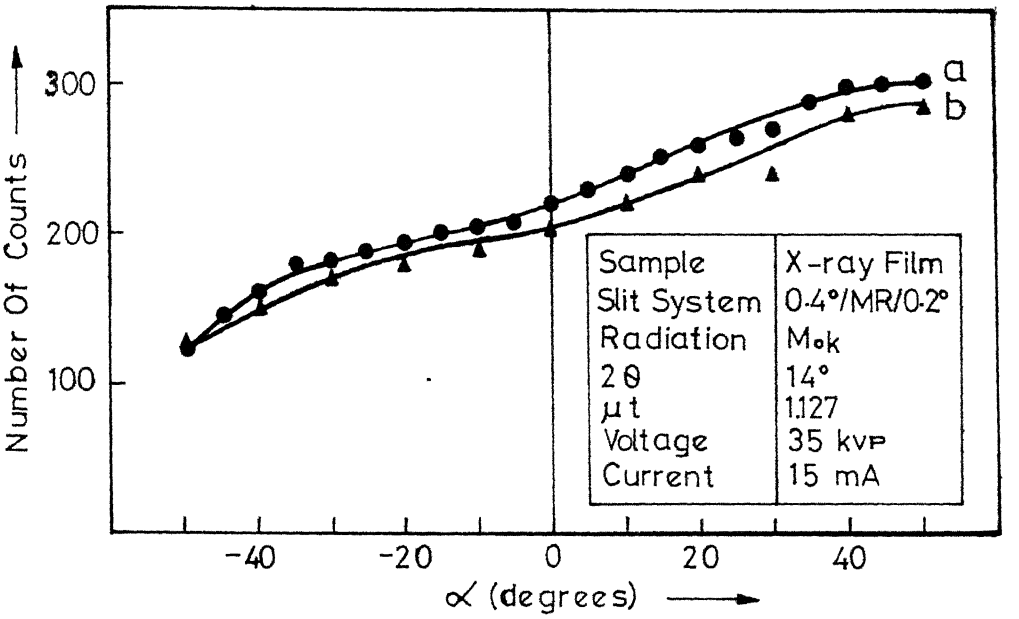

FIG 17(a). Variation Of I Measured With ∝ For X-ray Film. (a) Present Work b) Data By Decker etal

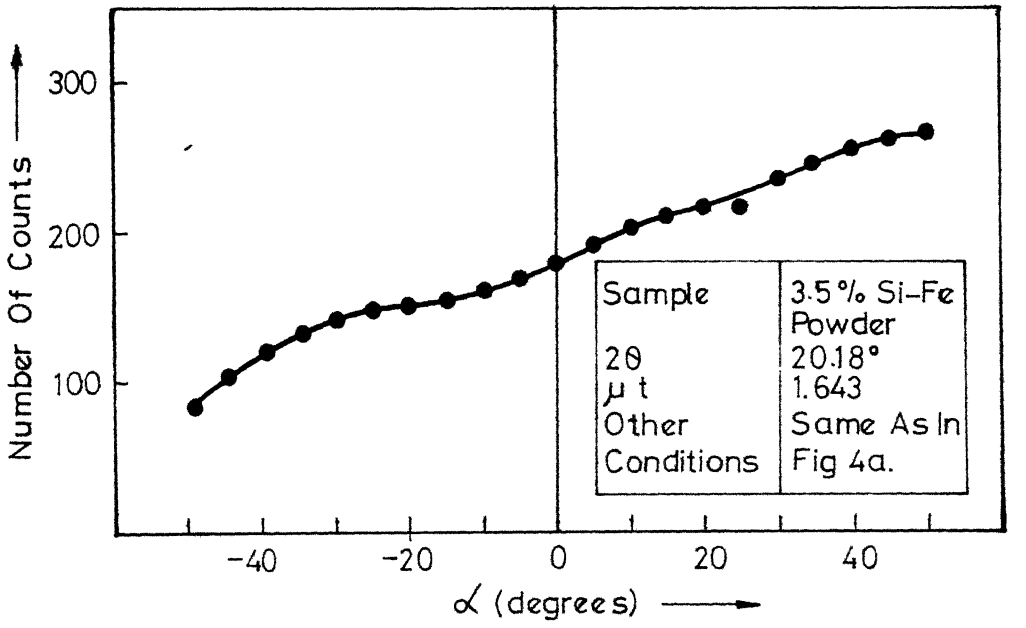

FIG 18(a). Variation Of I Measured With ∝ For 3.5% Si-Fe Random Sample

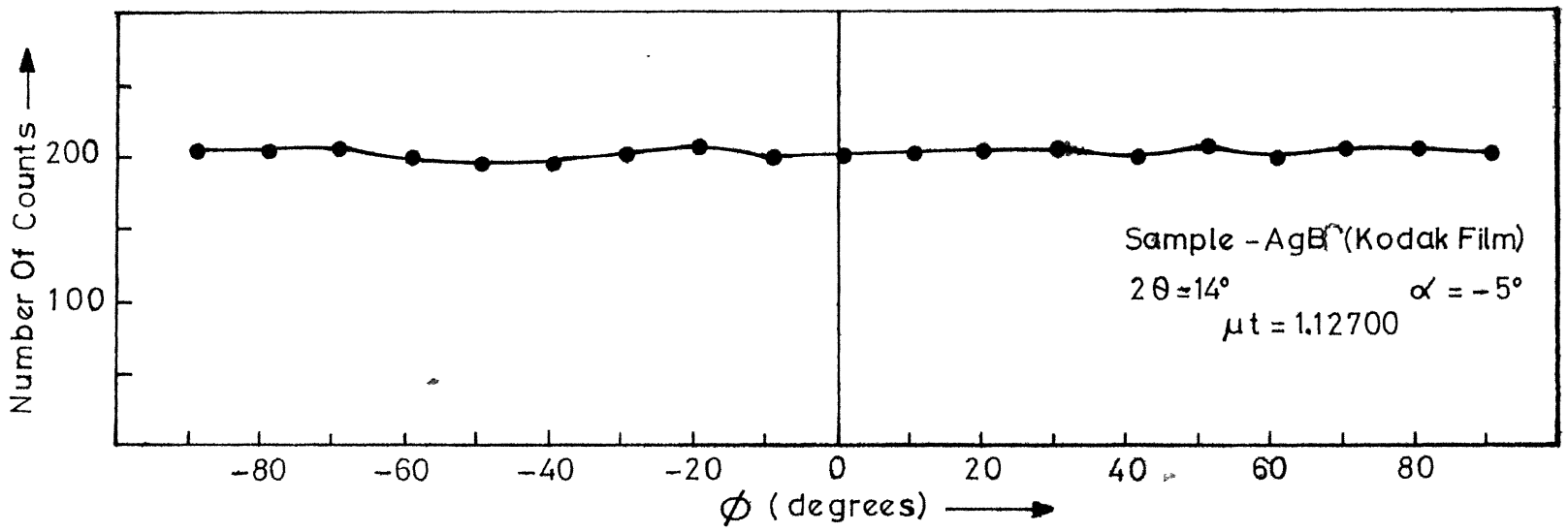

FIG 17b. Variation Of I Measured With φ For X-ray Film

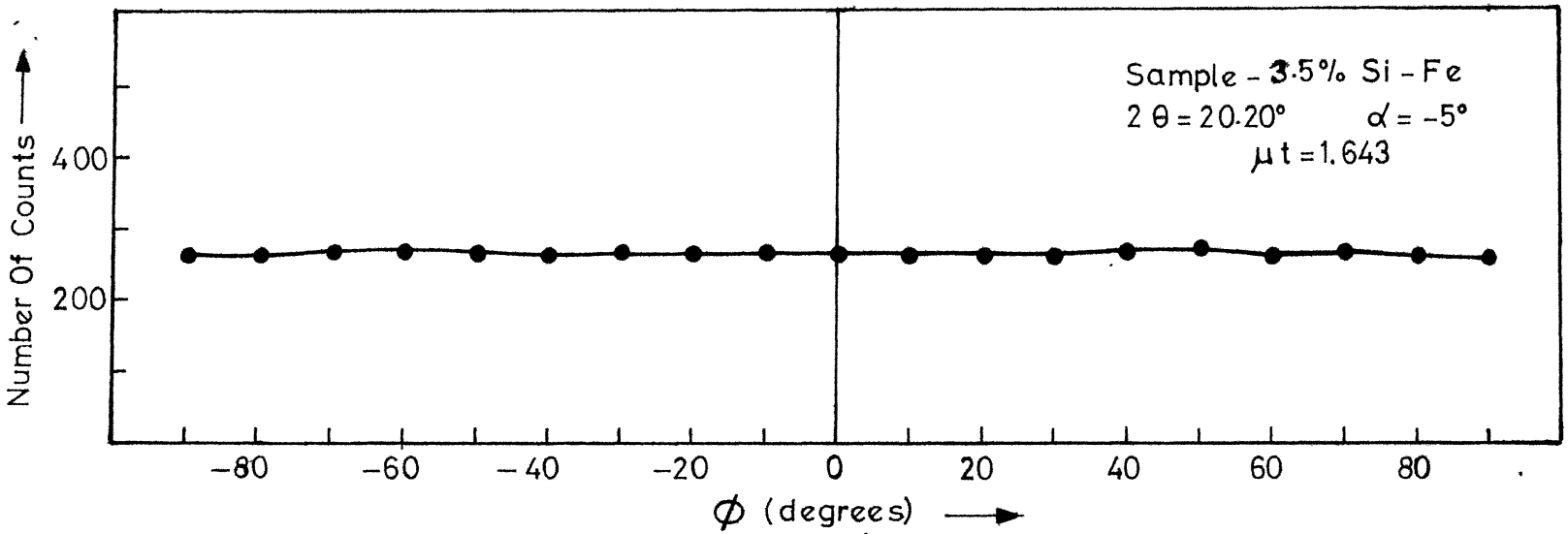

FIG 18 b. Variation Of I Measured With φ For 3.5% Si-Fe Random Sample

Fig. Transmission Goniometer Fitted on Deffractometer

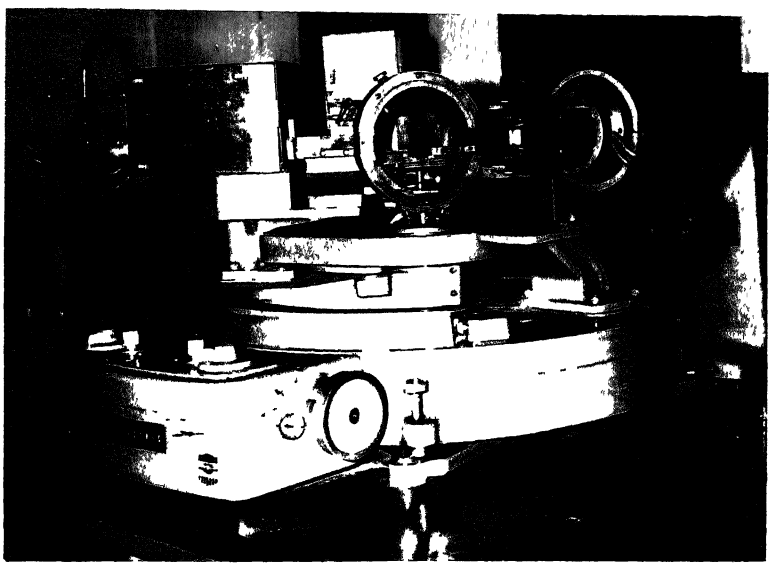

III EXPERIMENTAL PROCEDURE

A. MAKING, SHAPING AND HEAT TREATMENT OF Fe-Si ALLOYS

The grain orientation study with Fe-Si alloys was made with two alloy compositions, namely, high purity 3.5% Si-Fe and commercial purity 3.5% Si-Fe. The alloy preparation involved melting and homogenisation, forging, rolling and annealing.

1) Melting & homogenisation of alloys: Two alloys each containing 3.5% Si were prepared by melting together 1) High purity electrolytic iron and pure silicon of 99.9% purity supplied by Semi Elements Incorporated, New York, and 2) pure silicon and commercial purity low carbon steel. The composition of the commercial purity low carbon steel was .029% C, 0.21% Mn 0.025% P, 1.58% Si and 0.027% S and was supplied by Rourkela Steel Plant, Rourkela. 664 gms of high purity and 800 gms of commercial purity alloys were induction melted in alumina crucibles under a protective atmosphere of purified argon gas. The furnace chamber was evacuated to a vacuum of about 20 microns of Hg before flushing with argon and the process was repeated twice to remove all air from the furnace chamber. The molten alloys were allowed to solidify, cool down in the furnace to about 1150°C and annealed at this temperature for 2 hours for composition homogenisation and finally cooled down to room temperature. The total melting losses amounted to 0.3% and 0.4% for the high purity and commercial purity alloys, respectively. The ingots obtained were approximately 2" dia x 1½" long

(pure alloy) and 2.3" dia x 4" long (commercial purity alloy).

The ingot surfaces were ground on a grinding wheel to remove small blow holes. A bigger blow hole, about 1/8" deep, formed at the bottom of the commercial purity alloy and was eliminated by machining.

1) Forging of homogenised alloys:- The ingots were heated to a temperature about 1200°C in a Globar muffle furnace and cast structures of the ingots were broken down by hot forging in the temperature range of 1150°C - 900°C. The forged pieces were made in suitable sizes, the high purity alloy was forged to a 9.2" x $1\frac{1}{8}$" x $\frac{1}{2}$" size flat & the commercial purity alloy was forged into two $7\frac{1}{2}$" x $1\frac{1}{8}$" x 0.47" flats, to suit subsequent rolling operation. The forged flats were cleaned on coarse emery paper. The high purity alloy flat was cut into six pieces of about $1\frac{1}{2}$" x $1\frac{1}{8}$" x $\frac{1}{2}$" size. The commercial purity flats were cut into two sizes i) $1\frac{1}{2}$" x $1\frac{1}{8}$" x 0.47" and ii) 2.5" x $1\frac{1}{8}$" x 0.47".

3.) Solution treatment and aging of commercial purity alloy.

Grain stability of commercial purity alloy requires proper distribution of inclusions before giving any treatment. This is important for primary grain growth inhibition which is necessary for ensuring secondary recrystallization. In order to find out the distribution of inclusions, a piece of hot forged commercial alloy

was polished and investigated metallographically at 500 magnification. The as polished specimen microstructure (Fig.19) showed a non uniform distribution of inclusions and inclusion sizes were large. In order to achieve uniform dispersion of inclusion in the matrix, five samples were cut from the forged sample and annealed at 1350°C for ½ hour, 1 hour, 2 hours & 2½ hours respectively and then directly quenched in a bath of ice cold brine. Metallographic examination showed that a solution treatment at 1350°C for 1½ hours (Fig.20) took about 40-45% impurities in solution. For determining aging time at 1000°C, to obtain best distributions of inclusions, five more samples were cut from hot forged flat, solution treated at 1350°C for 1½ hour and aged at 1000°C for ½ hour, 1½hour, 2 hours, 2½hours, 3 hours. It was found that an aging treatment of 2½ hours (Fig.21) gave a fairly uniform distribution of inclusions. In view of these observations, the two commercial purity forged samples were given solution and aging treatment at 1350°C for 1½ hour, and 1000°C for 2½ hours, respectively, in purified argon atmosphere.

4) Hot Rolling: Hot rolling of forged high purity alloy and forged, solution treated and aged commercial purity alloy specimens were carried out in the temperature range of 1150°C - 900°C. All high purity samples and one commercial purity alloy sample (specimen I, 1½" x 1$\frac{1"}{8}$ x 0.47" size) were hot rolled lengthwise whereas

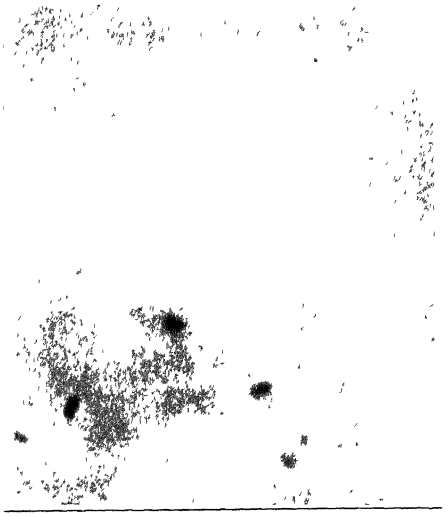

Fig. 19 Commercial purity 3.5% Si-Fe alloy (A_{Comm}). Hot forged
500 X

Fig. 20 Commercial purity 3.5% Si-Fe alloy (A_{Comm}). Hot forged and solution treated at 1350°C for 1½ hrs
500 X

Fig. 21 Commercial qurity 3.5% Si-Fe alloy (A_{Comm}). Hot forged, solution treated at 1350°C for 1½ hrs and aged at 1000°C for 2½hrs
500 X

the other commercial purity sample was hot rolled widthwise (sepcimen II). The specimens were heated to 950°C in controlled atmosphere (argon) furnace and then heated to 1200°C in a "Globar" rod muffle furnace so as to keep the hot specimen for minimum time in air thereby avoiding large scale oxidation. During rolling the specimen temperature was measured by a surface pyrometer. The reduction in the first pass was invariably higher (thickness reduced by about 0.030") and all subsequent reductions per pass were about 0.020". The final hot rolled nominal thickness of the high purity samples were either 0.2" or 0.1", whereas the commercial purity samples were hot rolled to about 0.1" thickness. The thickness of all the hot rolled products are given in Tables I_A and II_A.

The high purity sample on analysis using vacuum fusion technique available at N.M.L., Jamshedpur showed O_2 and N_2 contents 0.006% and 0.007%, respectively.

e) Cold rolling and intermediate annealing:- The hot rolled samples were cleaned on coarse emery paper before further heat treatment to remove very thin oxide layer formed during hot rolling. The hot rolled high purity samples were cut into two or three parts. The commercial purity sample hot rolled lengthwise was cut into two parts and designated as A_{comm} and B_{comm}. Trial runs on both these alloys indicated that these

alloys tend to crack when cold rolled at room temperature. Hence the alloys were warm cold rolled (37) in the temperature range of 400°-200°C. The 0.2" and 0.1" thick specimens of high purity alloys were cold rolled to 0.1" and 0.035", respectively. At this stage only a few specimens were given an intermediate anneal at 950°C for 5 mins. in purified argon atmosphere and finally cold rolled to about 0.014". All other specimens were cold rolled to the final thickness of 0.017" without any intermediate annealing.

One part of the commercial purity specimen I (designated A_{Comm}) was cold-rolled directly to the final thickness 0.012" and another part of the same specimen (designated B_{Comm}) was cold rolled to an intermediate thickness of 0.030", annealed at 950°C for 5 mins. and finally cold rolled to 0.012" thickness.

The reduction to final size was done through a number of cold rolling passes in order to maintain the cold rolling temperature. Only 2-3 passes were allowed between two reheatings. The reduction in first pass was invariably higher, about 0.015", whereas in the subsequent passes the reduction varied between 0.005" to 0.010" depending on whether two or three passes were given in one stage of reduction before reheating.

HEAT TREATMENT OF ALLOYS:-

1) Matrix Stabilization:- Matrix stabilization is essential to ensure secondary recrystalization. To have matrix stability in thin high purity Fe-Si alloy sheet the grain size should be about one to two times the sample thickness.[11] In order to find the time and temperature suitable for producing this condition few metallographic samples were cut from cold rolled product of about 0.014" and thinned down to about 0.004". Specimen D_a (TableIII) was given vacuum annealing (about 50 μ of Hg) at 775°C for ½ hour, 1 hour, 1½ hours, 2 hours, 2½ hours and 3 hours, polished (after mounting in bakelite), etched and grain size was determined by comparing with ASTM grain size chart. The absolute value of average grain size was determined from these grain size (TableIII). Since the annealing time found suitable (3 hours) was too large and there was possibility of oxidation of the thin specimens, specimens were annealed at 980°C for 15 to 20 mins. It produced sufficiently large grain size comparable with those annealed at 775°C for longer periods of time (Fig.22). Hence the latter temperature and time conditions were used in the subsequent work.

Table III - Grain size produced in thin 3.5% Si-Fe alloy as a result of annealing at different time and temperature.

Specimen	Specimen thickness in inches	Annealing Temp. °C	Annealing Time Hrs.	Average Gr. Size ASTM size	Average Gr. Size Gr. diameter in inches
	0.003	775	½	8	0.001
	0.003	775	¾	8	0.001
	0.003	775	1	8	0.0014
D	0.003	775	1½	7	0.002
	0.003	775	2	6	0.0028
	0.003	775	2¼	5	0.0038
	0.003	775	3	4	0.0057
	0.003	775	3½	4	0.0057
A	0.003	950	15 mins	2	0.008
E	0.003	950	15 mins	2	0.008

I. I. T. KANPUR
CENTRAL LIBRARY
15896

Fig. 22(a) High purity 3.5% Si-Fe alloy (D_a) annealed at 750°C for 1 hr 100 X

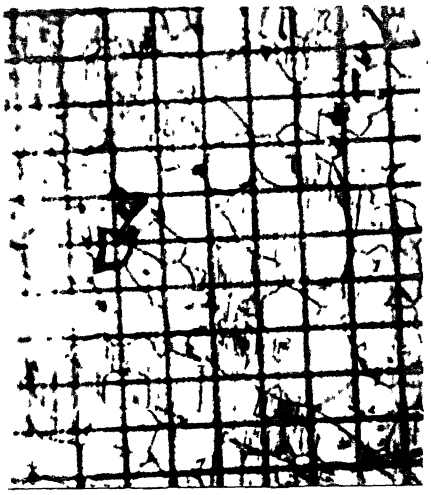

Fig. 22(b) High purity 3.5% Si-Fe alloy (D_a) annealed at 750°C for 2 hrs 100 X

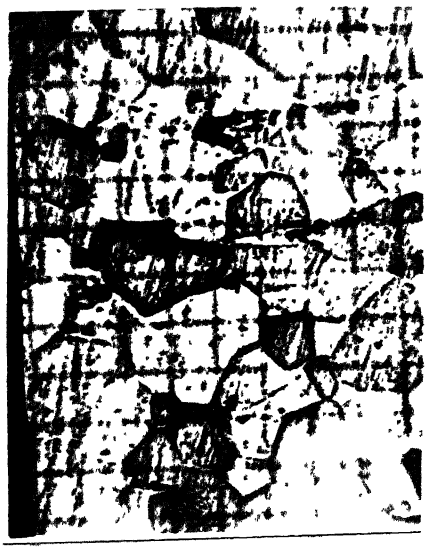

Fig. 22(c) High purity 3.5% Si-Fe alloy (D_a) annealed at 750°C for 3 hrs 100 X

Fig. 22(d) High purity 3.5% Si-Fe alloy (A_a) annealed at 950°C for 15 mins 100 X

2) Primary Recrystallization: The cold rolled high purity and commercial purity samples were cut into specimens 1.25" long x $1\frac{1}{8}$" wide. Two specimens of D_a were primary recrystallized at 775°C for $2\frac{1}{2}$ hours in purified argon atmosphere. The other specimens were thinned down to about 0.004" and given a primary recrystallization treatment in vacuum of about 50 microns of Hg at temperatures varying from 950°C - 980°C for 15-20 mins. The details of the treatment given to the specimen are shown in Table I_B.

A few commercial purity specimens of both A_{Comm} and B_{Comm} were thinned down to about 0.004" and recrystallized at 750°C for 2 hours and a few specimens of these samples, without thinning, were recrystallized at 750°C for 2 hours in vacuum of 40 microns of Hg.

3) Secondary recrystallization: All high purity specimens were recrystallized at 1150°C-1200°C for 2-10 mins. in vacuum of about 50 microns of Hg. The two primary recrystallized specimens (specimen D_a) were secondary recrystallized, one at 1050°C for $3\frac{3}{4}$ hours and the other at 1100°C for 4 hours in a purified argon gas atmosphere.

Commercial purity thinned and primary recrystallized specimen were secondary recrystallized at 1150°C for 5-10 mins. Two thick samples (0.012") of A_{comm} and B_{comm} , primary recrystallized at 750°C for 2 hours, were secondary recrystallized at 1150°C

for 4 hours in vacuum of the order of 50 microns of Hg, and two other similar specimens each from A_{Comm} and B_{Comm}, were secondary recrystallized in purified argon gas atmosphere at 1150°C for 4 hours. In the latter case before flushing argon a vacuum of the order of 60 microns of Hg was achieved in the heat treatment tube.

B) SPECIMEN THINNING:

The accurate determination of texture by transmission method requires thin specimens so that the value of μt (where μ = linear absorption coefficient and t is thickness of the sample) is about one. This required specimens of thickness ranging from 0.003" to 0.004". Preparation of specimens of .003" thickness, uniform over a whole area of 1" x 1" is difficult and hence considerable experimentation had to be done. Careful mechanical polishing was tried first, but the main draw back of this procedure was that it was too time consuming, laborious, and the final thickness achieved was invariably quite large, about 0.008". For quicker means of specimen thinning from about 0.014" to 0.003", both chemical and electrolytic etching methods were tried. The electrolytic etching set up was made by fixing two parallel stainless steel cathodes at a distance of 2" from each other and the specimen to be thinned, the anode, was placed between them at a distance

of 1" from the cathodes. Several solutions were tried for chemical and electrolytical thinning and their respective effects are tabulated in Table IV_A and IV_B The best solution for cold rolled specimen was fresh etchant E for thinning directly from about 0.014" to 0.002". The same solution, however, was found unsuitable for producing very thin specimen out of recrystallized samples; the smallest thickness that could be produced without producing pits and holes was 0.005". The etchant E kept for a long time, however, was suitable for thinning down commercial purity alloy samples directly from 0.012" to 0.003". The rate of reaction was, however, reasonably slow.

For the texture investigation the procedure adopted for thinning the cold-rolled and recrystallized samples were,

1) Cold rolled samples of both high purity and commercial purity alloys :- chemical thinning by etchant E to the final size.

2) Recrystallized samples:

a) High purity specimens were thinned down to 0.005" by solution E, followed by careful

TABLE IV_A

Electrolytic thinning solutions used and their Characteristics

No.	Composition of Electrolyte	Electrothinning conditions: Current density amp/sq.cm.	Electrothinning conditions: Voltage Volts	Performance and characteristics
A	Chromic Acid 100 gms/lit of H_2O	6-8	10-12	Very slow reaction, heavy cathode corrosion, localized pit formation in specimen
B	Citric Acid 10gm/lit of H_2O Nacl 100gm/lit of H_2O Hcl Few Ml.	8-10	10-13	Fast reaction, very rapid reaction at the specimens edges. Cold rolled specimens are of uniform thickness(except for the edges) and without pits. Pits form in recrystallized specimens.
C	HNO_3 10ml HF 20ml Glycerol 20-40 ml	7-12	5-11	Fast reaction, localized pit formation in specimen.

TABLE IV_B

Chemical thinning solution used and their characteristics

No.	Solution	Performance and characteristics
D	HNO_3 5ml Alcohol 100ml	Very slow reaction, composition change rapidly due to evaporation of alcohol, suitable for removal of small amount of material from both cold rolled and recrystallized specimens.
E	HNO_3 30ml Acetic Acid 10ml HCl 30ml H_2O 30ml	Very fast reaction, uniform thinning of specimen all over, no preferential reaction at the specimen edges. No pit formation for cold rolled specimen even down to specimen thickness of 0.002", pits form in recrystallized specimen of thickness 0.005".

mechanical polishing to 0.030" and followed by etching chemically with etchant A.

b) The commercial purity alloy samples were chemically thinned by aged etchant E to 0.030".

(C) TEXTURE DETERMINATION:

Texture determination involved:

1) Determination of $\theta_{(hkl)}$
2) Determination of μt of each specimen.
3) Determination of Intensity correction factor.
4) Measurement of intensity data and plotting the pole figure.

1) Determination of θ_{hkl}: Since (110) reflection was chosen for texture work for both high purity and commercial purity specimens, $\theta_{(110)}$ was determined by powder diffraction technique. The high purity alloy powder was prepared by filing with a jeweller's file and annealed at 800°C for 2 hours in an evacuated and sealed silica capsule. A specimen for back reflection focussing camera was prepared using the annealed powder. The highest angle reflection of the diffraction pattern was used for the lattice parameter determination.

Mo radiation was used for this purpose. The lattice parameter determined gave the $2\theta_{(110)}$ to be 19.95°. For the commercial purity alloy the Bragg angle was determined by the diffractometer and $2\theta_{(110)}$ was found to be 20.05°.

1) Determination of μt: The value of μt for each specimen is required for the evaluation of the corresponding correction factor R. μt of specimens was determined by using a strong diffracted beam from a Parmaquartz specimen ($2\theta = 12.15^{\circ}$) and measuring the intensity of diffracted beam with and without the specimen in the path of the diffracted x-ray beam. Then using the general absorption equations,

$$I_t = I_o \, \bar{e}^{\mu t} \qquad \ldots(1)$$

where I_o and I_t are the intensities of incident and transmitted X-rays respectively, μ is the linear absorption coefficient and t is the specimen thickness, the μt was determined.

2) Determination of correction factor: In the transmission technique of texture determination, as the specimen is rotated, the path length as well as the diffracting volume vary. Therefore, the measured intensity requires correction so that the intensities for the different orientations of the specimen can be compared with each other. Theoretical calculations

of the correction factor has been made by Decker, Harker and Asp[41] which is given as:

$$I_c = I_m \; R.$$

where

$$R = I_{o/I\pm\alpha} = \frac{\mu t}{\cos\theta} \exp[-\mu t \cos\theta] \; x$$

$$\frac{[\cos(\theta\pm\alpha)/\cos(\theta \mp \alpha)] - 1}{\exp\left[\frac{-\mu t}{\cos(\theta\pm\alpha)}\right] - \exp\left[\frac{-\mu t}{\cos(\theta_{\mp}\alpha)}\right]} \qquad \ldots(2)$$

(+) sign is for anticlockwise rotation of α from zero position.

(-) sign is for clockwise rotation of α from zero position and

I_c = $I_{(corrected)}$

I_m = $I_{(measured)}$

θ = Bragg angle for (hkl) plane used for texture work.

α = rotation of specimen around the diffractometer axis.

μ = Linear absorption coefficient.

t = Specimen thickness.

The value of R (for $\mp\alpha$) were calculated (Appendix I) using IBM 7044 digital computer for variable μt and variable α (from 5^o to 50^o) using $\theta_{(110)}$ determined experimentally. Since the difference between the $2\theta_{(110)}$ values of high purity and commercial purity alloys was very small and is not expected to show large change in the value of R, so the calculated values

of R for high purity alloy specimens were also applied to the commercial purity alloy specimens. R as a function of μt for constant α and R as a function of α for constant μt have been plotted in Figs 23 to 25, so that the extrapolation of the data for intermediate values of μt could be easily made.

4) Measurement of intensity data and plotting of pole figures: For a given Fe-Si specimen, the counter was fixed at the correct $2\theta_{(110)}$ to receive the diffracted beam corresponding to the (110) reflection and the specimen in the goniometer was positioned initially with the rolling direction vertical i.e., coincident with the diffractometer axis, and with the plane of the specimen bisecting the angle between the incident (So) and diffracted (S) beams (Fig.15). This corresponds to $\alpha = 0^{\circ}$ and $\phi = 0^{\circ}$. For obtaining good intensity and less of scatter the diffractometer conditions found most suitable were the following:

Slit at the source - 1°MR Sollar Slit.

Slit at the Counter - 0.2° and MR Sollar Slit

Counter:- Scientillation counter (Counting efficiency 100% for Mo radiation).

Voltage - 35 Kv.

Milliamperes - 15 MA.

Preset time - 100 Seconds.

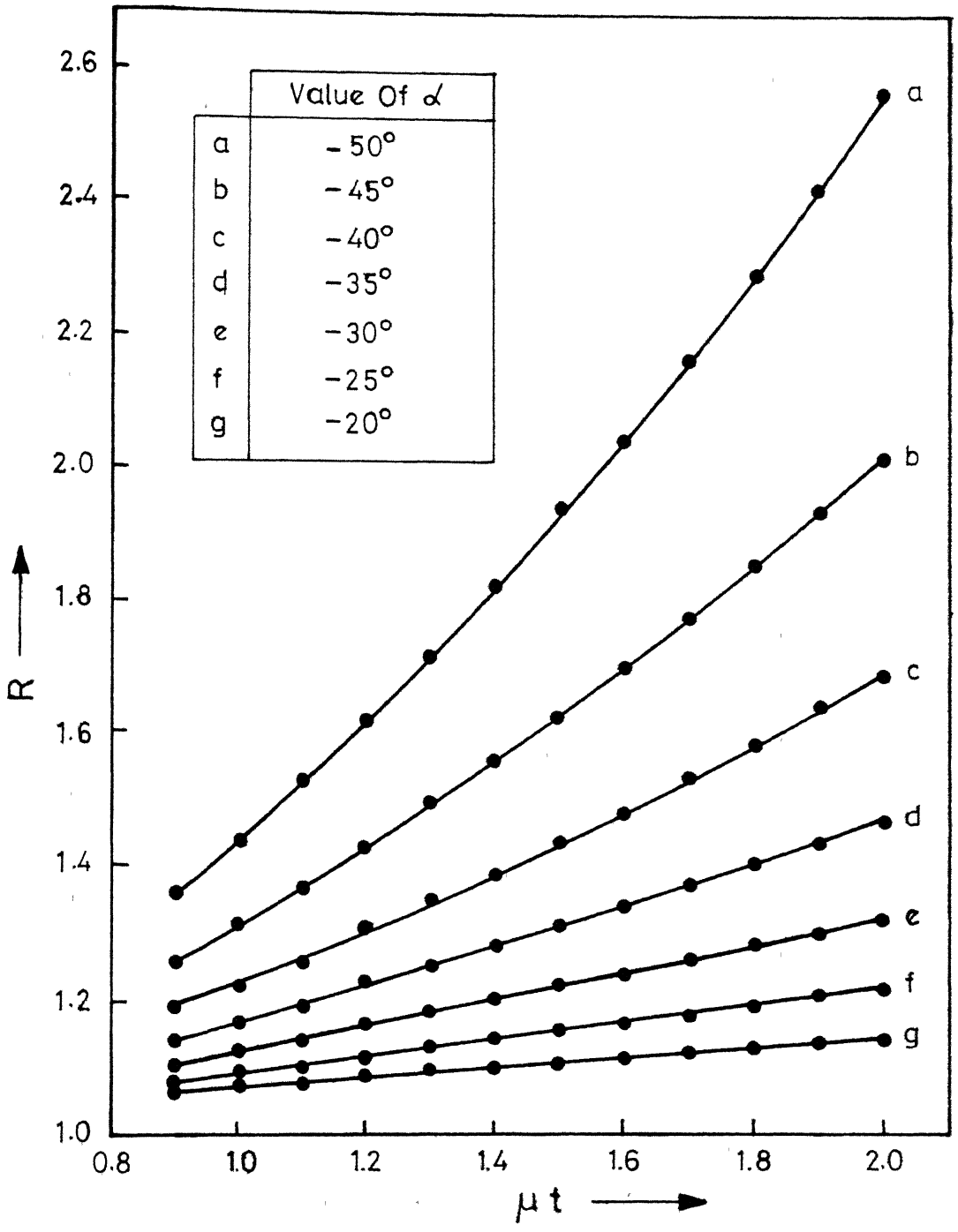

FIG 23. Correction Factor R As Function Of μt For Constant Value Of α

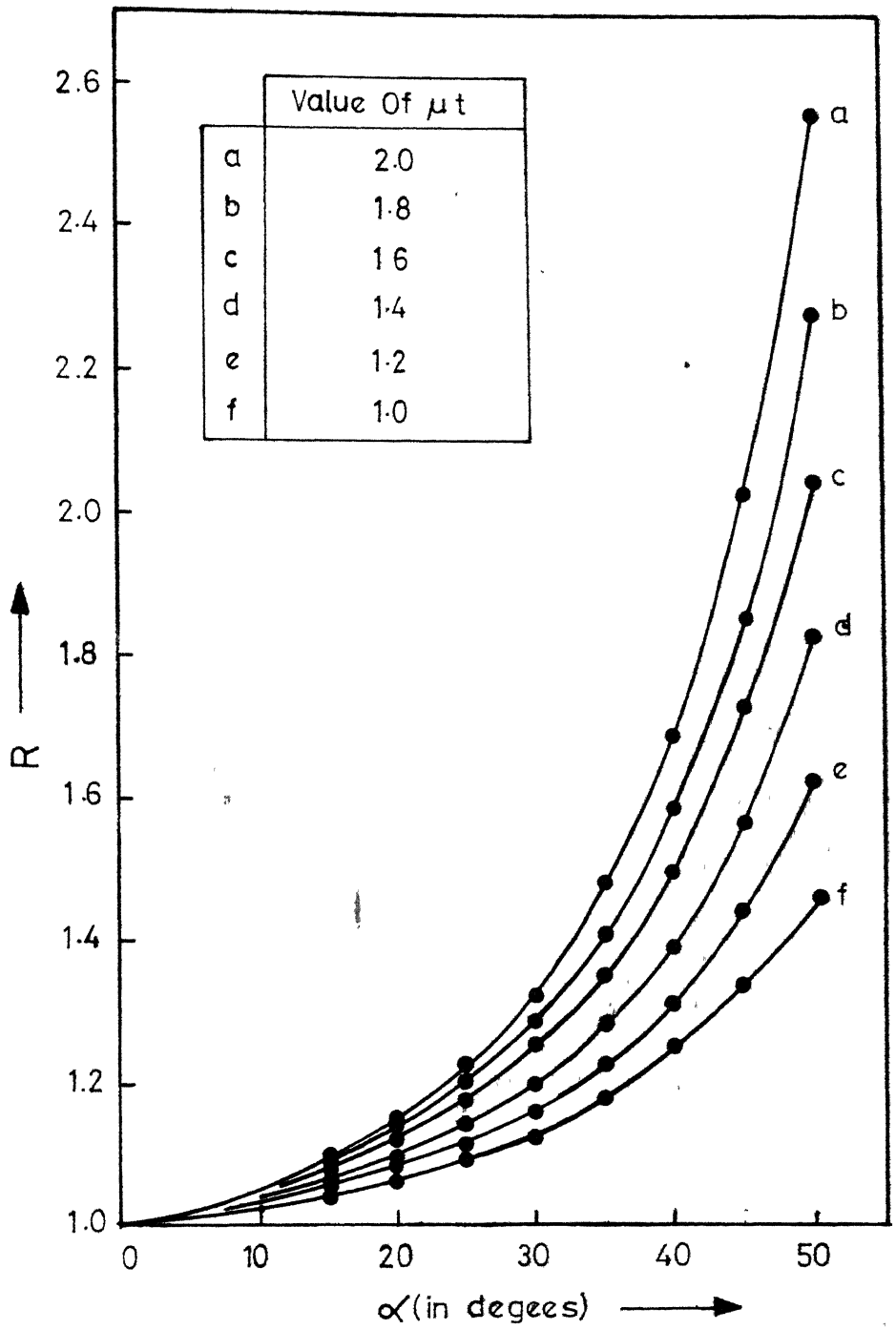

FIG 24. Correction Factor R As Function Of ∝ For Constant Value Of μt

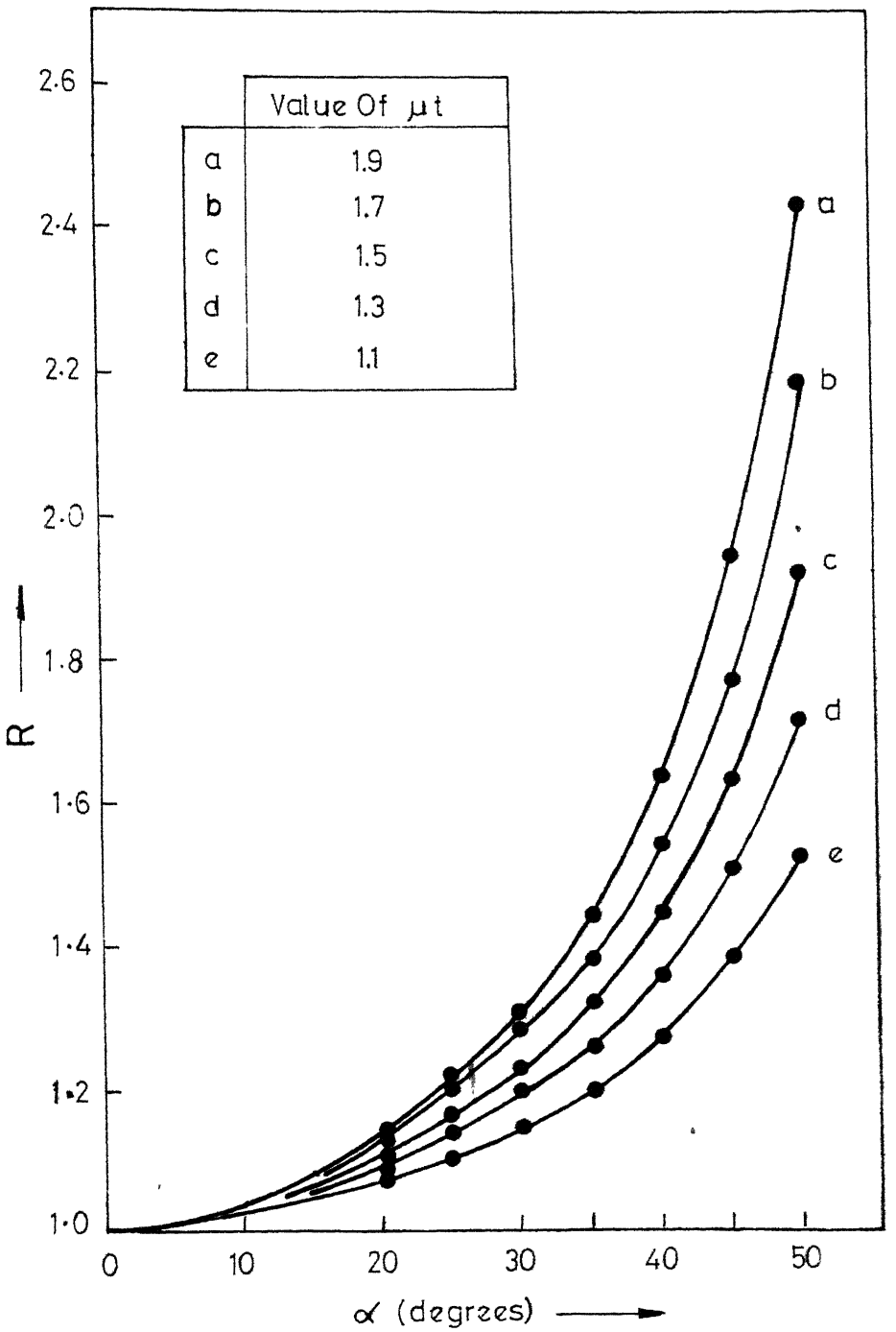

FIG25. Correction Factor R As Function Of ∝ For Constant Value Of μt

With a 1 rmp motor and the 100 seconds counting time 6 to 7 oscillations could be given to the specimen. To explore a quarter of a pole figure specimens were surveyed usually at 5° intervals of $-\alpha$ up to 50° for fixed ϕ and 10° intervals of $+\phi$ up to 90° for fixed $-\alpha$. Only quarter of pole figure in each case was determined. In the regions of high intensity or drastic changes in intensity over smaller angular regions, intensity data at smaller angular intervals were taken. The data collected in terms of counts/sec., which are propertional to pole densities, were corrected making use of the respective μt of the specimen and the value of α involved in the measurement. The corrected values were plotted on a polar (equatorial) stereographic net drawn at 2° intervals (Fig.26).

To plot the pole of the reflecting plane on the pole figure, it is evident that it coincides with the left cross direction for the initial setting i.e. when $\alpha = \phi = 0^{\circ}$. A rotation of the specimen by $+\phi$ degrees in its own plane then moves the pole of the reflecting plane ϕ degrees around the circumference of the pole figure and a rotation of $-\alpha$ about the diffractometer axis moves it $-\alpha$ degrees from the circumference along a radius (Fig.27). In this way all the corrected data were plotted on the pole figures using the respective ϕ and $-\alpha$ values, and contour lines

passing through equi-intensity points were drawn to indicate the pole densities. The pole figure was interpreted with the help of a single standard stereogram showing [110] poles for different planes of projection (Fig.28).

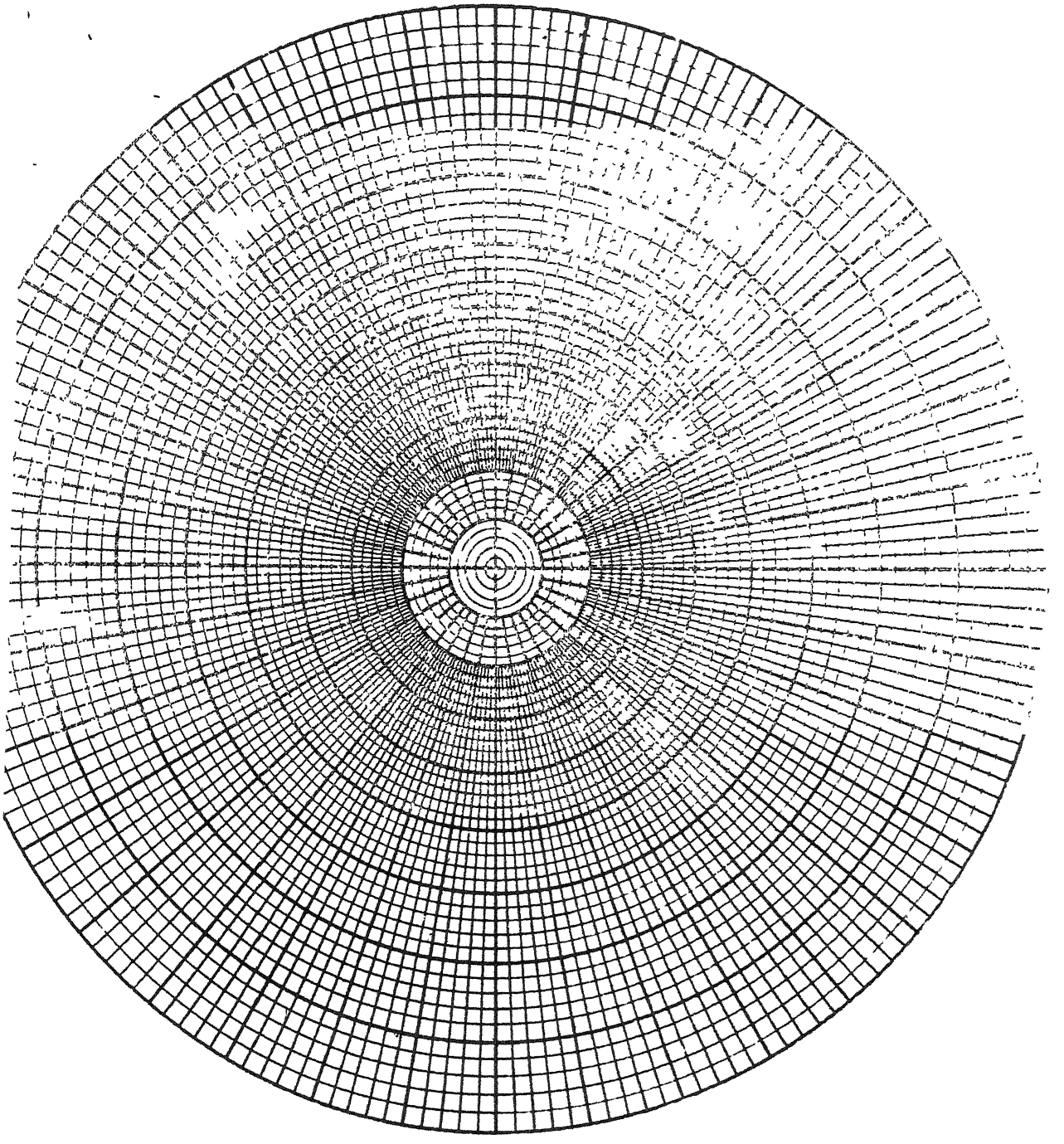

Fig. 26. Polar (equatorial) stereographic net drawn to 2° intervals.
Mfd. by N. P. Nies, 969 Skyline Dr., Laguna Beach, Calif.

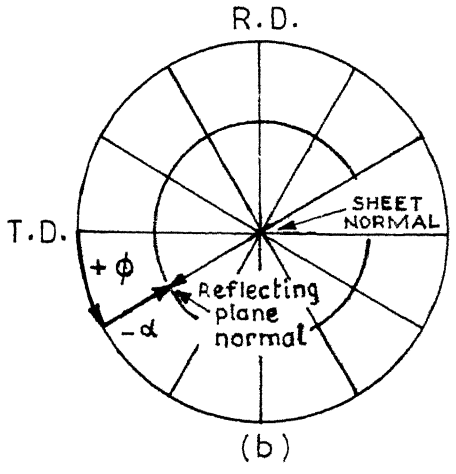

Fig.27. Angular relationships in the tranmission pole figure method on the stereographic projection (On the projection the position of the reflecting plane normal is shown for $\phi = 30^\circ$ and $\alpha = -30^\circ$)

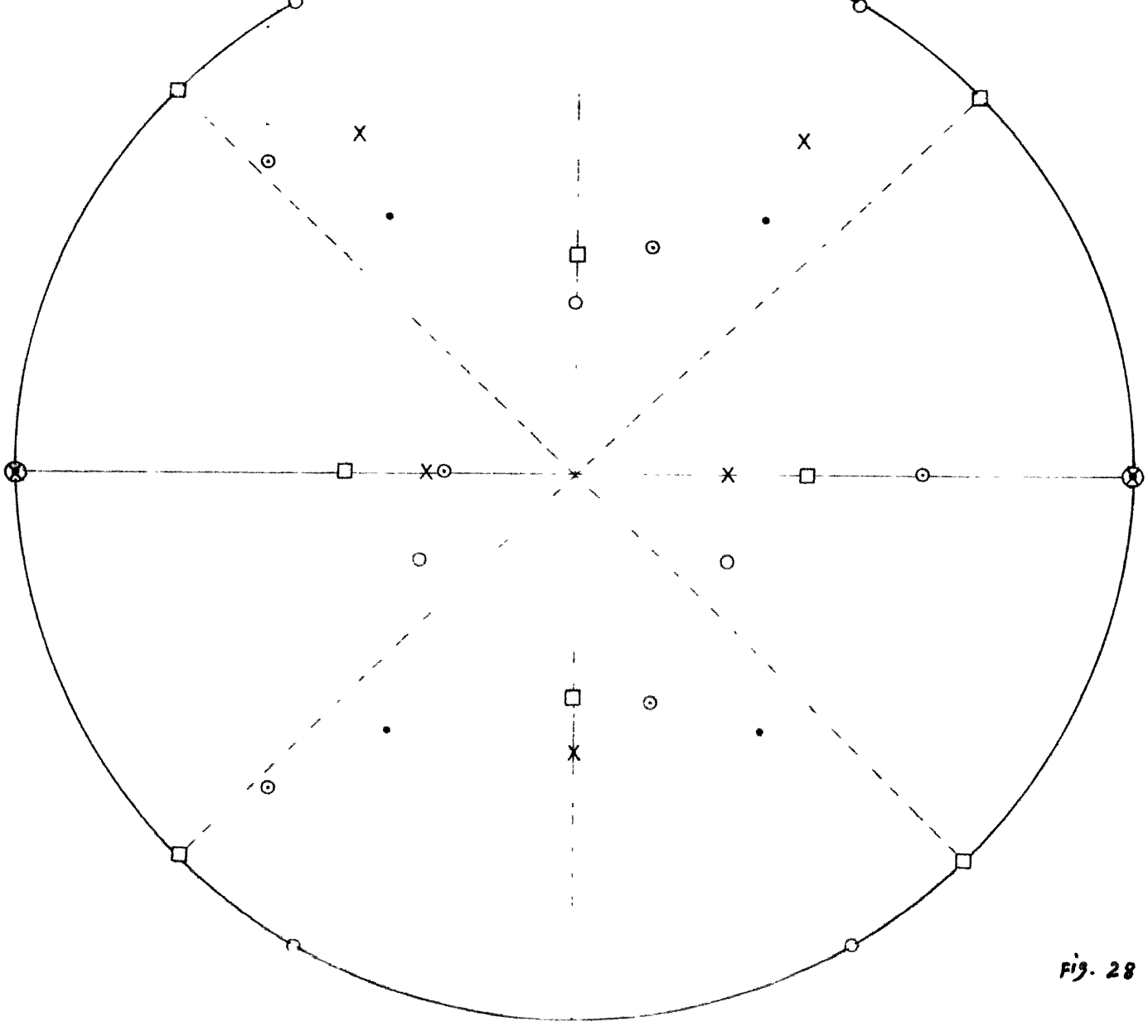

Location of [110] poles in

(130) Projection ⊙

(110) Projection •

(211) Projection x

(111) Projection o

(001) Projection □

----- Rolling and transverse directions for (001) [11$\bar{1}$] texture (cold rolled texture)

——— Rolling and transverse direction for a (011) [100] texture (cube on edge texture) and (b) (001) [100] texture (cube texture)

Fig. 28

IV RESULTS AND DISCUSSION

Results and Discussions:-

Two Fe-Si alloys, high purity and commercial purity, containing 3.5%Si were processed through hot forging and hot rolling followed by cold rolling, through an intermediate annealing or no intermediate annealing. Details of the forming treatment schedules are given in Table I_A and II_A respectively. The specimens were then primary recrystallized and secondary recrystallized as given in Table I_B and II_B. For each of these specimens texture was determined, the details of which are shown in Tables I_C and II_C and in Figs. 33 to 62. For the high purity alloy the most suitable primary recrystallization annealing treatment was determined by finding time and temperature which produced stable grain structure. The details of this study is shown in Table III and a few representative microstructures are shown in Fig. 22. The chemical and electrolytic etchants tried for the specimen thinning and their respective performances are given in Tables IV_A and IV_B.

The commercial purity alloy was prepared with a steel supplied by Hindustan Steel Ltd. The steel contained a higher amount of C (.029%C) than is usually desired ($\leqslant$ 0.01%) in grain oriented alloys. The effect of increased carbon concentration 1) it increases the hysteresis loss (Fig. 29) and 2) it affects the γ loop of Fe-Si system (Fig. 30). From Fig. 31 it is clear that small changes in %C can cause large extension

Table I_A - Cold rolling schedule of High Purity 3.5% Si-Fe. Alloy

Specimen	Hot rolled thickness in inches	Cold Rolling		Intermediate Annealing.		Final cold Rolling		Total % Red.
		Final thickness in inches	% Red.	Temp. °C	Time Mins.	Final thickness in inches	% Red.	
A_a	0.202	0.104	49	950	5	0.017	83	91
A_b	0.202	-	-	-	-	0.017	91	91
D_a	0.105	0.037	65	903	5	0.014	54	87
E_a	0.106	0.38	65	950	5	0.015	54	86

Table II_A - Cold rolling schedule of Commercial Purity 3.5% Si-Fe Alloy

Specimen	Hot rolled thickness in inches	Cold Rolling		Intermediate Annealing		Final cold Rolling		Total % Red.
		Final thickness in inches	% Red.	Temp. °C	Time Mins.	Final thickness in inches	% red.	
$A_{Comm.}$	0.102	-	-	-	-	0.012	88	88
$B_{Comm.}$	0.102	0.030	70	950	5	0.012	60	88

Table I_B - Primary & Secondary recrystallization schedule for high purity 3.5% Si-Fe. Alloy.

Specimen	Recrystallization						Figure No.o correspondi
	Primary			Secondary			
	Temp. °C	Time Mins.	Atmos-phere	Temp. °C	Time Mins.	Atmos-phere	Pole figure
A_a	-	-	-	-	-	-	33
	980	20	*Vac.	-	-	-	34
	980	20	Vac.	1150	2½	Vac.	35
	980	25	Vac.	1150	3	Vac.	36
	980	30	Vac.	-	-	-	37
	980	30	Vac.	1150	3½	Vac.	38
A_b	-	-	-	-	-	-	39
	980	18	Vac.	-	-	-	40
	980	18	Vac.	1150	3	Vac.	41
D_a	-	-	-	-	-	-	42
	750	15)	Argon	1050	225	Argon	43
	750	15)	Argon	1100	240	Argon	44
	-	-	-	-	-	-	45
	950	20	Vac.	-	-	-	46
	950	20	Vac.	1200	5	Vac.	47
	950	120	Vac.	-	-	-	48
	950	120	Vac.	1200	8	Vac.	49
E_a	-	-	-	-	-	-	50
	900	15	Vac.	1150	5	Vac.	51
	980	18	Vac.	1150	5	Vac.	52

* Vacuum.

Table II_B - Primary & Secondary recrystallization schedule for Commercial purity 3.5% Si-Fe. Alloy

Specimen	Recrystallization						Figure No. of corresponding polc figure
	Primary			Secondary			
	Temp. °C	Time Mins.	Atmos-phere	Temp. °C	Time Mins.	Atmos-phere	
$A_{Comm.}$	-	-	-	-	-	-	53
	750	120	* Vac.	-	-	-	54
	750	120	Vac.	1150	5	Vac.	55
	750	120	Vac.	1150	10	Vac.	56
	750	120	Vac.	1150	240	Vac.	57
	750	120	Vac.	1150	240	Argon	58
$B_{Comm.}$	-	-	-	-	-	-	59
	750	120	Vac.	-	-	-	60
	750	120	Vac.	1150	10	Vac.	61
	750	120	Vac.	1150	240	Vac.	62

* Vacuum.

Table I_C - Texture of cold rolled, Primary recrystallized and secondary recrystallized specimens of high purity 3.5% Si-Fe Alloy

Sepcieen	Figure No.of corresponding pole figure	Texture
A_a	33	Strong (100) [011] texture, with spread about 10° around R.D. and C.D. central peak 10° off from ideal position
	34	(100) [011] texture, weaker in C.D. with Central peak disappeared. Texture more random than cold rolled texture.
	35	Strongly developed (100) [011] texture, with Central peak off by 10° from ideal position.
	36	Very strong (100) [011] ideal cold rolled texture with very little spread around R.D. and C.D.
	37	Texture similar to 20 mins. primary recrystallized specimen, but with pole density stronger around R.D. and low intensity central peak
	38	Very strong (100) [011] ideal cold rolled texture
A_b	39	Strong (100) [011] texture with some spread in pole densities around R.D. and C.D.
	40	Strong (100) [011] texture with more spread around R.D. and C.D. than the cold rolled state. Central peak weak and displaced from ideal location.
	41	Strong (100) [011] texture with some spread around R.D. and C.D. All pole densities (at the ideal locations) are equally strong.
D_a	42	Weak (100) [011] texture with central peak missing and scater about R.D. and C.D. is considerable
	43	(100) [011] texture with central peak of low intensity and 5° off from the ideal location.
	44	Weak (100) [011] texture similar to specimen recrystallized at 1050°C. with central peak of slight more intensity but shifted 10° from ideal location.

Contd.

Specimen	Figure No. of corresponding pole figure	Texture
D_a	45	Weak (100) [01$\bar{1}$] texture with central peak of low intensity and large spread around R.D. and C.D.
	46	Weak (100) [01$\bar{1}$] texture similar to cold rolled state.
	47	Weak (100) [01$\bar{1}$] texture but slightly sharper than cold rolled and primary recrystallized state.
	48	Stronger (100) [01$\bar{1}$] texture than the specimen primary recrystallized for 20 mins.
	49	Strong (100) [01$\bar{1}$] texture but with some spread around R.D. and C.D. Pole densities at ideal locations are almost equal.
E_a	50	Weak (100) [01$\bar{1}$] texture with low central peak intensity similar to D_a cold rolled specimen.
	51	Weak (100) [01$\bar{1}$] texture with considerable spread around R.D. and C.D. The central peak disappeared.
	52	Same as above (E_a), recrystallized specimen with slight improvement in the intensities at R.D. and C.D. A new component (111) [11$\bar{2}$] off from the ideal position by about 10° is also produced

Table II_C - Texture of cold rolled, primary recrystallized and secondary recrystallized specimens of Commercial quality 3.5% Si-Fe Alloy

Specimen	Figure No. of corresponding pole figure	Texture
$A_{Comm.}$	53	Srtong (100) [011] texture with small spread around R.D. and C.D.
	54	Strong (100) [011] texture but with slight spread about C.D. and weak central peak
	55	Strong cold rolled texture with spread around both R.D. and C.D. and central peak slightly weak.
	56	Similar to specimen secondary recrystallized for 5 mins with improvement in central peak intensity.
	57	The intensity at C.D. considerably increased and peak at R.D. almost eliminated. The texture is strong (110) [001] with central peak off from ideal position by about 15^{o}.
	58	Similar to vacuum annealed thick specimen but with central peak off from ideal position by 10^{o}.
$B_{Comm.}$	59	A fairly strong colled rolled texture with spread about 10^{o} around R.D. and 20^{o} around C.D.
	60	Weak cold rolled texture with considerable scater around R.D. and C.D. and very low central peak intensity.
	61	Strong cold rolled texture compared to primary recrystallized state with large spread around R.D. and C.D.
	62	Intensity at C.D. considerably increased and intensity at R.D. decreased indicating possible development of cube-on-edge texture.

TABLE V

Comparative study of the intensity data for specimen A_a (secondary recrystallized for $3\frac{1}{2}$ mins*) due to scientillation and proportional counter**

Setting of Goniometer		Measured intensity in counts/Sec.	
α in degrees	ϕ in degrees	Scientillation Counter	Proportional Counter
0	0	3763	1833
0	+90	3815	1994
-45	+45	3651	1853
-50	0	22	101
-50	90	17	100

* For specimen refer to Table I_A

** For pole figures refer to Figs. 38 and 64.

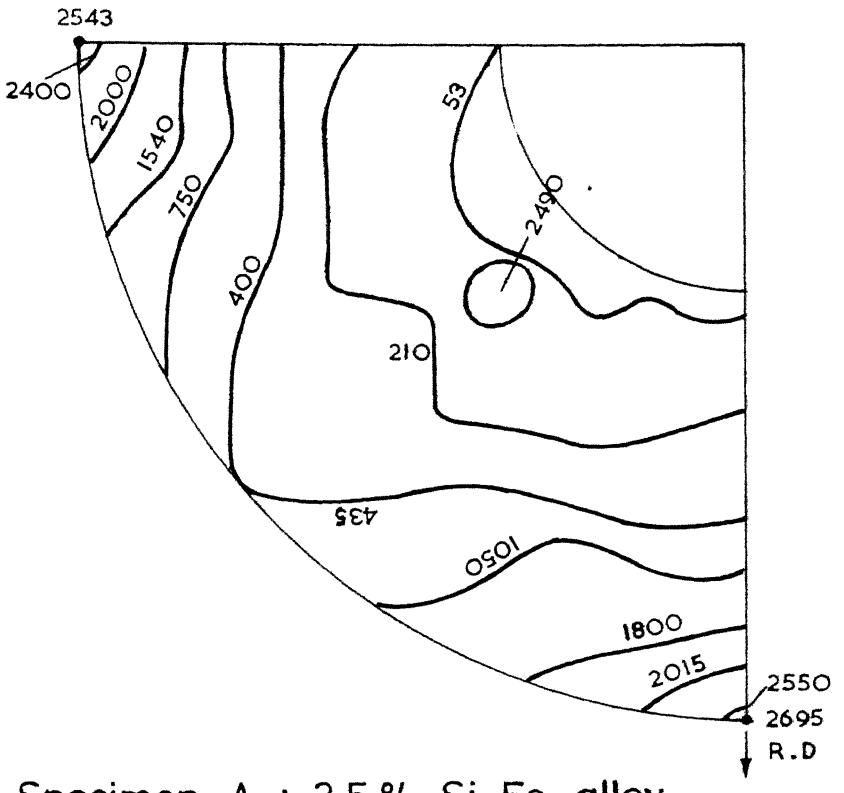

Fig. 33 Specimen A_a: 3.5 % Si-Fe alloy, cold rolled.

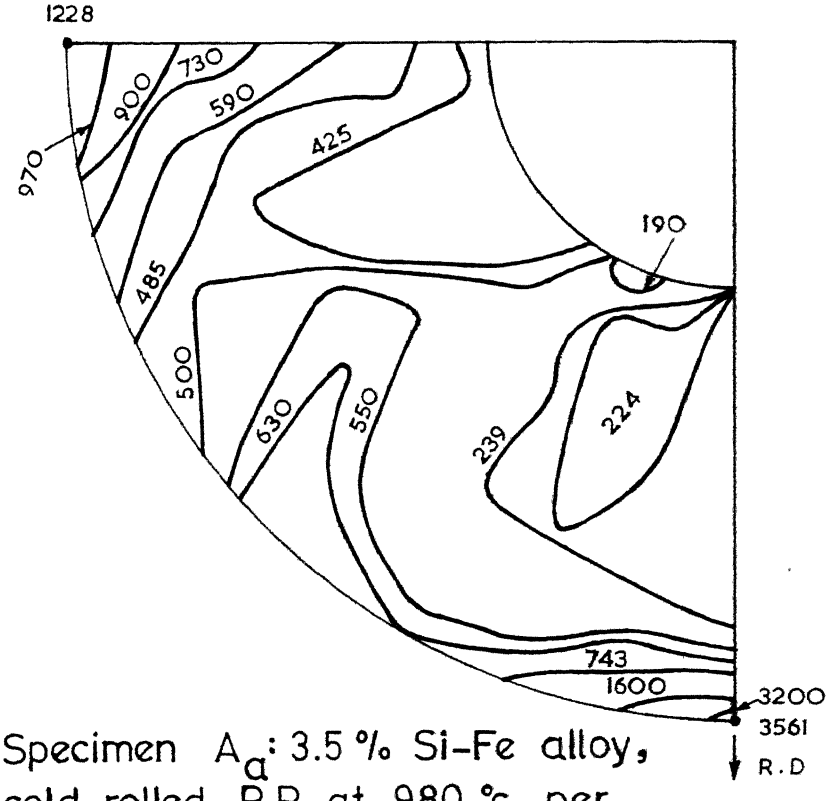

Fig. 34. Specimen A_a: 3.5 % Si-Fe alloy, cold rolled, P.R. at 980 °c per 20 mins.

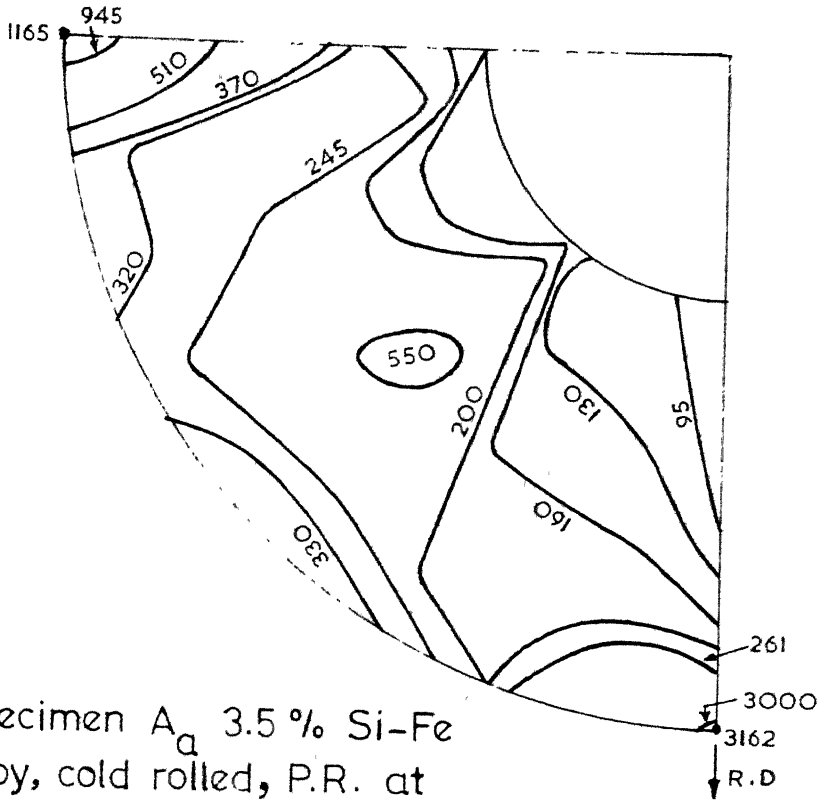

Fig. 37 Specimen A_a 3.5 % Si-Fe alloy, cold rolled, P.R. at 980 °c per 30 mins.

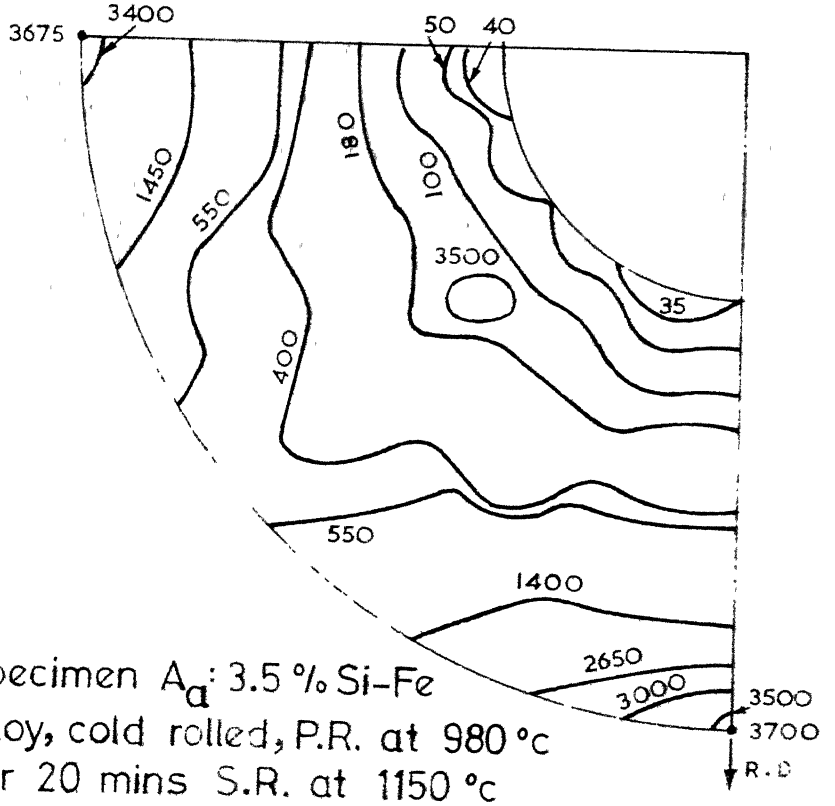

Fig. 35 Specimen A_a: 3.5 % Si-Fe alloy, cold rolled, P.R. at 980 °c per 20 mins S.R. at 1150 °c per $2\frac{1}{7}$ mins.

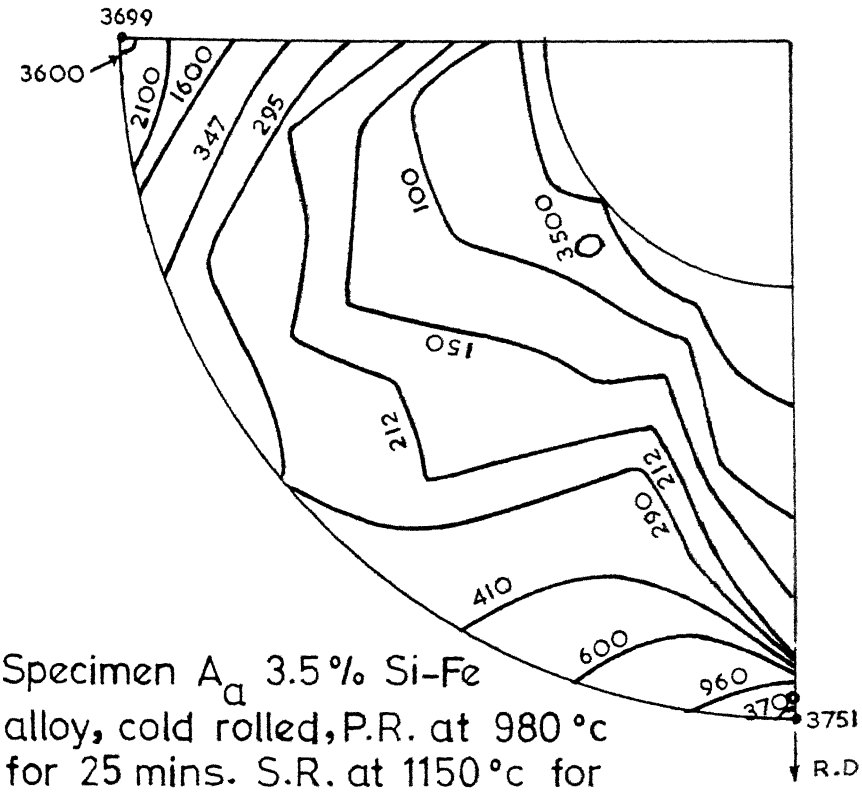

Fig.36 Specimen A_a 3.5% Si-Fe alloy, cold rolled, P.R. at 980 °c for 25 mins. S.R. at 1150 °c for 3 mins.

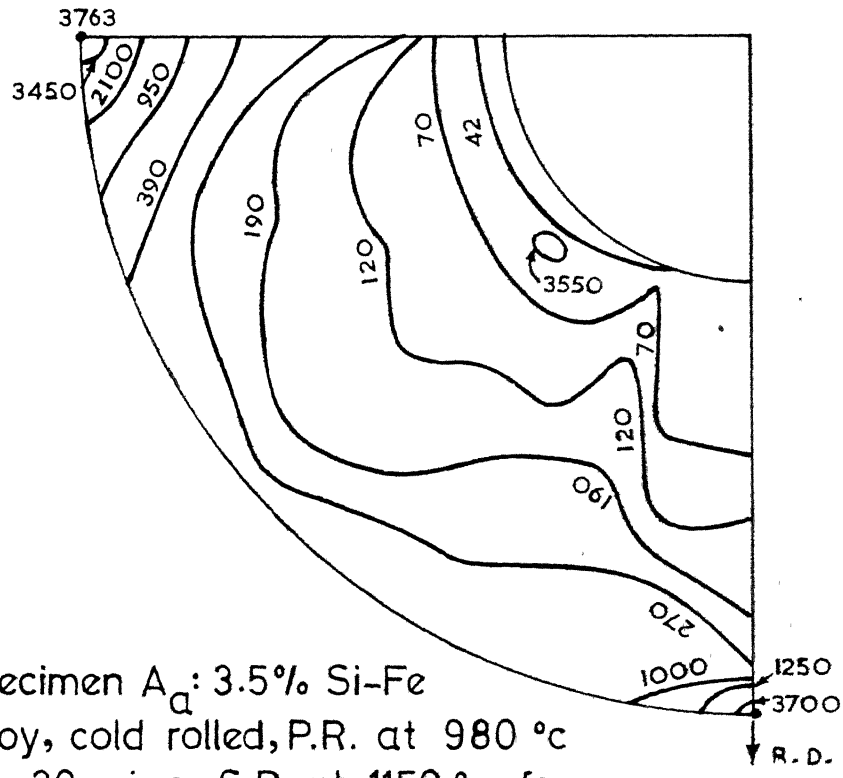

Fig.38 Specimen A_a: 3.5% Si-Fe alloy, cold rolled, P.R. at 980 °c for 30 mins. S.R. at 1150 °c for $3\frac{1}{2}$ mins.

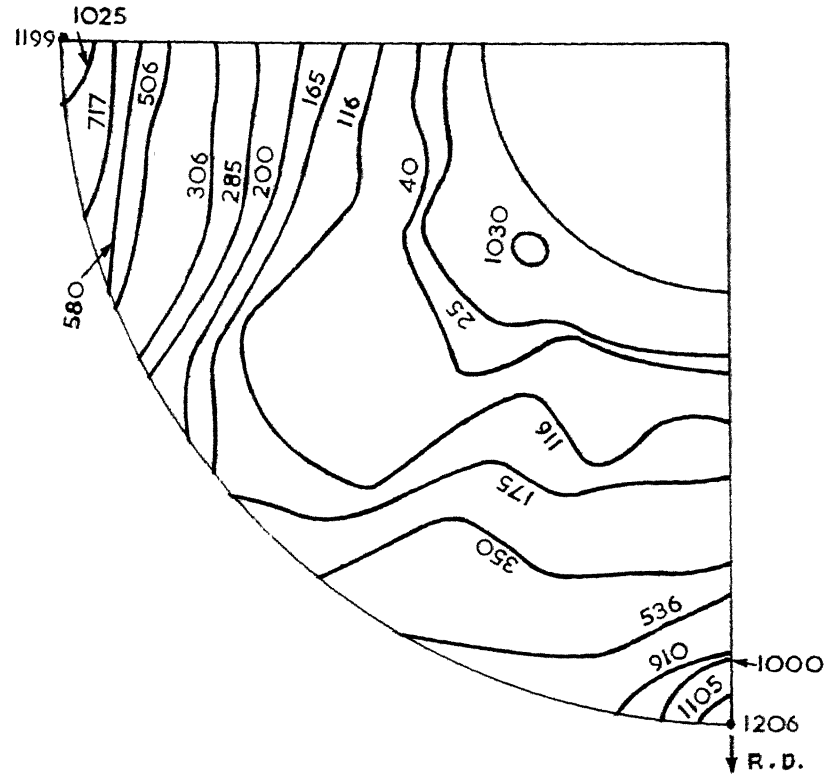

Fig. 39 Specimen A_b: 3.5 % Si-Fe alloy, cold rolled.

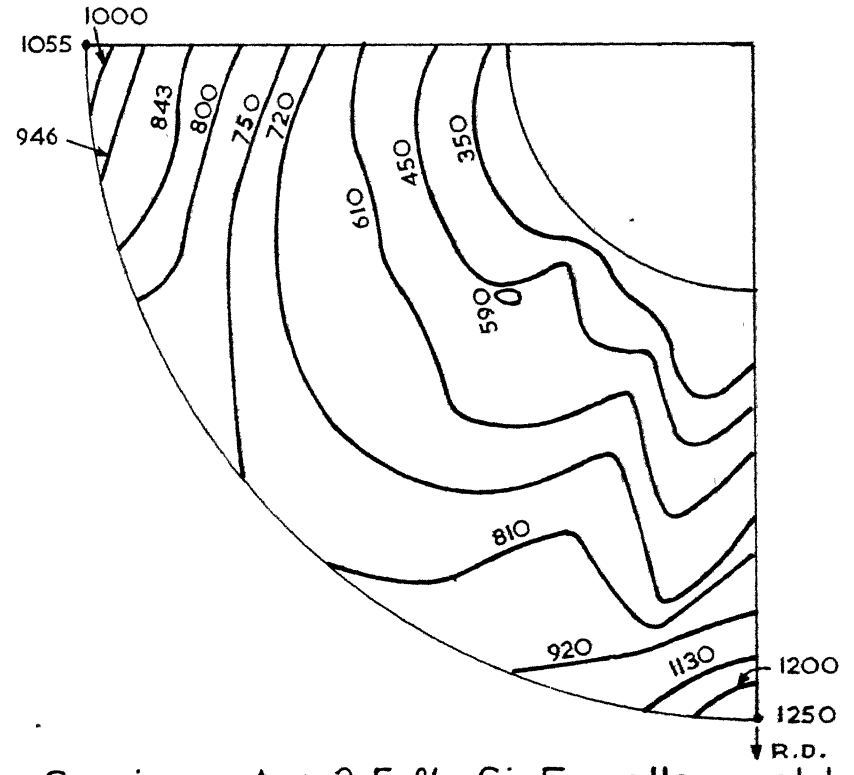

Fig. 40 Specimen A_b: 3.5 % Si-Fe alloy cold rolled P.R. at 980 c for 18 mins.

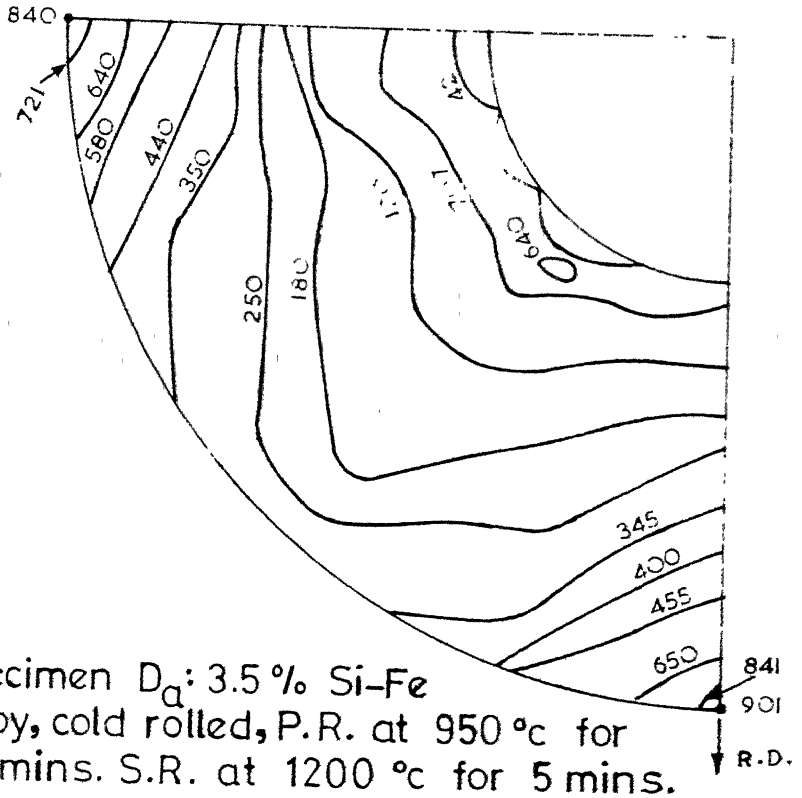

Fig. 47. Specimen D_a: 3.5 % Si-Fe alloy, cold rolled, P.R. at 950 °c for 20 mins. S.R. at 1200 °c for 5 mins.

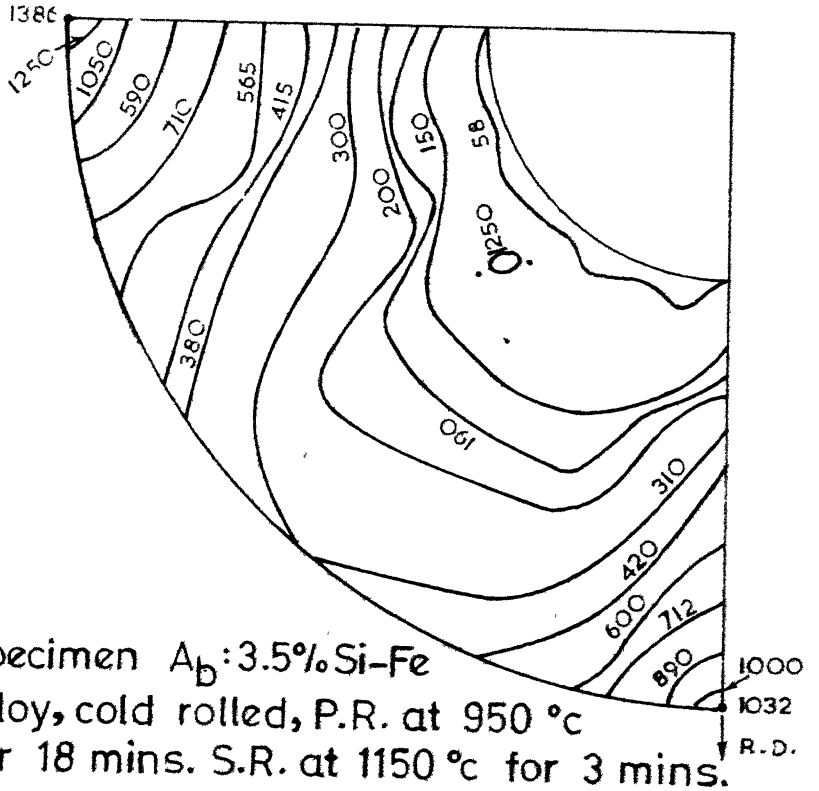

Fig. 41. Specimen A_b: 3.5% Si-Fe alloy, cold rolled, P.R. at 950 °c for 18 mins. S.R. at 1150 °c for 3 mins.

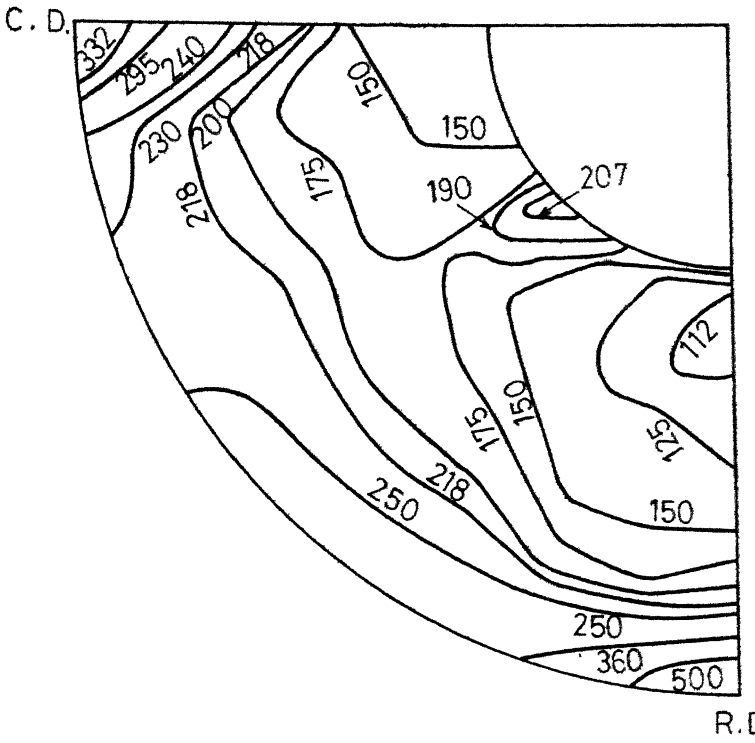

Fig. 43 Specimen D_a: 3.5% Si-Fe alloy, cold rolled, P.R. at 750 °c for $2\frac{1}{2}$ hrs. in argon, S.R. at 1045 °c for $3\frac{3}{4}$ hrs. in argon.

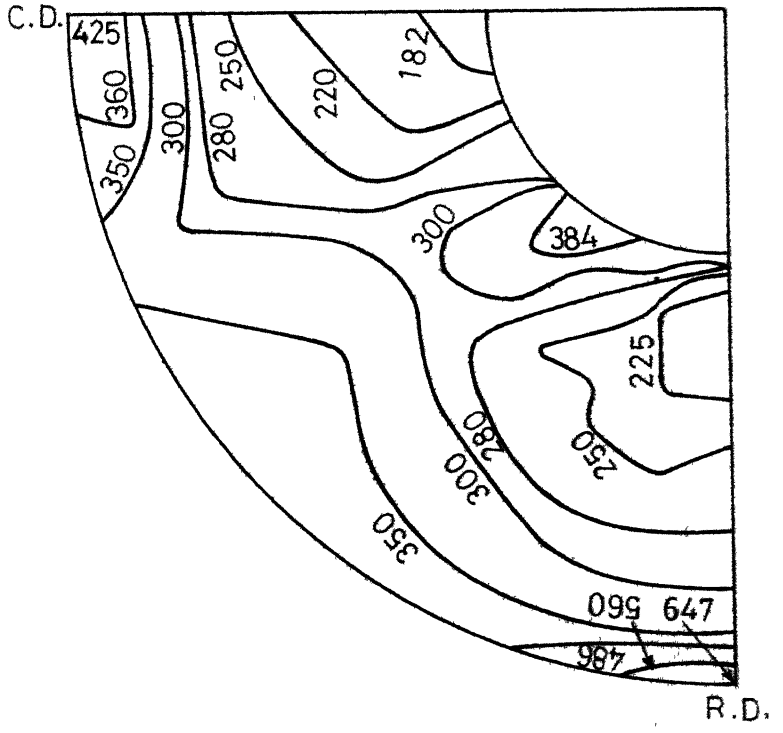

Fig. 44. Specimen D_a: 3.5% Si-Fe alloy, cold rolled, P.R. at 750 °c for $2\frac{1}{2}$ hrs. in argon, S.R. at 1150 °c for 4 hrs. in argon.

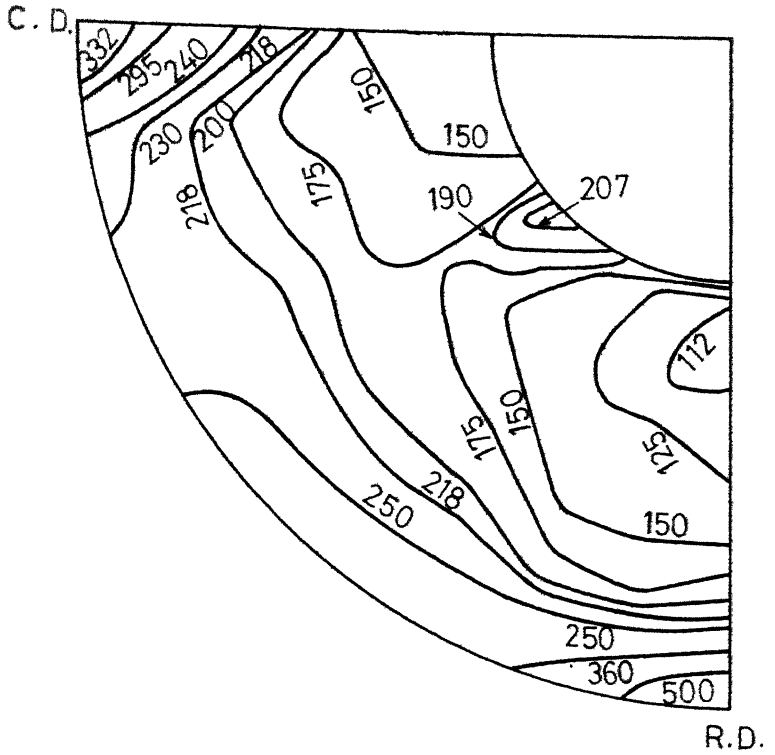

Fig. 43 Specimen D_a: 3.5% Si-Fe alloy, cold rolled, P.R. at 750 °c for $2\frac{1}{2}$ hrs. in argon, S.R. at 1045 °c for $3\frac{3}{4}$ hrs. in argon.

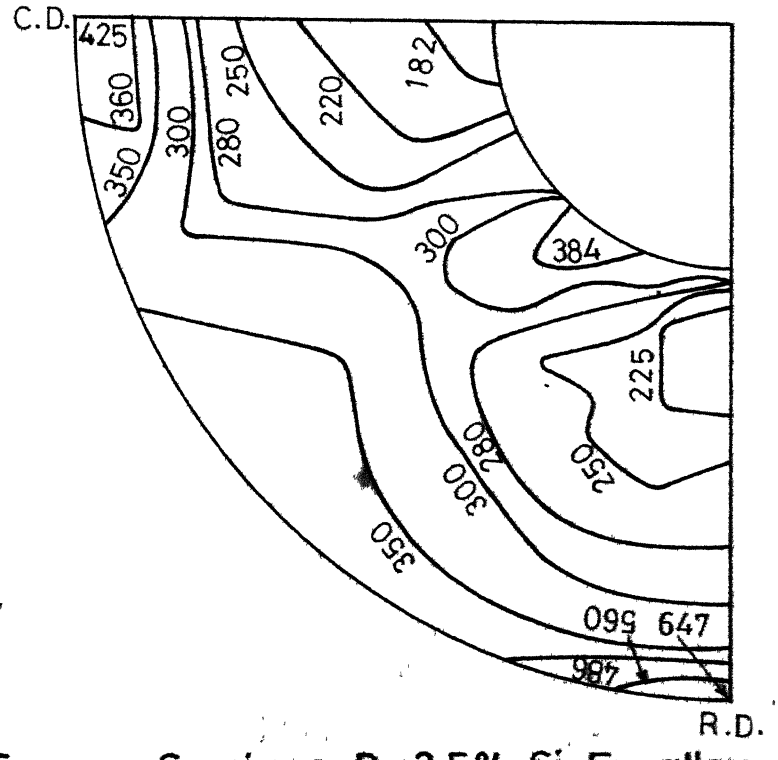

Fig. 44 Specimen D_a: 3.5% Si-Fe alloy, cold rolled. P.R. at 750 °c for $2\frac{1}{2}$ hrs. in argon, S.R. at 1150 °c for 4 hrs. in argon.

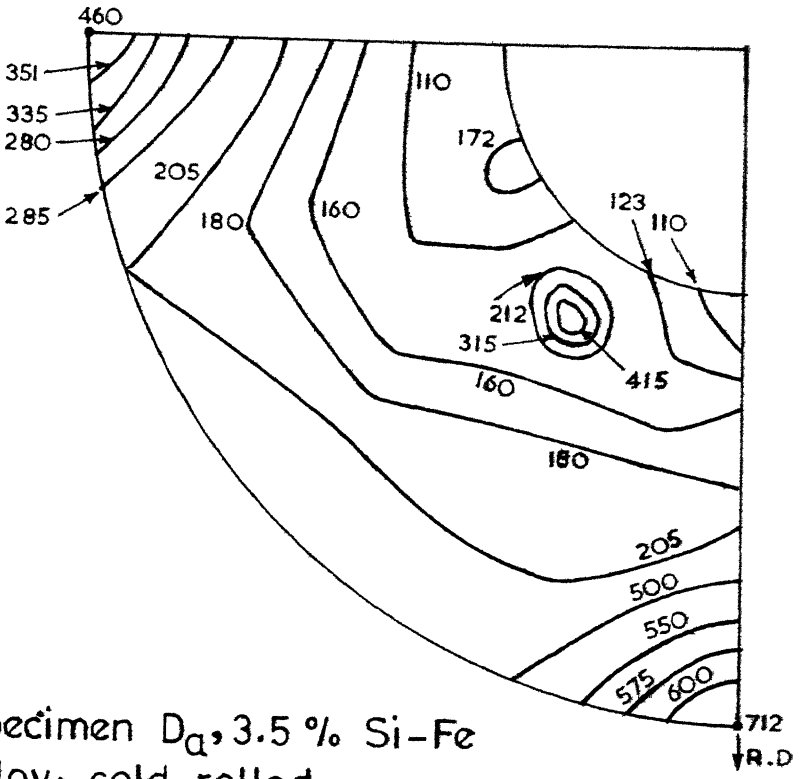

Fig.45 Specimen D_a, 3.5 % Si-Fe alloy, cold rolled.

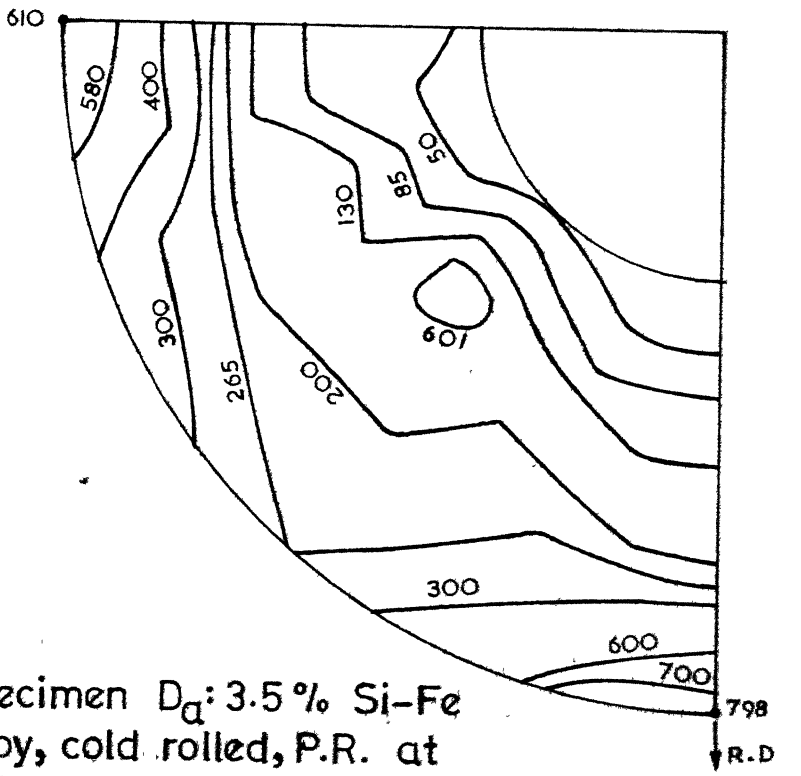

Fig.46 Specimen D_a: 3.5 % Si-Fe alloy, cold rolled, P.R. at 950 °c for 20 mins.

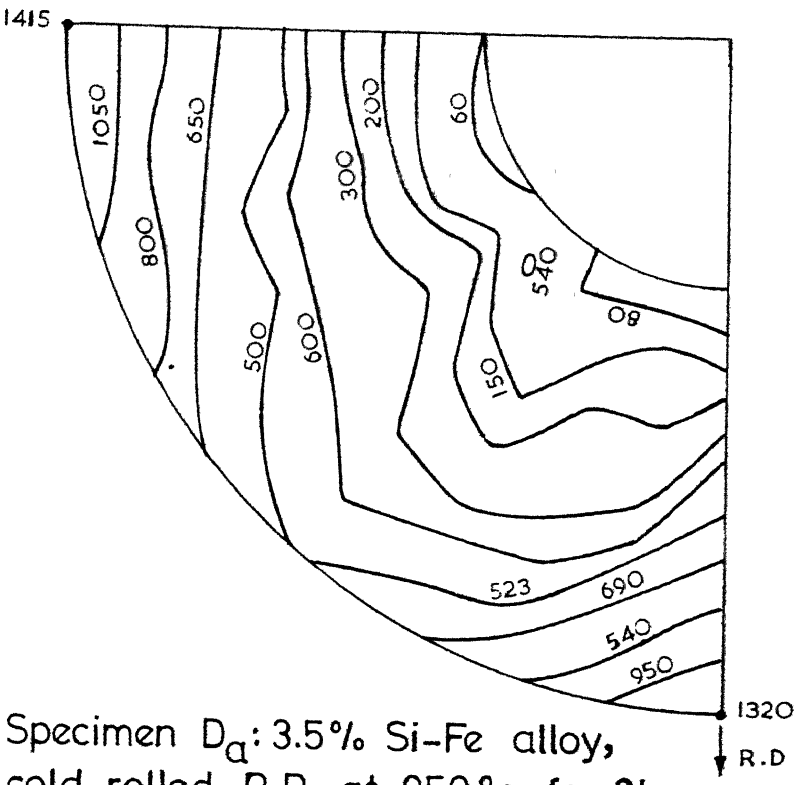

Fig. 48 Specimen D_a: 3.5% Si-Fe alloy, cold rolled, P.R. at 950 °c for 2hrs.

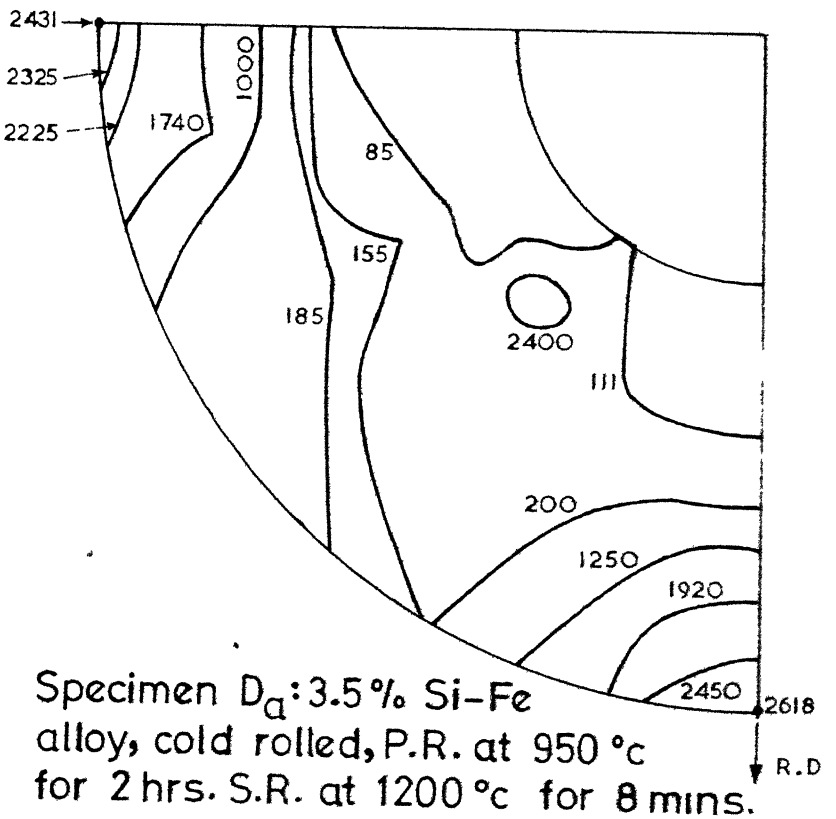

Fig. 49 Specimen D_a: 3.5% Si-Fe alloy, cold rolled, P.R. at 950 °c for 2 hrs. S.R. at 1200 °c for 8 mins.

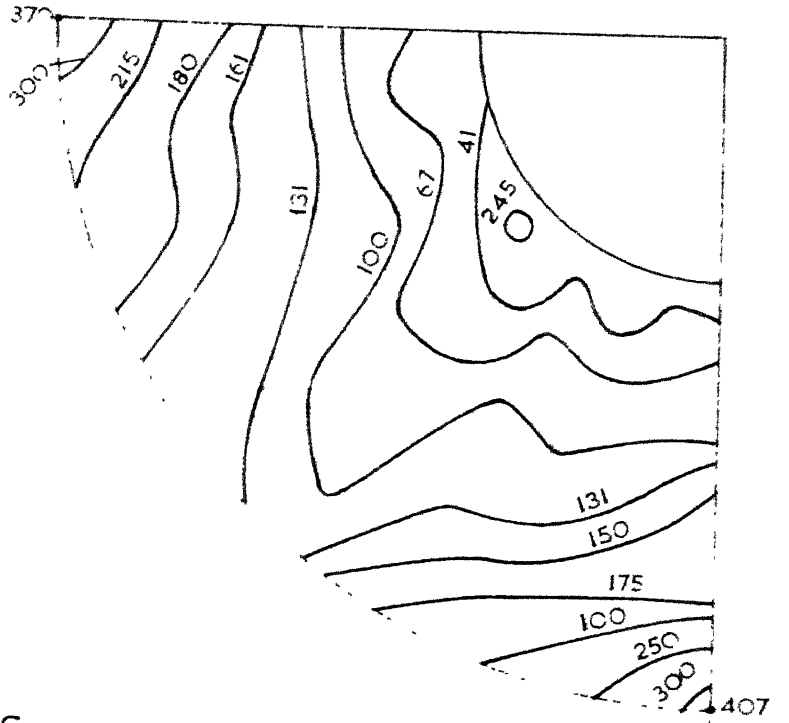

Fig. 50 Specimen E_a, 3.5 % Si-Fe alloy, cold rolled.

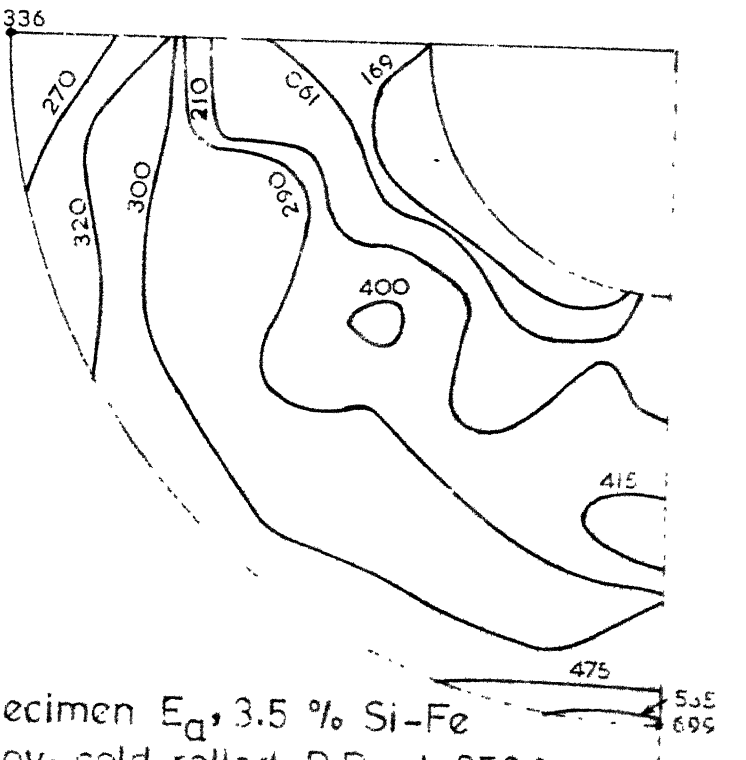

Fig. 52 Specimen E_a, 3.5 % Si-Fe alloy, cold rolled. P.R. at 950 °c for 18 mins. S.R. at 1150 °c 5 mins.

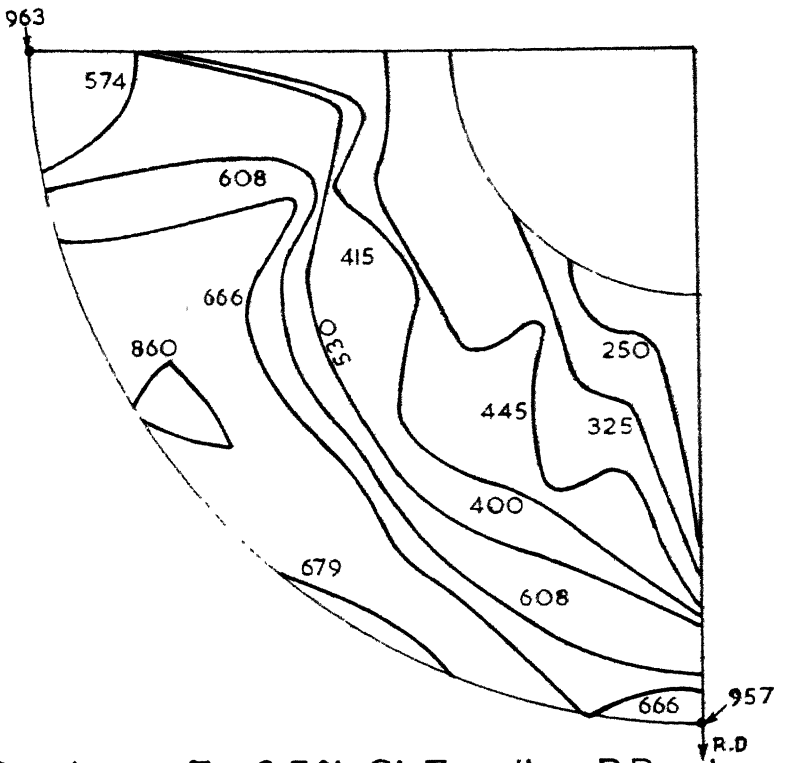

Fig.51 Specimen E_a 3.5% Si-Fe alloy, P.R. at 900 °c for 5 mins S.R. at 1150 °c for 5 mins.

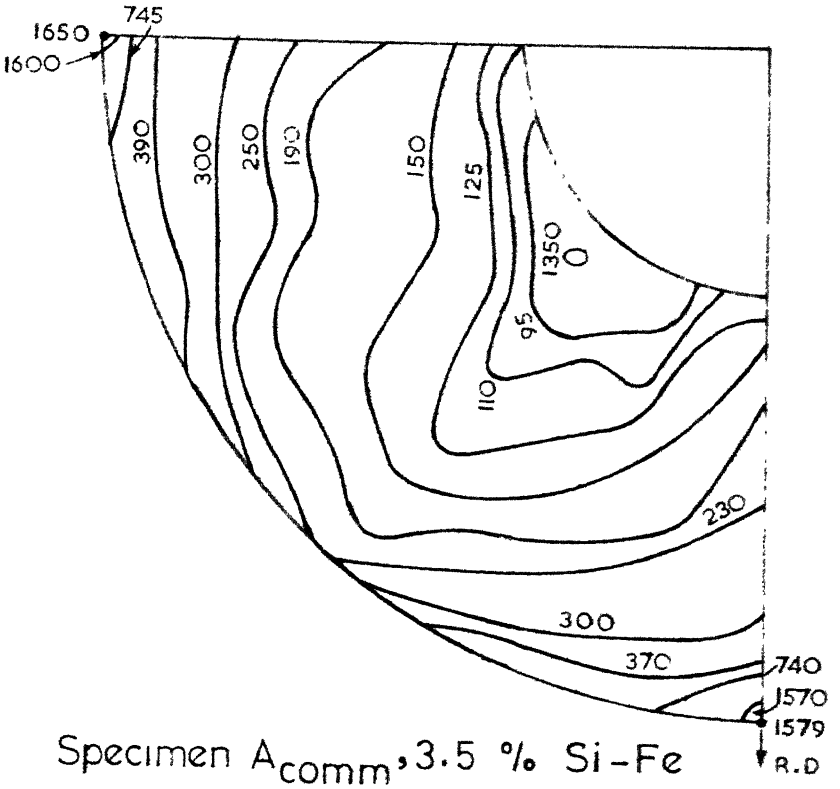

Fig.53 Specimen A_{comm}, 3.5 % Si-Fe alloy, cold rolled.

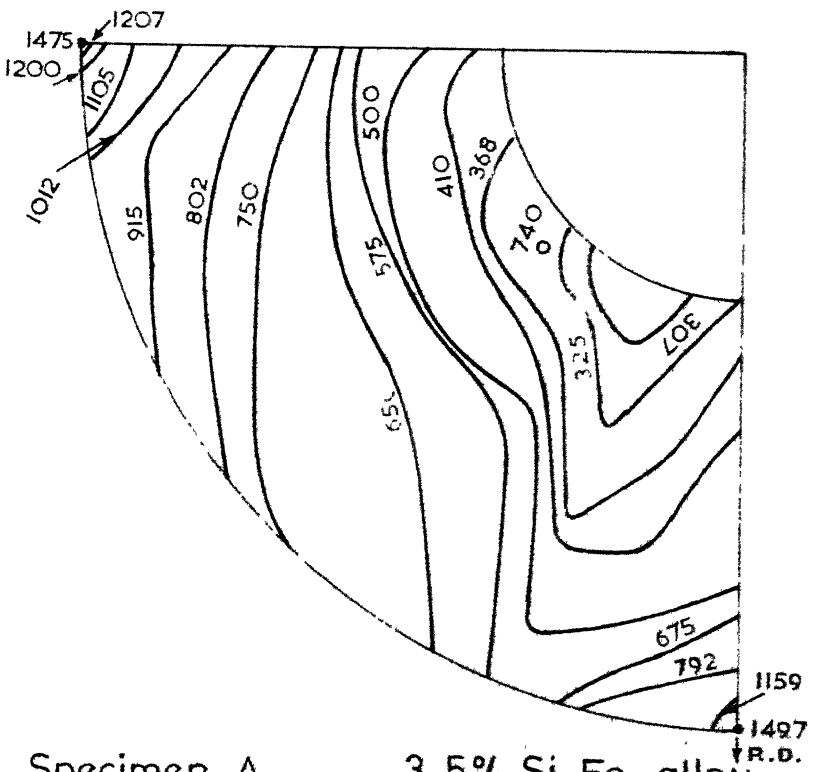

Fig.54. Specimen A_{comm}, 3.5% Si-Fe alloy, cold rolled, PR at 750°c for 2hrs.

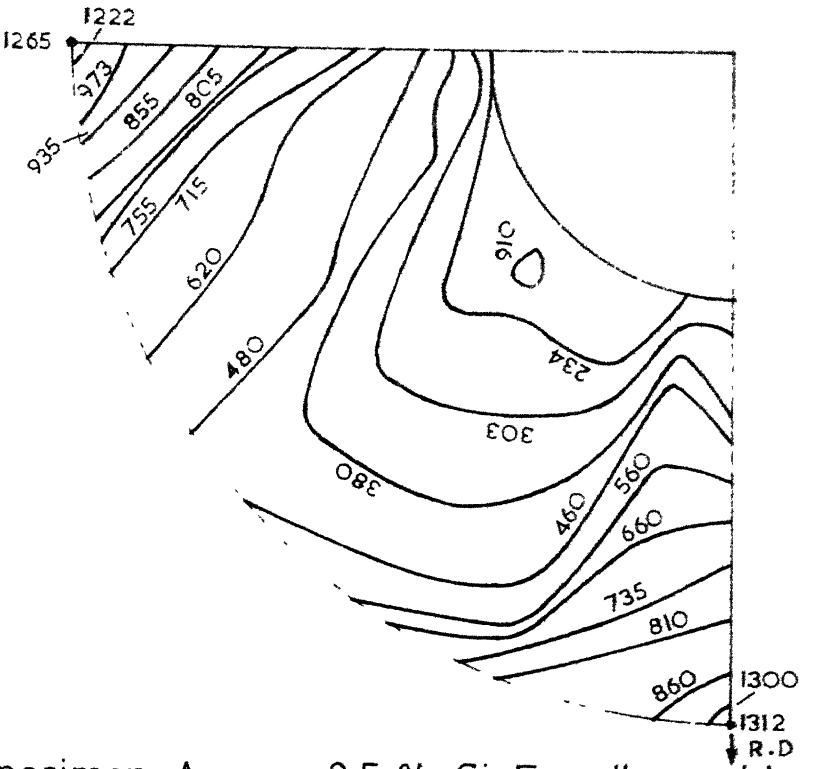

Fig.55 Specimen A_{comm} 3.5 % Si-Fe alloy, cold rolled, P.R. at 750°c for 2 hrs., SR at 1150 °c for 5 mins.

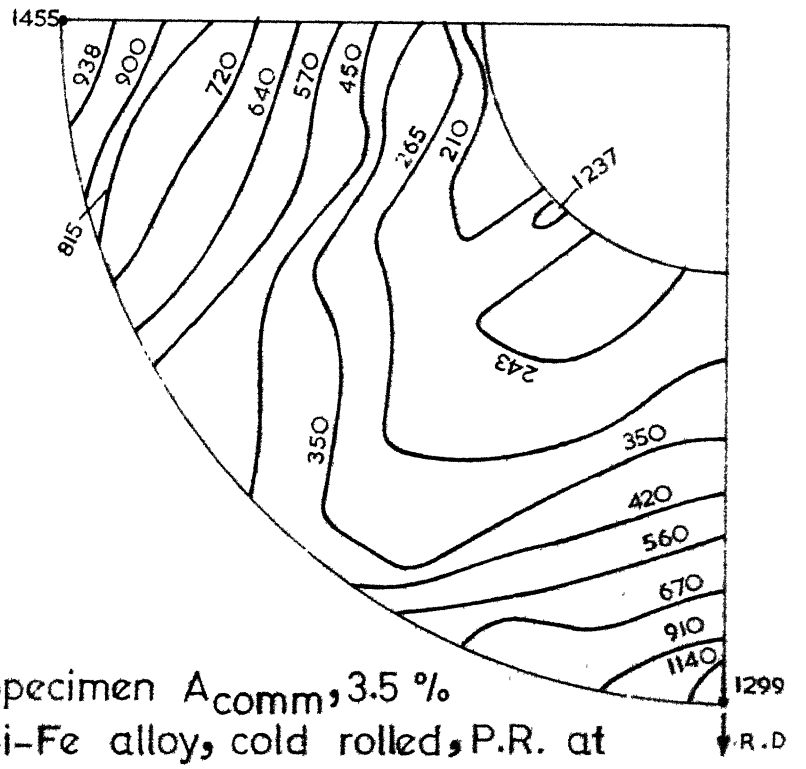

Fig.56 Specimen A_{comm}, 3.5 % Si-Fe alloy, cold rolled, P.R. at 750 °c for 2 hrs., S R at 1150 °c for 10 mins.

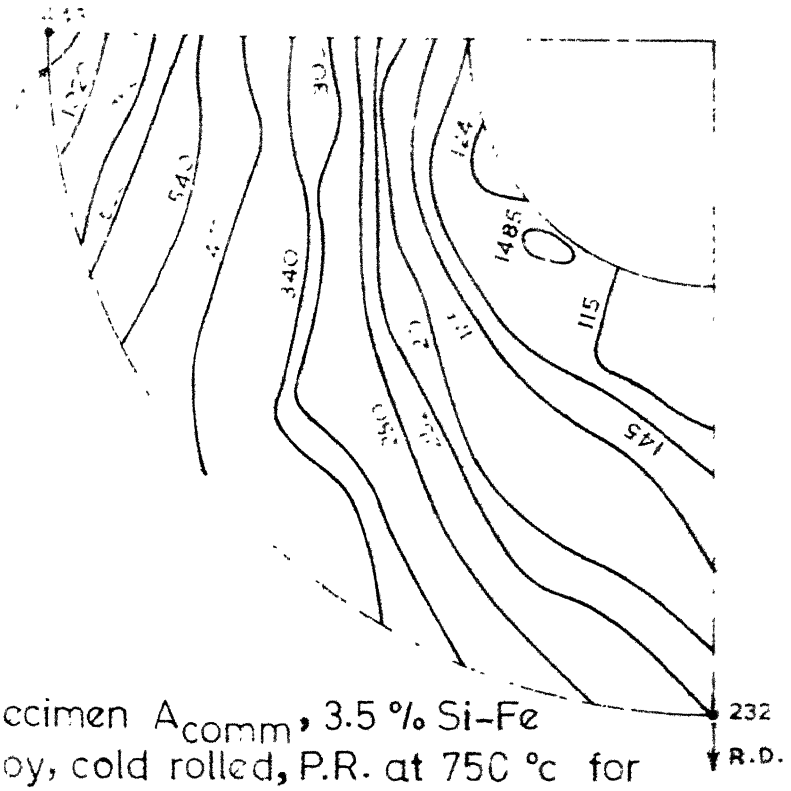

Fig.58 Specimen A_{comm}, 3.5 % Si-Fe alloy, cold rolled, P.R. at 750 °c for 2 hrs., S.R. at 1150 °c for 4 hrs. in purified argon atmosphere

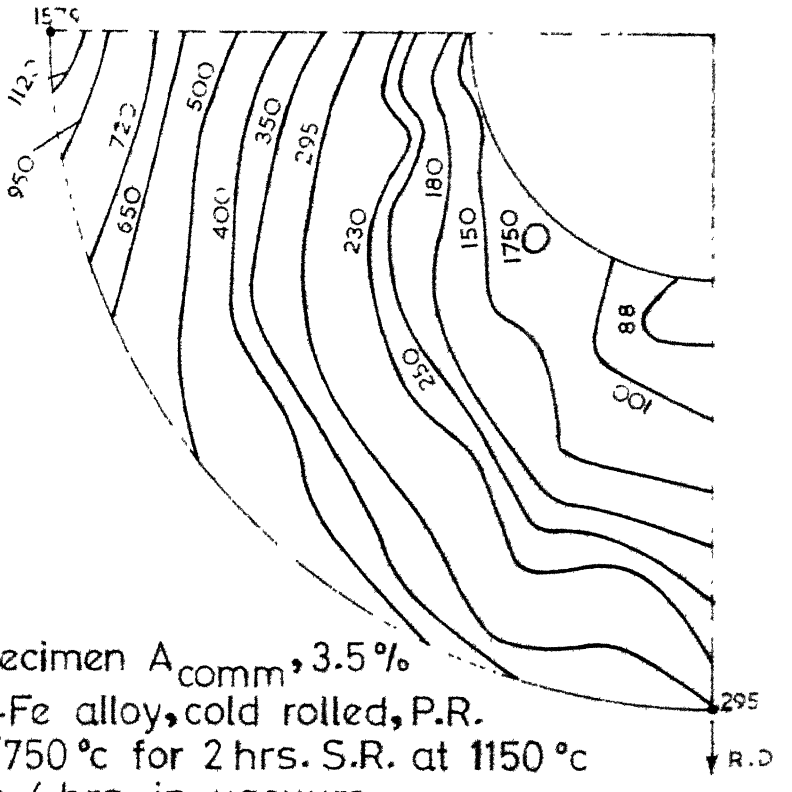

Fig.57 Specimen A_{comm}, 3.5 % Si-Fe alloy, cold rolled, P.R. at 750 °c for 2 hrs. S.R. at 1150 °c for 4 hrs. in vacuum.

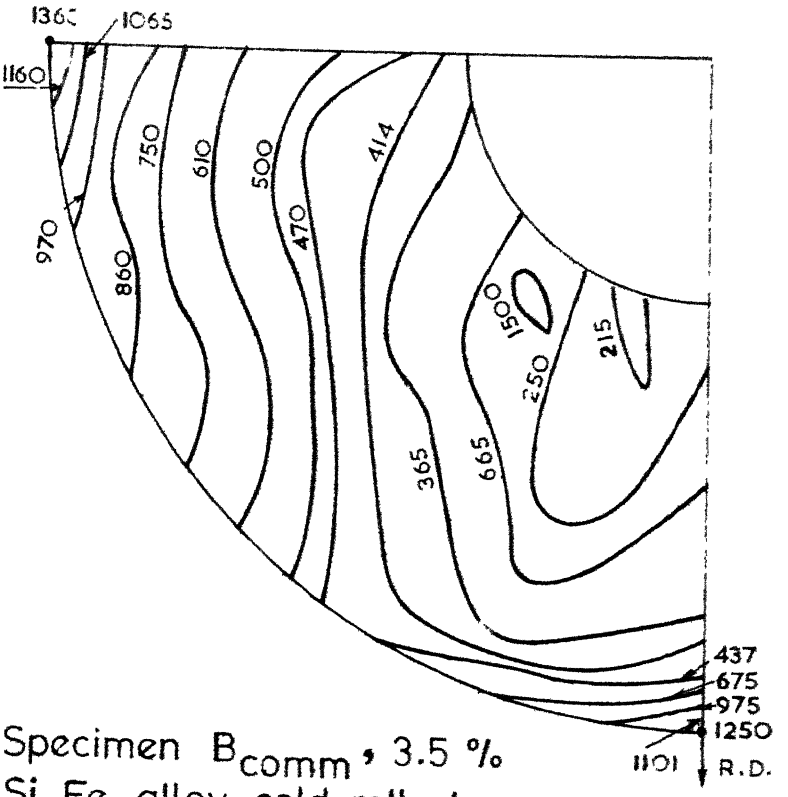

Fig. 59 Specimen B_{comm}, 3.5 % Si-Fe alloy, cold rolled

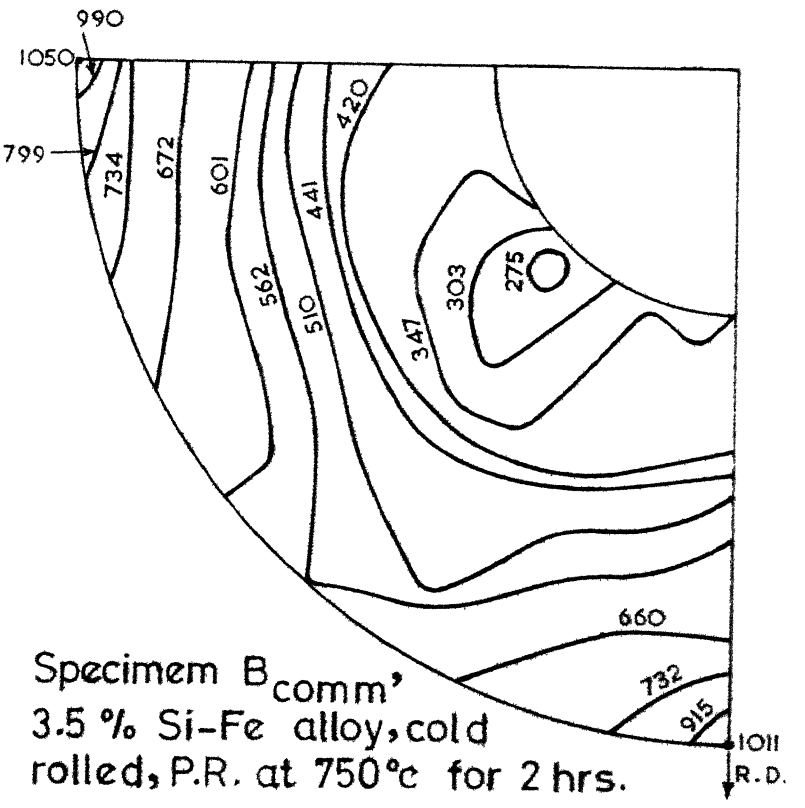

Fig. 60 Specimem B_{comm}, 3.5 % Si-Fe alloy, cold rolled, P.R. at 750°c for 2 hrs.

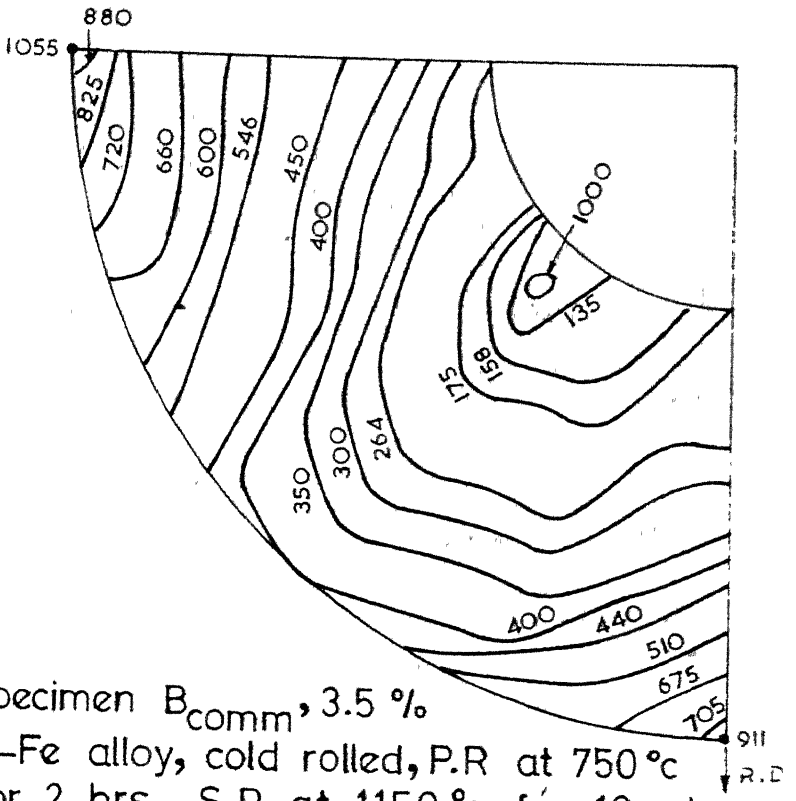

Fig. 61 Specimen B_{comm}, 3.5 % Si-Fe alloy, cold rolled, P.R at 750 °c for 2 hrs. S.R. at 1150 °c for 10 mins.

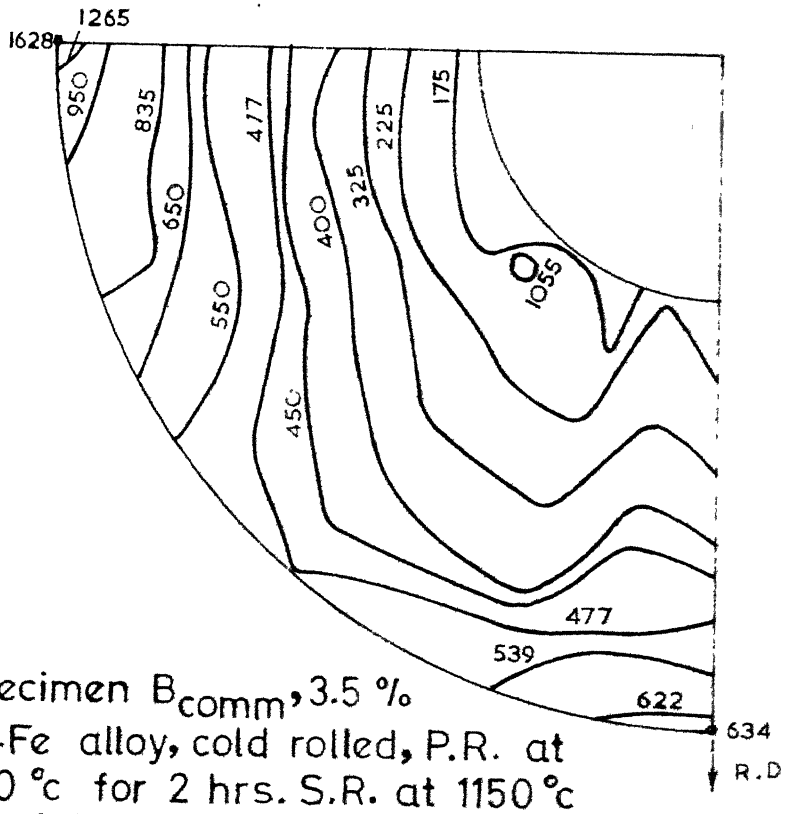

Fig. 62 Specimen B_{comm}, 3.5 % Si-Fe alloy, cold rolled, P.R. at 750 °c for 2 hrs. S.R. at 1150 °c for 4 hrs.

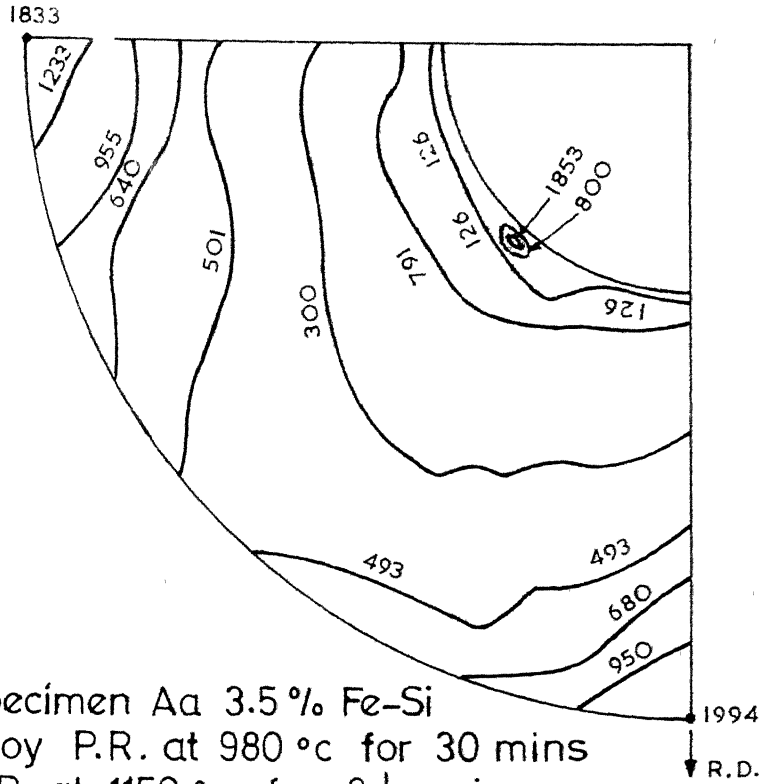

Fig. 64 Specimen Aa 3.5 % Fe-Si alloy P.R. at 980 °c for 30 mins S.R. at 1150 °c for $3\frac{1}{2}$ mins.

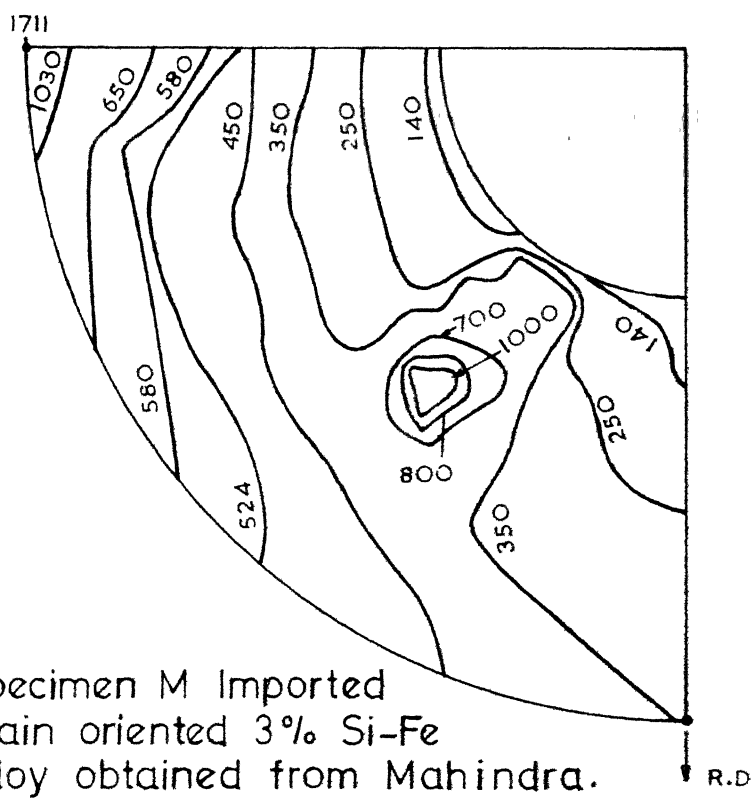

Fig. 63 Specimen M Imported grain oriented 3% Si-Fe alloy obtained from Mahindra.

Fig. 29. Effect of Impurities on the Change in Hysteresis loss W_h (with respect to pure Fe) of 4% Si-Fe alloy at B=10000 Gauss.

Fig. 30. Fe-Si phase Diagram.

Fig. 31. Modification of Fe-Si Diagram with variation in C concentration.

Fig. 32(a). Hysteresis loss W_h, coercive force H_c, Total loss W_t and Maximum permeability μ_m as a function of Si content for hot rolled commercial Si-Fe alloys.

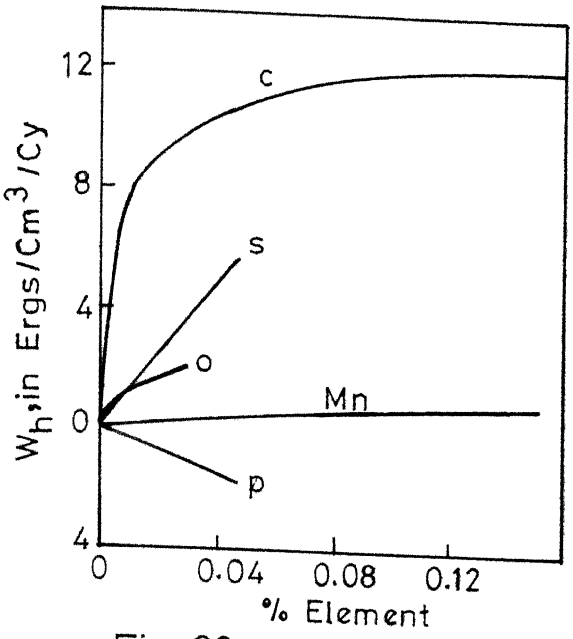

Fig. 29

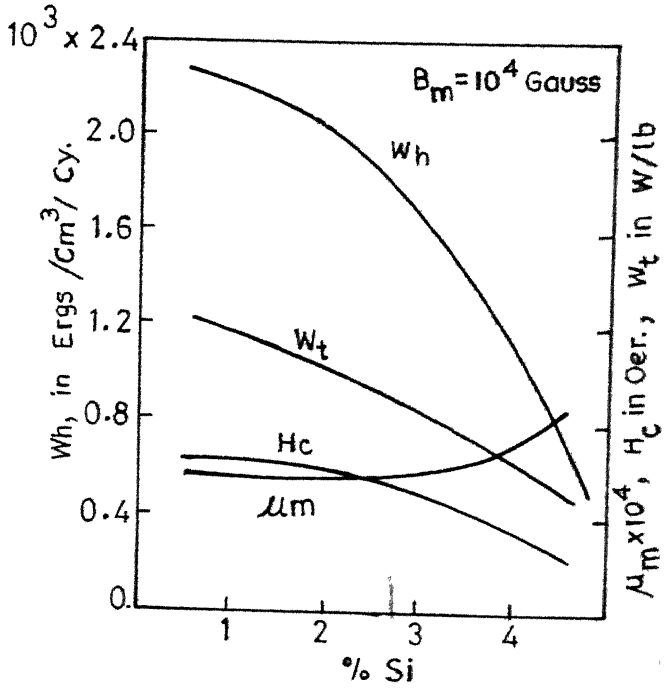

Fig 32 (a)

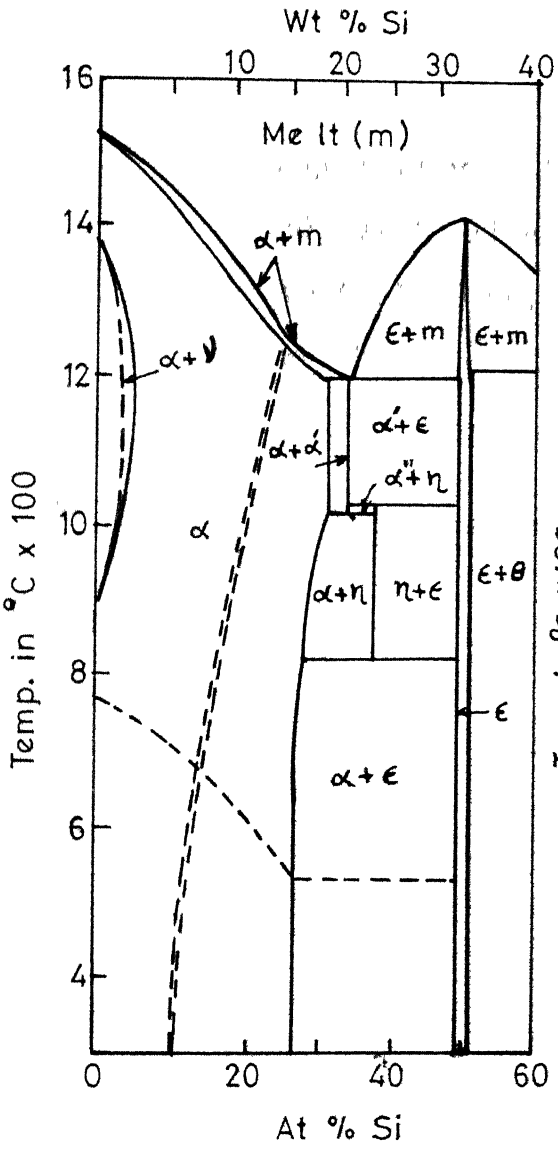

Fig. 30

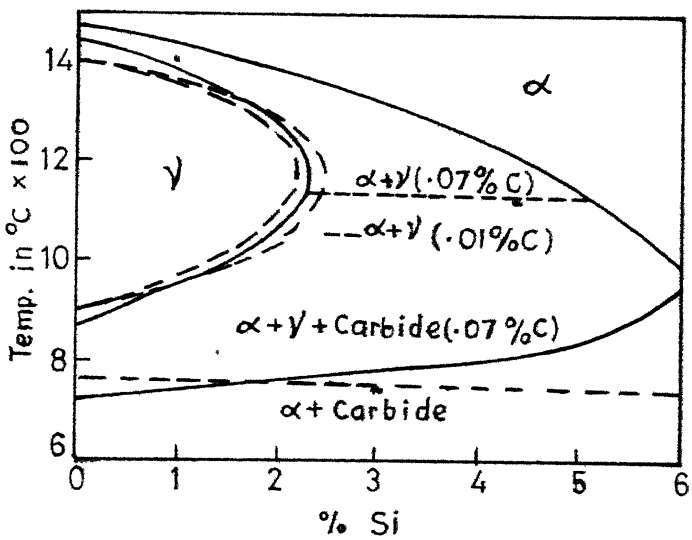

Fig. 31

Fig. 32(b). Average grain size vs. Annealing temperature for (A) high purity Fe-Si alloy containing 3.3% Si and .003%C, (B) Fe-Si alloy containing 2.84% Si, 0.046% S 0.006%C and 0.110 % Mn. Curve (A) is typical of normal grain growth process and curve (B) is typical of abnormal grain growth process.

Fig. 32(c). Effect of sulphur on the formation of cube texture.

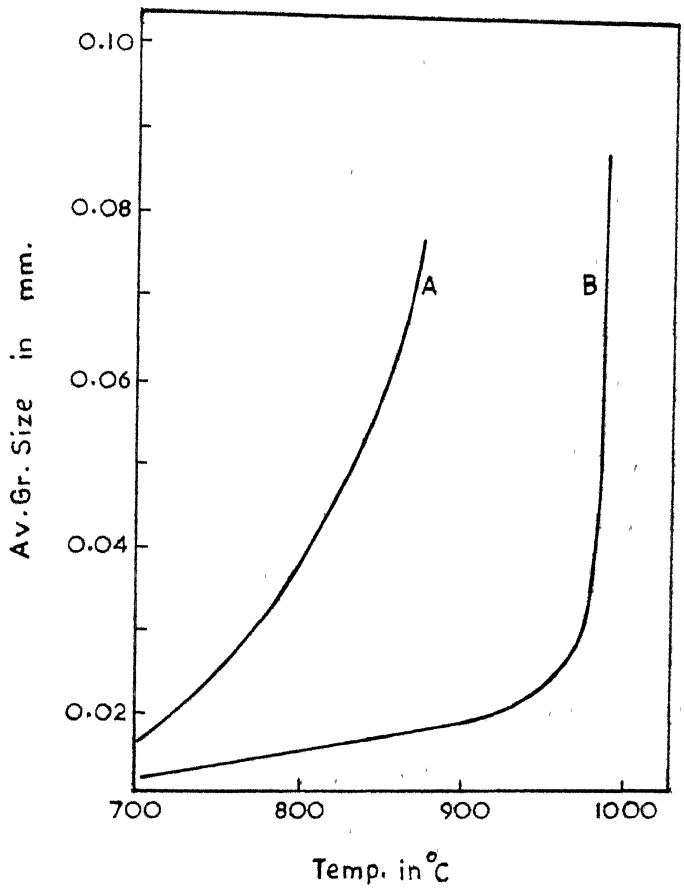

Fig 32 (b)

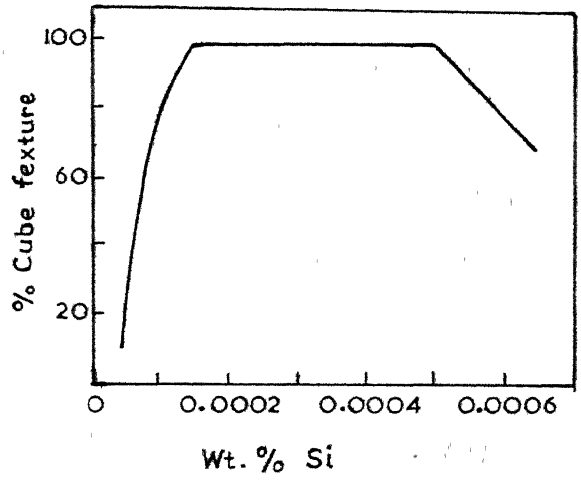

Fig 32 (c)

of γ and $\alpha+\gamma$ region and this will cause heat treatment difficulty because the recrystallization temperature falls in the γ loop. However, with .029% C and as high as 3.5% Si is not expected to extend the loop too far. Hence no difficulty is expected in heat treatment.

From Fig. 29, we find that the variation in hysteresis loss in Fe-Si alloys in the range of 0.01% C to 0.03% C is rather small compared to the range of 0.0%C to 0.01%C. Since as large as about 0.01% C is used for the production of grain oriented steel, in the present study no attempt was made to bring down the % C by alloying the available commercial material with high purity Fe. However, since Si was added to increase the level of Si concentration, the % C is expected to go down slightly. Because of the higher % C, however, the total loss due to slight higher % C will not be too different from that of 0.01% C. Further, increase in silicon content to 3.5% than the usual 3% Si content will nullify to some extent the effect (hysteresis loss) due to increased % C (Fig.32). The Mn, S, P, contents of the alloy (0.21% Mn, 0.027% S and 0.025% S) are also slightly higher than the usual contents (Mn 0.015% S 0.01% and P 0.01%[44] in the grain oriented steels. A slight higher Mn and S may be tolerated in producing grain oriented steel provided these elements can be retained as dispersed MnS[12,42]. Mangnese is

practically inert as far as magnetic properties are concerned (Fig. 29) and is known to improve the ductility and workability of the alloy especially at higher temperatures[42]. Sulphur when in dissolved state in Fe-Si alloys has detrimental effect on both magnetic properties, (Fig.29), as well as secondary recrystallization process (Fig.32). But when present as MnS, it helps stabilization of grain structure in the primary recrystallized stage[12]. Phosphorous improves the hysteresis loss, (Fig.29), and takes care of oxygen because of its strong affinity for it[43]. Thus the supplied commercial alloy may be suitable for grain oriented material of practical importance. However, still better material will be Fe-Si alloy containing less than 0.01% C, 0.015% S, 0.01% P and 0.015% Mn; smaller the carbon the better.

The stabilization of grain size during primary recrystallization was achieved by determining suitable time and temperature for primary recrystallization of pure Fe-Si alloy. As suggested by Beck[10] and Walters[11] stable grain size was found by annealing for atleast 3 hours at 775°C or 15-20 mins. at 950°-980°C, the grain size was approximately 2½ times the specimen thickness. In some cases, however, due to delay in taking the specimen out from the furnace, primary recrystallization has been done at 950°C for as long

as 30 mins . Fiedler[45] with an alloy containing 3.27% Si, 0.06% Mn, 0.004% C, 0.026% S showed that at or above 1300°C the MnS inclusions can be dissolved and more uniform precipitation can be achieved by air cooling at the rate of 150°C/ min or by brine quenching followed by high temperature aging. In the present case a solution treatment at 1350°C for 1½ hrs. was found to dissolve 40-45% of the inclusions (Fig. 20). Specimens when annealed for different times at 1000°C followed by air cooling showed a good and uniform distribution of inclusions (Fig. 21) for annealing time of 2½ hrs. Compared to Fiedler's data the inclusions in the present case were more in amount. As observable in the Figs.19 & 20 all inclusions did not go into solution as it happened in Fiedler's alloys. This is possibly because the amount of inclusions were more and the time allowed was not sufficient to take all these particles into solution, or it may be due to insoluble inclusions other than MnS being present. No attempt was made to take all the inclusions into solution because in that case all of it would be reprecipitated as uniformly distributed inclusions and it might have caused adverse effect due to too many fine inclusions being present. The heat treatment used was found at a later stage to be suitable for producing the desired texture.

Hot rolling of material does not produce preferred orientation[42] . The hot rollings and hot forgings were primarily used to bring down the size of

ingots to the workable sizes. Preliminary cold-rolling studies with high purity 3.5% Si-Fe alloy indicated that it behaves slightly different compared to high purity 3% Si-Fe alloy[40]. The essential difference being that 3% Si alloy was workable at all temperatures whereas 3.5% Si alloy was workable only at elvated temperatures. Since no data on 3.5% Si alloy is available in the literature it was thought appropriate to investigate the effect of 1) straight rolling to final thickness 2) one intermediate annealing followed by a) heavy reduction (more than 80%) and b) critical reduction (about 50-60 %).

Since Fe-Si alloys are bcc, the strongest Bragg reflection is the (110) reflection. Moreover, since the transmission technique was being used, it was necessary to find in the pole figure as many ideal [110] pole locations for the (110) [001] texture or the (100) [011] texture as possible. Because of these facts (110) pole figure was chosen for representing the texture of the Fe-Si alloys. One of the limitations of the transmission goniometer is that the investigation can be carried out only between α = 0 to 40° or 50°. The highest angle (50°) is permissible provided that the frame of the goniometer does not obstruct the diffracted beam. To achieve this condition Mo radiation was chosen so that the Bragg angle $\theta_{(110)}$ was small. This allowed rotation of the sample up to 55°. Moreover, Mo radiation had the added advantage of

low absorption in air compared to the other radiations of longer wave lengths. Since Mo radiation was used, for better counting efficiency a scintillation counter (~100% efficient for Mo radiation) was used. The texture study of high purity alloy specimens was carried out using scientillation counter, but the commercial purity alloy specimens were studied using a Xenon filled proportional counter because the scientillation counter went out of order. The proportional counter is about 40% efficient for Mo radiation. Hence, the intensities of different pole figures, expressed as counts/second, cannot be directly compared. It will be, however, possible to compare the intensity variations in two pole figures by comparing the ratio of intensities, of any position with respect to a fixed position, of one pole figure with that of the other pole figure. Table V shows the effect of use of the two counters for a given specimen. Pole figures of cubic metals and alloys are usually symmetrical around cross direction and rolling direction. Hence it is not necessary to plot intensity data in a full stereogram. In the present case also, preliminary tests for plotting half of the pole figure showed that the pole figure is symmetrical around the cross and rolling directions. Hence only one quarter of the pole figure was determined for each case.

The ideal (100) [01$\bar{1}$] texture will show three

intensity maxima, at(1) $\phi = 0^{\circ}, \alpha = 0^{\circ}$ i.e. coincident with the cross direction (C.D.), 2) $\phi = 90^{\circ}, \alpha = 0^{\circ}$ i.e. coincident with the rolling direction (R.D.) and 3) $\phi = 45^{\circ}, \alpha = -45^{\circ}$. For easy identification of the peak at $\alpha = -45^{\circ}$, $\phi = 45^{\circ}$ it has been called the central peak. The ideal (110) [001] texture will show only two intensity maximas 1) $\alpha = 0^{\circ}$, $\phi = 0^{\circ}$ and 2) $\alpha = -30^{\circ}$, $\phi = 45^{\circ}$. To interpret the pole figures, a single standard stereogram showing only the [110] pole locations for the (001), (110), (111), (112) and (130) standard projections. (Fig. 28) was used. Following the general convention, the textures were interpreted in terms of the ideal texture even when there was considerable deviation from ideal behaviour.

The cold rolled texture produced in high purity Fe-Si alloys can be divided into two basic groups, those which were given heavy (more than 80%) final reduction and those which were given just the cr tical amount (less than 50%) of final reduction. The cold rolled texture for heavily rolled material was found to be sharply developed (100) [011] texture with uniform spread, varying from 5° to 10° around the R.D. and C.D. (Table I_C, Fig.33,39). The central peak, however, was found to be comparatively quite sharp i.e. with less spread. The specimens A_a and A_b (Table I_A) were both cold rolled to the same amount but A_a went through an intermediate annealing stage. The final reduction of A_a was slightly lower than the specimen A_b. The textures of these two specimens (Table I_C, Figs. 33,39)

were found equally sharp with only a minor increase in spread for the A_a specimen. This showed that the intermediate annealing has practically no effect on the texture produced so long as the final reduction is very high (above 80%). But when the %age reduction is small, less than 60% (specimen D_a and E_a), the cold rolled texture developed was weak with large spread around the R.D. and C.D. and the central peak was also weak(Table I_C, Figs.42,45,50). The similarity between the textures of specimens D_a and E_a (Table I_C,Figs.45,50) indicates that the texture was reproducible, even through the subsequent heat treatments. The cold rolled textures of high purity alloys are in agreement with the work of other investigators [12,9]. As for example, Dunn[8] reported sharp (100) [01] texture at and above 70% reduction. Brown's[9] work also indicate that in one stage process of 75% reduction or 70% reduction following an intermediate annealing produces sharp (100) [01] texture, whereas a two stage process involving an intermediate annealing followed by 50-60% reduction produces complex duplex texture. In the present investigation, however, no duplex texture could be seen and this is possibly due to the difference in composition of the alloys. The cold rolled texture is dependent on composition can be seen by comparing the present data with that of Narula[40].

The primary recrystallization textures of heavily cold rolled (83%to 91%) specimens A_a and A_b showed that the cold rolled textures were retained as strong textures but with small decrease in pole density around the C.D.. This treatment, however, caused larger spread around the rolling

and the cross directions than that produced in the cold rolled state. The central peak in these cases was either completely eliminated or became very insignificantly low in intensity (Table I_C, Figs. 34, 37,40). Primary recrystallization of specimen D_a (54% final reduction) at 950°C for 15-20 mins. showed weak cold rolled texture with about a 10° shift of peak positions away from the R.D. and with no trace of the central Peak (Table I_C, Figs.46). These observations on primary recrystallization texture of 3.5% Si-Fe alloys are similar to the observation of Brown[9], Fiedler[45], May and Turnbull[12], Dunn and Walters[20], that the texture becomes more random on primary recrystallization. However, unlike the observations on other Fe-Si alloy data[9,12] the heavily cold rolled specimens A_a & A_b retained strong (100) [011] texture. This behaviour is similar, however, to that of Mo which also shows strong (100) [011] texture in both cold rolled and annealed state[44]. A very marked behaviour of specimen D_a, which was given only 54% final reduction, was that the specimen annealed for very long time (2 hrs.) produced considerably sharper (100) [011] texture than the cold reduced state. The texture of this specimen, however, was very much weaker than the heavily cold rolled material.

The high temperature annealing treatment, which is called here secondary recrystallization, of heavily cold rolled and primary recrystallized specimens of high purity alloy (Table I_A and I_B) showed strong cold rolled texture (100) [011] with the central peak at the ideal position (Table I_C Figs.36, 38,41). On the other hand the specimens of high purity alloy

cold rolled in two stage process (Table I_A) on secondary recrystallization produced some what improved (100) [01] texture than the primary recrystallization textures (Table I_C, Figs.43,44,47,52). However, the improvement was not very strikingly significant. The specimen D_a, primary recrystallized for 2 hrs., on secondary recrystallization produced a very sharp (100) [01] texture (Table I_C Fig. 49). The reason for this behaviour is not apparent because whether the specimen is being recrystallized at 950°C or 1150°C the change taking place appears to be similar to primary recrystallization. From this point of view the texture should become random as is obtained in 3% Si-Fe alloy[40]. The present data on high purity 3.5% Si-Fe alloy is in agreement with the work of May and Turnbull[12] who also failed completely to achieve (110) [00] annealing texture but instead produced a reasonably sharp cold rolled texture on secondary recrystallization of high purity 3.39% Si-Fe alloy. This behaviour appears to be characteristic only of high Si Fe-Si alloys. The texture observed for 3.5% Si-Fe alloy is, however, about 7 times sharper than May and Turnbull's texture of 3.39% Si-Fe alloy. These results thus indicate that for pure Fe-Si alloys, the sharp (100) [01] texture can be produced either by heavy reduction or by low reduction followed by long primary recrystallization and a high temperature annealing. The behaviour of 3.5% Si-Fe alloy is again similar to Mo[44] in which high temperature anneal has been found to produce sharp cold rolled texture.

Heavily cold rolled(in one stage) commercial purity alloy specimen A_{Comm} (Table II_A) showed a very strong (100) [01]

texture with small spread (≤10°) around the R.D. and C.D. (Table II_C, Fig. 53). The commercial purity alloy B_{Comm} cold reduced in a two stage process (Table II_A), unlike pure alloy produced a sharp cold rolled texture but with about 10° spread around the R.D. and 15° around the C.D. (Fig. 59). Primary recrystallization of heavily cold rolled specimen A_{Comm} retained sharp cold rolled texture (Table II_C, Fig. 54) with 10° spread around the C.D., and the central peak was of very low intensity. The primary recrystallization texture of the specimen B_{Comm} (Table II_C, Fig. 60) was similar to the primary recrystallization texture of the specimen A_{Comm}.

Secondary recrystallization of thin commercial purity specimens, A_{Comm} and B_{Comm}, for 5-10 mins showed retention of the strong cold rolled texture but the spread around the R.D. and C.D. was about 15°-20° (Table II_C, Figs. 55,56,61). Thick commercial purity A_{Comm} specimens on secondary recrystallization in vacuum or in argon atmosphere showed considerable increase in the intensity at the C.D. and at the central position. But the intensity at the R.D. decreased quite considerably (Table I_C Fig. 57,58). On comparing this with the standard projection (Fig. 28) it is clear that this is what is ideaIy required for the development of cube-on-edge texture. The central peak, however, was found in its original location (with respect to (100) [01$\bar{1}$] texture) and off by about 15° from the ideal location of (110) [00$\bar{1}$] texture. Except for this deviation, the texture (Table II_C, Figs. 58, 59) is similar to the texture observed for 3% Si-Fe grain oriented

sheet supplied by Mahindra and Mahindra Co., Poona (Fig.63). The texture was slightly more sharp in specimens secondary recrystallized in argon. Thick B_{Comm} specimen, cold reduced in two stages and primary recrystallized, on secondary recrystallization showed development of weak cube-on-edge texture (Table I_C, Fig. 62) with about 15-20° spread around the rolling direction.

The results are in agreement with the work of most of the investigators[12,38,24,36] who on secondary recrystallization achieved cube-on-edge texture in commercial purity alloy. The achievement of the (110) [001] texture in the present investigation indicated that it is not necessary to use H_2 atmosphere annealing (as prescribed by many investigators) for achieving this texture. But it seems that a slightly higher temperature and longer annealing time or a low vacuum may develope the ideal cube-on-edge texture in commercial purity alloy.

CONCLUSIONS

CONCLUSIONS

From the present investigation on high purity and commercial purity 3.5% Si-Fe alloys the following conclusions can be drawn:

1. Straight single stage reduction involving more than 80% reduction is required to produce sharp cold rolled texture (100) [01].

2. Sharp cold rolled texture can be produced even in two stage reduction process provided the reduction in the final stage is more than 60%.

3. Intermediate annealing has no effect on the sharpness of cold rolled texture provided the final reduction is above 80%.

4. In specimens straight cold reduced by more than 70% primary recrystallization retains the cold rolled texture as the major (with spread of 10^{0} around R.D. and C.D.) texture.

5. The primary recrystallization texture is more random in samples with about 54% final reduction.

6. Secondary recrystallization of high purity specimens produces sharp cold rolled texture.

7. Sharp cold rolled texture in high purity alloys can be produced either by heavy reduction in the final stage or by low reduction ($\sim$ 54%) followed by long primary recrystallization and a high temperature annealing.

8. Short time secondary recrystallization of commercial purity thin specimens sharpens the cold rolled texture related to the primary recrystallization texture.

9. Long primary annealing time and high temperature is essential for producing secondary recrystallization textures in thick (0.014") commercial purity alloys specimens.

10. Low vacuum or purified argon atmosphere can be used for producing grain oriented Fe-Si alloys.

REFERENCES

References

1. S.Kaya and K. Hunda, Sc.Repts., Tohoku Imp. Univ. 15, (1926), 721.
2. H.J. Williams, Phys. Rev., 52, (1937), 747.
3. G. Kurdjunow and G.Sachs, Z.Physik, 62, (1930), 592.
4. C.J. Smithells & C.E. Ransley, J.Inst. Metals, 60, (1937), 172.
5. C.E. Ransley and M.P. Rooksby, J.Inst. Metals, 62,(1938), 205.
6. H.T. Clark, Trans. AIME, 188, (1950), 1154
7. H.Hu, J. Metals, 9, (1957), 1164.
8. C.G. Dunn Acta. Met, 1, (1954), 163.
9. J.R. Brown. J. Appl. Phys. 29, (1958), 339.
10. P. Beck. 1) Trans. AIME 175, (1948) 163.
    2) Trans. AIME 212, (1958) 769.
11. Mullins, Acta Met. 6, (1958), 414
    C.G. Dunn & Watters Trans AIME, 175, (1948) 372.
12. J.E. May and D. Turnbull, Trans AIME, 2127 (1958),769.
13. H.C. Fiedler, J. Appl. Phys. 29 (1958), 361.
14. K.V. Gregorov and Coworkers, Physic of Metals and Metallography I, No. 2, (1959), 147
15. C.G. Dunn, Acta Met., 2, 1954, 173.
16. C.G. Dunn & P.K. Koh, Trans. AIME, 167, (1946), 357.
17. C.G. Dunn & P.K. Koh, J.Metals, 8, (1958), 1017
18. C.G. Dunn & P.K. Koh, J.Metals, 9, (1957), 81
19. C.G. Dunn, J. Metals, 6, (1954), 549
20. J.L. Watters and C.G. Dunn, Acta Met, 8, (1960), 497
21. G. Wiener, J. Appl. Phys., 35, 1964, 856.
22. K. Detert, Acta Met., 7, (1959), 589.

23. Yu-Avraami. and others, Physics of Metals and Metallography No.2, (1967), 162.

24. B.F. Deckrand D. Harker, J. Appl. Phys. 22, (1951), 900.

25. K. Foster, Trans. AIME., 227, (1963), 185

26. J.C. Walters and C.G. Dunn, Trans. AIME 218, (1960), 914

27. J.C. Walters and C.G. Dunn, J.Metals. 1958, 573.

28. J.C. Walters and C.G. Dunn, J.Metals. (1959), 559.

29. J.C. Walters and C.G. Dunn, Trans.AIME 215, (1959), 465

30. Kramer, See E. Adams. J.Appl. Phys. 35, (1964), 856.

31. N. Morril, Metal Progress, 54, (1958), 675.

32. K. Sixtus, Physica, 6, (1935), 105.

33. J.C. Walters, N.R. Hibbard, H.C. Fiedler, W.E. Grenoble, H.R. Pry and P.G. Frishmann, J. Appl. Phys., 29, (1958), 363.

34. P.A. Albert, R.N. Trapp, G. Wiener, and M.F. Litman, J.Appl. Phys., 29, (1958), 366.

35. K. Detert, G. Ibe and F. Assmous, Z. Metal, 48, 1957, 344.

36. J. C. Walters and C.G. Dunn, Trans. AIME, 218, (1960), 448

37. N.P. Goss, Trans. ASM, 23, (1939), 511.

38. G. Wiener and L. Corcoran J.Metals, 9, (1956), 901.

39. C.S. Barret, Ansel and A.E. Mehl, Trans, AIME, 123,(1937),516

40. M.L. Narula, M.Tech. Thesis Jan 1972 submitted to Met. Engg. Dept., IIT, K.

41. B.F.Docker,D.Harker and E.T.Asp,J.Appl.Phys.19,388,(1948)

42. T.D. Yensen, See N.P. Goss Iron Age, 171, Feb.5, (1953), 147

43. See R.M. Bozorth, Ferromagnetism, Van-Nostrand Co.,Inch,151

44. M.Semchysen, G.A. Teonom, TMS-IIME, 194,(1927), 279

45. See 44.

APPENDIX

APPENDIX I

Programme for calculating correction factor and calculated data

```
CCC   DETERMINATION OF CORRECTION FACTOR USED
CCC   FOR INTENSITY CORRECTION
      DIMENSION ALPHA(20), B(20), C(20), D(20), GUT(31)
      PIM = 3..4159/180.
      THETA = 9.975*PIM
      A = COS(THETA)
      DO 5    L = 1,10
      ALPHA(L) = FLOAT(L)*5.*PIM
      B(L) = COS(THETA+ALPHA(L))
      C(L) = COS(THETA-ALPHA(L))
    5 D(L) = B(L)/C(L)
      DO 10   M = 1,22
      GUT(M) 3 0.8+.1*FLOAT(M)
      PRINT 1T GUT(M)
      E = GUT(M)/A
      EE = EXP(-E)
      DO 10   N = 1,10
      F = EXP((GUT(M)/B(N))
      G = EXP((GUT(M)/C(N))
      FACTN = E*EE*(1./D(N)-1.)/(G-F)
      FACTP = E*EE*(D(N)-1.)/(F-G)
      H = 5.*FLOAT(N)
      PRINT 2 ,H,FACTP,FACTN
    1 FORMAT(1X,F10.3)
   10 CONTINUE
    2 FORMAT(11X,F10.2,2E20.4)
      STOP
      END
```

31 Where, $GUT = \mu t$

$FACTN = I_0/I_{-\alpha}$

$FACTP = I_0/I_{+\alpha}$

(Refer equation - (2))

(MT*)	(ALPHA)	(C.F. ALPHA)	(C.F.-ALPHA)
0.900			
	5.00	0.9845E 00	0.1015E 01
	10.00	0.9685E 00	0.1031E 01
	15.00	0.9522E 00	0.1046E 01
	20.00	0.9358E 00	0.1064E 01
	25.00	0.9196E 00	0.1084E 01
	30.00	0.9044E 00	0.1109E 01
	35.00	0.8912E 00	0.1141E 01
	40.00	0.8817E 00	0.1187E 01
	45.00	0.8786E 00	0.1254E 01
	50.00	0.8868E 00	0.1357E 01
1.000			
	5.00	0.9849E 00	0.1016E 01
	10.00	0.9701E 00	0.1032E 01
	15.00	0.9558E 00	0.1050E 01
	20.00	0.9422E 00	0.1071E 01
	25.00	0.9298E 00	0.1096E 01
	30.00	0.9194E 00	0.1127E 01
	35.00	0.9124E 00	0.1169E 01
	40.00	0.9110E 00	0.1226E 01
	45.00	0.9186E 00	0.1311E 01
	50.00	0.9415E 00	0.1441E 01
1.100			
	5.00	0.9853E 00	0.1016E 01
	10.00	0.9717E 00	0.1034E 01
	15.00	0.9594E 00	0.1054E 01
	20.00	0.9486E 00	0.1078E 01
	25.00	0.9400E 00	0.1108E 01
	30.00	0.9346E 00	0.1146E 01
	35.00	0.9341E 00	0.1196E 01
	40.00	0.9411E 00	0.1267E 01
	45.00	0.9602E 00	0.1370E 01
	50.00	0.9993E 00	0.1529E 01
1.200			
	5.00	0.9857E 00	0.1016E 01
	10.00	0.9733E 00	0.1036E 01
	15.00	0.9630E 00	0.1058E 01
	20.00	0.9551E 00	0.1086E 01
	25.00	0.9503E 00	0.1120E 01
	30.00	0.9501E 00	0.1165E 01
	35.00	0.9562E 00	0.1225E 01
	40.00	0.9722E 00	0.1309E 01
	45.00	0.1003E 01	0.1432E 01
	50.00	0.1060E 01	0.1622E 01

(MT*)	(ALPHA)	(C.F. ALPHA)	(C.F.-ALPHA)
1.300			
	5.00	0.9861E 00	0.1017E 01
	10.00	0.9749E 00	0.1037E 01
	15.00	0.9665E 00	0.1062E 01
	20.00	0.9615E 00	0.1093E 01
	25.00	0.9608E 00	0.1132E 01
	30.00	0.9657E 00	0.1184E 01
	35.00	0.9798E 00	0.1254E 01
	40.00	0.1004E 01	0.1352E 01
	45.00	0.1048E 01	0.1496E 01
	50.00	0.1124E 01	0.1721E 01
1.400			
	5.00	0.9865E 00	0.1017E 01
	10.00	0.9796E 00	0.1039E 01
	15.00	0.9701E 00	0.1066E 01
	20.00	0.9680E 00	0.1100E 01
	25.00	0.9713E 00	0.1145E 01
	30.00	0.9815E 00	0.1203E 01
	35.00	0.1002E 01	0.1283E 01
	40.00	0.1037E 01	0.1396E 01
	45.00	0.1095E 01	0.1563E 01
	50.00	0.1192E 01	0.1824E 01
1.500			
	5.00	0.9869E 00	0.1018E 01
	10.00	0.9780E 00	0.1041E 01
	15.00	0.9737E 00	0.1070E 01
	20.00	0.9746E 00	0.1108E 01
	25.00	0.9818E 00	0.1157E 01
	30.00	0.9976E 00	0.1223E 01
	35.00	0.1025E 01	0.1313E 01
	40.00	0.1071E 01	0.1441E 01
	45.00	0.1144E 01	0.1632E 01
	50.00	0.1263E 01	0.1933E 01
1.600			
	5.00	0.9872E 00	0.1018E 01
	10.00	0.9796E 00	0.1042E 01
	15.00	0.9773E 00	0.1074E 01
	20.00	0.9811E 00	0.1115E 01
	25.00	0.9925E 00	0.1170E 01
	30.00	0.1014E 01	0.1243E 01
	35.00	0.1049E 01	0.1344E 01
	40.00	0.1105E 01	0.1488E 01
	45.00	0.1194E 01	0.1704E 01
	50.00	0.1338E 01	0.2048E 01

(MT*)	(ALPHA)	(C.F. ALPHA)	(C.F.*ALPHA)
1.700			
	5.00	0.9876E 00	0.1019E 01
	10.00	0.9812E 00	0.1044E 01
	15.00	0.9809E 00	0.1078E 01
	20.00	0.9877E 00	0.1123E 01
	25.00	0.1003E 01	0.1183E 01
	30.00	0.1030E 01	0.1263E 01
	35.00	0.1074E 01	0.1375E 01
	40.00	0.1141E 01	0.1536E 01
	45.00	0.1247E 01	0.1779E 01
	50.00	0.1417E 01	0.2163E 01
1.800			
	5.00	0.9880E 00	0.1019E 01
	10.00	0.9828E 00	0.1046E 01
	15.00	0.9845E 00	0.1062E 01
	20.00	0.9944E 00	0.1130E 01
	25.00	0.1014E 01	0.1195E 01
	30.00	0.1047E 01	0.1284E 01
	35.00	0.1099E 01	0.1407E 01
	40.00	0.1178E 01	0.1586E 01
	45.00	0.1301E 01	0.1856E 01
	50.00	0.1500E 01	0.2295E 01
1.900			
	5.00	0.9884E 00	0.1019E 01
	10.00	0.9843E 00	0.1047E 01
	15.00	0.9881E 00	0.1086E 01
	20.00	0.1001E 01	0.1138E 01
	25.00	0.1025E 01	0.1208E 01
	30.00	0.1124E 01	0.1440E 01
	40.00	0.1215E 01	0.1636E 01
	45.00	0.1357E 01	0.1937E 01
	50.00	0.1587E 01	0.2428E 01
2.000			
	5.00	0.9888E 00	0.1020E 01
	10.00	0.9859E 00	0.1049E 01
	15.00	0.9918E 00	0.1090E 01
	20.00	0.1008E 01	0.1146E 01
	25.00	0.1036E 01	0.1221E 01
	30.00	0.1081E 01	0.1326E 01
	35.00	0.1150E 01	0.1473E 01
	40.00	0.1254E 01	0.1688E 01
	45.00	0.1416E 01	0.2021E 01
	50.00	0.1678E 01	0.2568E 01

(MT*)	(ALPHA)	(C.F. ALPHA)	(C.F.-ALPHA)
2.100			
	5.00	0.9892E 00	0.1020E 01
	10.00	0.9875E 00	0.1051E 01
	15.00	0.9954E 00	0.1094E 01
	20.00	0.1014E 01	0.1153E 01
	25.00	0.1058E 01	0.1248E 01
	30.00	0.1116E 01	0.1368E 01
	35.00	0.1203E 01	0.1541E 01
	40.00	0.1335E 01	0.1797E 01
	45.00	0.1540E 01	0.2198E 01
	50.00	0.1876E 01	0.2870E 01
2.200			
	5.00	0.9896E 00	0.1021E 01
	10.00	0.9891E 00	0.1052E 01
	15.00	0.9990E 00	0.1098E 01
	20.00	0.1021E 01	0.1161E 01
	25.00	0.1058E 01	0.1248E 01
	30.00	0.1116E 01	0.1368E 01
	35.00	0.1203E 01	0.1541E 01
	40.00	0.1335E 01	0.1797E 01
	45.00	0.1540E 01	0.2198E 01
	50.00	0.1876E 01	0.2870E 01
2.300			
	5.00	0.9900E 00	0.1021E 01
	10.00	0.9906E 00	0.1054E 01
	15.00	0.1003E 01	0.1102E 01
	20.00	0.1028E 01	0.1168E 01
	25.00	0.1070E 01	0.1261E 01
	30.00	0.1134E 01	0.1390E 01
	35.00	0.1231E 01	0.1576E 01
	40.00	0.1377E 01	0.1854E 01
	45.00	0.1606E 01	0.2291E 01
	50.00	0.1982E 01	0.3033E 01
2.400			
	5.00	0.9904E 00	0.1021E 01
	10.00	0.9922E 00	0.1056E 01
	15.00	0.1006E 01	0.1106E 01
	20.00	0.1035E 01	0.1176E 01
	25.00	0.1081E 01	0.1274E 01
	30.00	0.1152E 01	0.1412E 01
	35.00	0.1259E 01	0.1612E 01
	40.00	0.1420E 01	0.1912E 01
	45.00	0.1674E 01	0.2388E 01
	50.00	0.2093E 01	0.3203E 01

(MT*)	(ALPHA)	(C.F. ALPHA)	(C.F.-ALPHA)
2.500			
	5.00	0.9908E 00	0.1022E 01
	10.00	0.9938E 00	0.1057E 01
	15.00	0.1010E 01	0.1110E 01
	20.00	0.1041E 01	0.1184E 01
	25.00	0.1093E 01	0.1288E 01
	30.00	0.1170E 01	0.1435E 01
	35.00	0.1287E 01	0.1649E 01
	40.00	0.1464E 01	0.1972E 01
	45.00	0.1744E 01	0.2489E 01
	50.00	0.2210E 01	0.3382E 01
2.600			
	5.00	0.9912E 00	0.1022E 01
	10.00	0.9954E 00	0.1059E 01
	15.00	0.1014E 00	0.1114E 01
	20.00	0.1048E 00	0.1924E 01
	25.00	0.1104E 00	0.1301E 01
	30.00	0.1189E 00	0.1458E 01
	35.00	0.1316E 00	0.1686E 01
	40.00	0.1510E 01	0.2033E 01
	45.00	0.1817E 01	0.2593E 01
	50.00	0.2333E 01	0.3570E 01
2.700			
	5.00	0.9915E 00	0.1023E 01
	10.00	0.9969E 00	0.1061E 01
	15.00	0.1017E 01	0.1118E 01
	20.00	0.1055E 01	0.1200E 01
	25.00	0.1116E 01	0.1215E 01
	30.00	0.1208E 01	0.1481E 01
	35.00	0.1346E 01	0.1724E 01
	40.00	0.1557E 01	0.2096E 01
	45.00	0.1893E 01	0.2701E 01
	50.00	0.2461E 01	0.3766E 01
2.800			
	5.00	0.9919E 00	0.1023E 01
	10.00	0.9985E 00	0.1062E 01
	15.00	0.1021E 01	0.1122E 01
	20.00	0.1062E 01	0.1207E 01
	25.00	0.1128E 01	0.1329E 01
	30.00	0.1227E 01	0.1504E 01
	35.00	0.1376E 01	0.1762E 01
	40.00	0.1605E 01	0.2160E 01
	45.00	0.1971E 01	0.2813E 01
	50.00	0.2596E 01	0.3973E 01